Phil. Trans. R. Soc. Lond. B **328**, 479–500 (1990) [479]
Printed in Great Britain

THE RESPONSE OF THE CEREBRAL HEMISPHERE OF THE RAT TO INJURY. I. THE MATURE RAT

By W. L. MAXWELL[1]†, R. FOLLOWS[2], DOREEN E. ASHHURST[1] and M. BERRY[2]

[1] *Department of Anatomy, St George's Hospital Medical School, London SW*17 0*RE, U.K.*
[2] *Department of Anatomy, United Medical and Dental Schools of Guy's and St Thomas's Hospitals, Guy's Campus, London SE*1 9*RT, U.K.*

(*Communicated by B. B. Boycott, F.R.S.* – *Received* 14 *August* 1989 – *Revised* 9 *February* 1990)

[Plates 1–11]

CONTENTS

The response to injury of the cerebrum of the mature rat was studied chronologically in stereotactically placed knife wounds by using both light and electron microscopical, and immunohistochemical, techniques.

Immediately after injury haematogenous cells fill the lesion and ischaemic necrosis occurs along the margins and a zone of cell swelling occupies the surrounding area.

† Present address: Department of Anatomy, University of Glasgow, Glasgow G12 8QQ, U.K.

This phase is transformed by the appearance of large numbers of macrophages and fibroblasts, and some reactive astrocytes in the zone of cell swelling at 4 days. Blood vessels grow into the lesion at this time. Collagen deposition begins in the subpial region of the wound and, with time, scarring progresses into the deeper parts of the wound. By 8 days, the lesion contains a matrix of collagen fibrils, capillaries, fibroblasts, macrophages and astrocytes. The wound margins are better defined as astrocytes become aligned and secrete the basement membrane of the glia limitans, initially in the subpial regions of the scar. By 16 days, a glia limitans is complete along the margins of the entire lesion and the scar tissue between is reduced in area and contains fibroblasts, scattered macrophages, collagen fibrils and a few extra-parenchymatous astrocytes. Subsequently the scar condenses to a thin layer and becomes less vascularized; few cells remain. The persistence of astrocytes within mesenchymatous scar tissue excluded from the cerebral neuropile is a new finding. No further changes are seen in the scar after 30 days.

The progressive development and maturation of scar tissue from the pial surface of the wound into the deeper regions of the cerebrum suggests that the major source of fibroblasts is from the meninges. The appearance of macrophages before fibroblasts in the wound may indicate that macrophages secrete a substance that is a trophic stimulus for fibroblasts. The organization of a glia limitans by astrocytes also proceeds inwards from the pial surface.

Within the neuropile, degeneration of damaged neural elements is the prominent feature in the first 8 days after injury. Macrophages and reactive astrocytes also appear among the debris and are numerous by 4 days at the junctions of viable and necrotic neuropile. Signs of a regenerative response of neural processes is first seen at 4 days as growth cones appear in the viable neuropile at the edges of the necrotic zone. Growth cones are most numerous at 8 days.

Evidence for new synapse formation is seen over the surface of dendritic swellings from 16 days onwards. Synapses of varying maturity are present, the most mature are adjacent to the dendritic shaft. This observation may suggest that these swellings are true growth cones, in which case, this new synaptogenesis is similar to that over dendritic growth cones during development.

It is not possible to judge the relative importance of either collateral sprouting or true regeneration in the reorganization of connections after injury, but neurite growth and the associated synaptogenesis described here could contribute to the recovery process. If the swellings on dendritic processes are true growth cones, then this is evidence for the regeneration of dendritic processes.

Introduction

The conditions that control axonal growth in the adult mammalian and avian central nervous systems (CNS) after axotomy have been controversial for many years (Berry 1979, 1983, 1985; Björklund & Stenevi 1979; Kiernan 1979; Vera & Grafstein 1981). In most cases growth is abortive (Ramon y Cajal 1928), but several groups of axons do exhibit true regeneration; these are central monoaminergic fibres, unmyelinated cholinergic axons (see Björklund *et al.* 1971; Björklund & Stenevi 1971), neurosecretory fibres (see review by Dellman 1973), primary olfactory axons (Barber 1981), retinal axons (Carter *et al.* 1988; McConnell & Berry 1982*a*, *b*), and neonatal axons (Kalil & Reh 1979). Moreover, all CNS axons in Amphibia and fish, and all peripheral nerves in birds and mammals regenerate, although the latter axons are unable to grow if the injury is in the CNS.

There are many theories which attempt to explain the failure of central axonal growth after injury in mammals and birds; these attribute the failure to an absence of trophic cues and/or

growth factors (Berry 1979; Kiernan 1979), or to the release of growth inhibitory substances (Berry 1982, 1983, 1985; Berry & Riches 1974). There are many light microscopical descriptions of the cellular events that follow injury to the central nervous system (Ramon y Cajal 1928; Cavanagh 1970; Hortega & Penfield 1928; Penfield 1927; Penfield & Buckley 1928). Thus, although the role of mesodermal and glial cells in scarring is generally known (Berry *et al.* 1983), the inter-relationships between these cells, the timing both of collagen secretion and of the formation of the glia limitans, are all poorly documented. Moreover, there is little information about the reaction of axons and dendrites to amputation (Kao *et al.* 1977*a*, *b*), the formation of growth cones and synaptogenesis (Bernstein & Bernstein 1973*a*, *b*).

This paper describes a detailed microscopical and immunohistochemical study of the cellular response of the cerebrum to a penetrating knife wound. Several techniques have been used previously to injure the cerebral cortex; these include dropping weights onto the exposed brain to produce a contusion (Feeney *et al.* 1981) and the application of cold instruments to the brain surface (Bakay 1968; Houthoff *et al.* 1981; Klatzo *et al.* 1968). The surgical penetration of the pia mater and underlying neuropile (Berry *et al.* 1983) has the advantage that both dendrites and axons are severed and that scarring is studied with minimal ischaemic necrosis; recovery is uncomplicated when compared with the severe consequences of spinal lesions.

Materials and methods

(*a*) *Preparation of lesions for microscopy*

The 30-day-old rats, of either sex, used for the experiments were taken from litters that had been reduced to 5 animals immediately after birth to standardize their masses. The experiment comprised seven groups of five rats; none was a litter-mate.

The rats were anaesthetized with an intraperitoneal injection of Avertin (tribromoethanol with amylene hydrate, Bayer). The head of the rat was placed in a stereotactic frame and a strip of the calvarium over the right cerebral hemisphere removed with a dental drill. The lesion was made, as shown in figures 1 and 2, using a disposable iridectomy knife. The groups of five rats were maintained for experimental periods of either 1, 2, 4, 8, 16, 30 or 60 days before being killed.

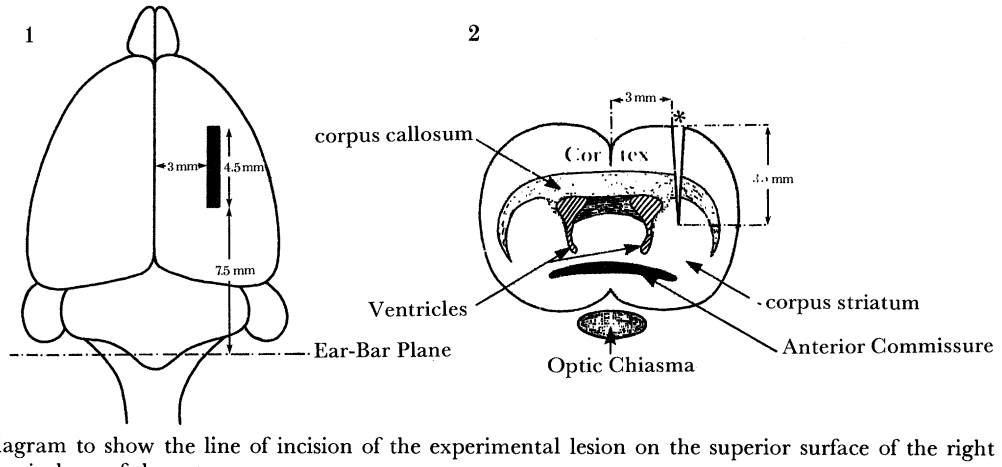

FIGURE 1. A diagram to show the line of incision of the experimental lesion on the superior surface of the right cerebral hemisphere of the rat.

FIGURE 2. A diagram to show the position of the lesion (*) as viewed in a coronal section. The lesion extends from the superior pial surface through the cortex and corpus callosum to penetrate part of the corpus striatum.

The animals were perfused at atmospheric pressure via the left ventricle under Avertin anaesthesia; the descending aorta was clamped and both external jugular veins were incised. Perfusion with physiological saline for 1 min was followed by fixative for 5 min. The fixative was 5% glutaraldehyde in 0.1 M phosphate buffer, pH 7.2, with 20 g l^{-1} sucrose added. The brain was removed from the cranium, taking particular care to separate the scar tissue from the calvarium overlying the lesion. The whole brain was then immersed in the fixative for about three hours at 4 °C. The brains were washed overnight in buffer, plus sucrose, at 4 °C. The site of the lesion was then cut coronally into 1.5 mm thick slices and postfixed for 1 h in osmium tetroxide (1% by volume) in phosphate buffer, plus sucrose, before ethanol dehydration, and embedding in TAAB resin via propylene oxide.

For light microscopical examination three serial sections at a microtome setting of 1.5 μm of the whole half cerebrum were cut with 1.0 cm glass knives with a Reichert Ultracut Om U4 ultramicrotome. The sections were floated on an aqueous ammonia (1% by volume) solution and flattened in an atmosphere saturated with chloroform. They were dried onto slides and stained with alkaline Toluidine Blue. The semi-thin sections were used for two purposes; firstly, for the selection of areas for examination with the transmission electron microscope, and secondly, for the quantitative analysis of the cells in the lesion.

For electron microscopy, mesas, 2.5 mm × 2.5 mm, were made to include selected areas of interest. Sections of silver–gold or gold interference colours were cut with glass or diamond knives, mounted on grids, stained with uranyl acetate and lead citrate, and examined in a Philips 201 or 301 electron microscope. Thus any ultrastructural detail could be located within the semi-thin section.

(b) Immunohistochemistry

Thirty-day-old rats were lesioned as described above. Groups of five animals were killed at experimental times of 1, 2, 4, 8, 16, 30 and 76 days. The cerebral hemispheres were removed and fixed for 1 h at 4 °C in paraformaldehyde (4% by volume) in phosphate buffered saline (PBS), pH 7.0. They were washed in PBS overnight at 4 °C dehydrated in graded ethanols and embedded in polyester wax, melting point 37 °C (Steedman 1957), and stored at 4 °C. Sections, 7 μm thick, were cut on a microtome fitted with a cooled chuck and floated onto a gelatin solution (10 g l^{-1}) on subbed slides and air-dried.

The antibodies used were rabbit anti-bovine glial fibrillar acidic protein (GFAP) (Dakopatt, Ltd, High Wycombe, U.K.) used at a dilution of 1:200, rabbit anti-calf-lens vimentin (Bio-Nuclear Services, Reading, U.K.) used at a dilution of 1:50, rabbit anti-mouse sarcoma laminin (Bethesda Research Laboratories, Gibco, Paisley, U.K.) used at a dilution of 1:100 and rabbit anti-carbonic anhydrase II (CAII) (donated by Dr N. Gregson, Guy's Hospital, London) used at a dilution of 1:250. All dilutions were made in PBS containing bovine serum albumin (BSA) (1% by volume).

The sections were dewaxed and rehydrated and placed in PBS containing Tween-20 (0.1% by volume) for 15 min. The sections were then incubated in the specific antibody for 1–12 h at room temperature. The slides were washed in three changes of PBS and then incubated in the labelled antibody for 1 h; this antibody was goat anti-rabbit IgG (whole molecule) conjugated with fluorescein isothiocyanate (FITC) (Sigma, Poole, U.K.), diluted to 1:100. The sections were washed in three changes of PBS and mounted in a non-quenching mountant. For controls, either the first or second antibody was omitted; all were negative.

The sections were examined with an Olympus BH-2 microscope with a fluorescence attachment. Photomicrographs were taken on Ilford HP5 film, rated at 400 ISO.

(*c*) *Quantitative analysis*

For each experimental period, one lesioned brain was selected at random for quantitative analysis of the numbers of the glial and mesenchymal cells present. The different cells counted were identified primarily by their nuclear morphology by using the following criteria (Ling *et al.* 1973).

(i) Monocytes have a kidney-shaped, eccentric nucleus with irregular granules of heterochromatin adjacent to the nuclear membrane; the cytoplasm is restricted to a thin layer.

(ii) Macrophages have an irregularly shaped nucleus with densely stained, punctate deposits of heterochromatin; the cytoplasm contains many lysosomes and phagocytotic vacuoles.

(iii) Fibroblasts are spindle-shaped and have an oval nucleus distinguished by the presence of several nucleoli.

(iv) Astrocytes have a palely stained nucleus, but the nuclear envelope is accentuated by a thin, deeply stained lining of heterochromatin.

(v) Oligodendrocytes have an indented, or angular, nucleus that contains large masses of heterochromatin; both nucleus and cytoplasm are densely stained.

(vi) Microglia have an elongated, or irregular, nucleus containing densely stained granules of heterochromatin.

Of the other cells present, the neurons were recognized by their large, round nuclei, whereas endothelial cells and pericytes were identified by their association with blood vessels.

The total area of the lesion within the boundaries of the normal tissue in a 1.5 μm section, stained with toluidine blue and taken from the central area of the lesion on a coronal plane, was photographed. Photographic montages at a magnification of 3500 diameters were assembled. The montages were covered with a square grid; the length of the sides of each square was equivalent to 100 μm on the prints. A line running vertically through the lesion from the pia mater to the corpus striatum was designated the lesion midline (figures 4, 8, 12, 17, 22, 27 and 30†); this was used as a reference line over which the central line of the grid was accurately positioned. The nuclei of each cell-type within each 100 μm square were counted, and the counts were corrected for actual number using the formula $N_v = N_{At} \times 1/D^- + t$‡ (Abercrombie 1946).

The montage was divided into bands of width 100 μm parallel to the midline, and the total numbers of the different types of mesenchymal and glial cells in these regions are shown on figure 36. The data were analysed with a statgraphics (STSC Inc.) programme. Multiple *X–Y–Z* line scatterplots, which show the variation in cell number with distance from the lesion midline at the different experimental times, were drawn (figure 36*a–f*).

† Figures 4–35 appear on plates 1–11.

‡ N_v = corrected nuclear number; N_{At} = number of nuclei per unit area in section of thickness t; D^- = mean diameter of nuclei; t = section thickness.

Results

(*a*) *Macroscopical changes of the lesioned areas*

The changes in the area of the lesion at the different experimental times are shown diagrammatically in figure 3. At 1 day (figures 3 and 4), the greatest coronal dimension of the lesion is in the superficial cortex and, including the zone of cell swelling, measures over 2000 μm, but by 4 days (figures 3 and 12), the lesion has altered and is now most extensive in the corpus callosum. At 8 days (figures 3 and 17), the region of cell swelling is much narrower and the central area of the wound is composed of scar tissue. By 16 days (figures 3 and 22), the scar tissue has contracted to a narrow band that is slightly wider in the corpus callosum; there is little gross change thereafter.

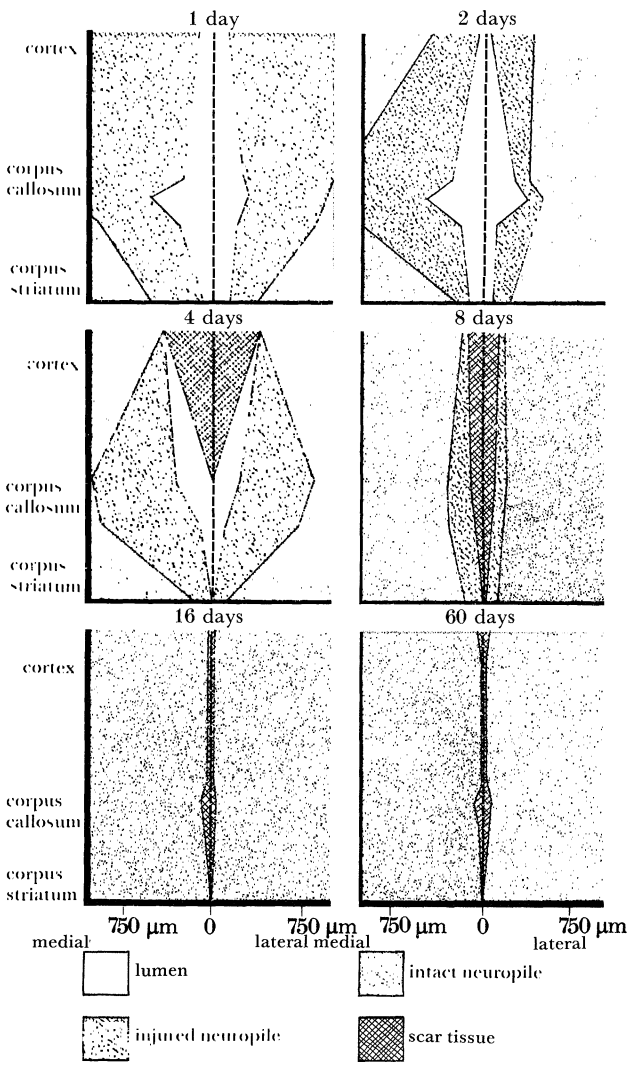

FIGURE 3. A histogram to show the widths of the lumen, injured neuropile, intact neuropile and scar tissue in the cortex, corpus callosum and corpus striatum at the different experimental times.

(*b*) *Microscopical studies of the lesioned areas*

Both the morphological and immunohistochemical observations are described here.

(i) *One- and two-day lesions* (*figures* 4 *and* 8)

Blood cells fill the lesion lumen, while the cortical area of cell swelling contains cellular debris and degenerating neurons and glia (figure 6). By two days, many monocytes lie in the cellular debris at the junction between the area of cell swelling and the intact neuropile, while near the midline the majority of the cells are macrophages. The number and distribution of reactive astrocytes, demonstrated by anti-GFAP binding, is the same as 1 day as in the control contralateral hemisphere (Mathewson & Berry 1985), but, by 2 days, the number of reactive cells near all parts of the lesion has increased. These cells, which are identified morphologically by the presence of many cytoplasmic filaments and glycogen granules (Blackwood 1976), are found peripheral to the injured neuropile at 2 days (figure 10) and their processes extend into the area of cell swelling.

Myelin figures are interspersed among erythrocytes, reactive astrocytes and cellular debris in the severed corpus callosum (figures 7 and 11), where a band of degeneration bulbs is present between 200 and 800 μm from the midline (figures 5 and 7). Around some bulbs, the myelin sheath is lost, whereas around others the sheath appears folded (figure 7). The axoplasm may either contain whorls of neurofilaments, aggregations of mitochondria and electron dense bodies, or be packed by vesicles with electron lucent contents and scattered disrupted mitochondria with large pericristal spaces. The electron dense bodies are found in the extracellular spaces of the zone of cell swelling, especially in the corpus callosum. They are between 0.2 and 0.6 μm in diameter, have a closely packed substructure (figure 9), and may be of lysosomal origin. Farther from the midline, the neuropile appears normal.

Oligodendrocytes possess the enzyme carbonic anhydrase and therefore can be distinguished by their binding of the antibody, CAII. They are present at 2 days (figure 35*c*) in the same number and distribution as in the uninjured brain.

(ii) *Four-day lesion* (*figure* 12)

A few erythrocytes are still present in the lesion lumen, particularly in the corpus callosum. The degenerating nuclei in the injured neuropile are much reduced in number and are restricted mainly to the corpus callosum, where oedema is still extensive. Monocytes are now present only at the junction of the injured and intact neuropile. Many macrophages appear in the developing scar tissue of the cortex, whereas in the corpus callosum, they extend from the scar tissue into the damaged neuropile. Scar tissue is forming between the edges of the cortical neuropile, but not in the corpus callosum or the corpus striatum. Many meningeal-derived fibroblasts, with much rough endoplasmic reticulum, are present in the cortical scar tissue (figure 15).

Reactive astrocytes are particularly numerous at the margin of the lumen (figure 14). In the cortex and corpus callosum, astrocyte processes are connected by gap junctions (figure 13). GFAP-positive astrocytes are located in the intact neuropile (figure 33*a*); few are in the zone of cell swelling. The processes of these astrocytes are preferentially orientated towards the lesion, as described by Mathewson & Berry (1985). Microglia and oligodendrocytes are found in the viable neuropile at the lesion edges, but do not extend into the oedematous region.

Although a band of degeneration bulbs persists in the corpus callosum between the intact and damaged neuropile, the first signs of regeneration are observed at 4 days. Growth cones that have a transverse diameter of 0.1 μm and contain small, electron lucent vesicles (see Kawana *et al.* 1971; Bunge 1977), are found in the debris of the area of cell swelling at the edges of the neuropile of the cortex and corpus striatum (figure 16).

Abbreviations used on figures

A	astrocyte
AC	anterior commisure
BV	blood vessels
CC	corpus callosum
DB	degeneration bulb
DC	degenerating cells
F	fibroblast
GL	glia limitans
IN	intact neuropile
L	lesion lumen
LE	leucocyte
M	macrophage
MD	midline of lesion
ME	mesenchymal cell
MI	microglia
N	neuron
NE	intact neuropile
ST	scar tissue
ad	degenerating axonal cytoplasm
ap	astrocyte process
ax	intact axon
ay	disrupted axon
b	electron dense bodies
bm	basement membrane
cf	collagen fibrils
d	post synaptic density
ds	dendritic swelling
f	glial fibrils
g	membrane ghosts
gc	growth cones
gl	glycogen granules
m	disrupted myelin sheath
mc	microtubules
mt	mitochondrion
n	neurofilaments
np	neurite process
rer	rough endoplasmic reticulum
s	synapse
sv	synaptic vesicle
ts	terminal swelling
v	vesicles

Description of plate 1

Figure 4. Diagram of a 1 day lesion to show the location of the micrographs in figures 5, 6 and 7. Key: 1, figure 6; 2, figures 5 and 7. The broken line delimits the area of damaged neuropile. AC, anterior commisure; CC, corpus callosum, MD, midline of lesion.

Figure 5. (Area 2, figure 4.) A photomicrograph to show the aggregation of degeneration bulbs (DB) within the damaged neuropile of the corpus callosum. The degeneration bulbs form a diagonal band (arrowheads). There is an area of disrupted myelin sheaths (m) on the right. To the left there is an area of intact neuropile (IN). Densely stained microglial nuclei are prominent among the degeneration bulbs. (Magn. ×470.)

Figure 6. (Area 1, figure 4.) An electron micrograph of the injured cortex. The neuropile consists of membrane ghosts (g), which may be disrupted dendritic processes, disrupted myelin sheaths (m) and scattered cytoplasmic organelles. A degenerating cell (DC) which has vacuolated mitochondria in the cytoplasm and clumped chromatin to the nucleus can be seen. (Magn. ×2650.)

Figure 7. (Area 2, figure 4.) An electron micrograph of an area in figure 5 to show the structure of the degeneration bulbs (DB). They are cytoplasmic swellings surrounded by disrupted myelin sheaths (arrows) and containing aggregations of vacuolated mitochondria (mt). An astrocyte (A) can be seen. The enlarged extracellular spaces contain membranous debris (arrowheads). (Magn. ×9050.)

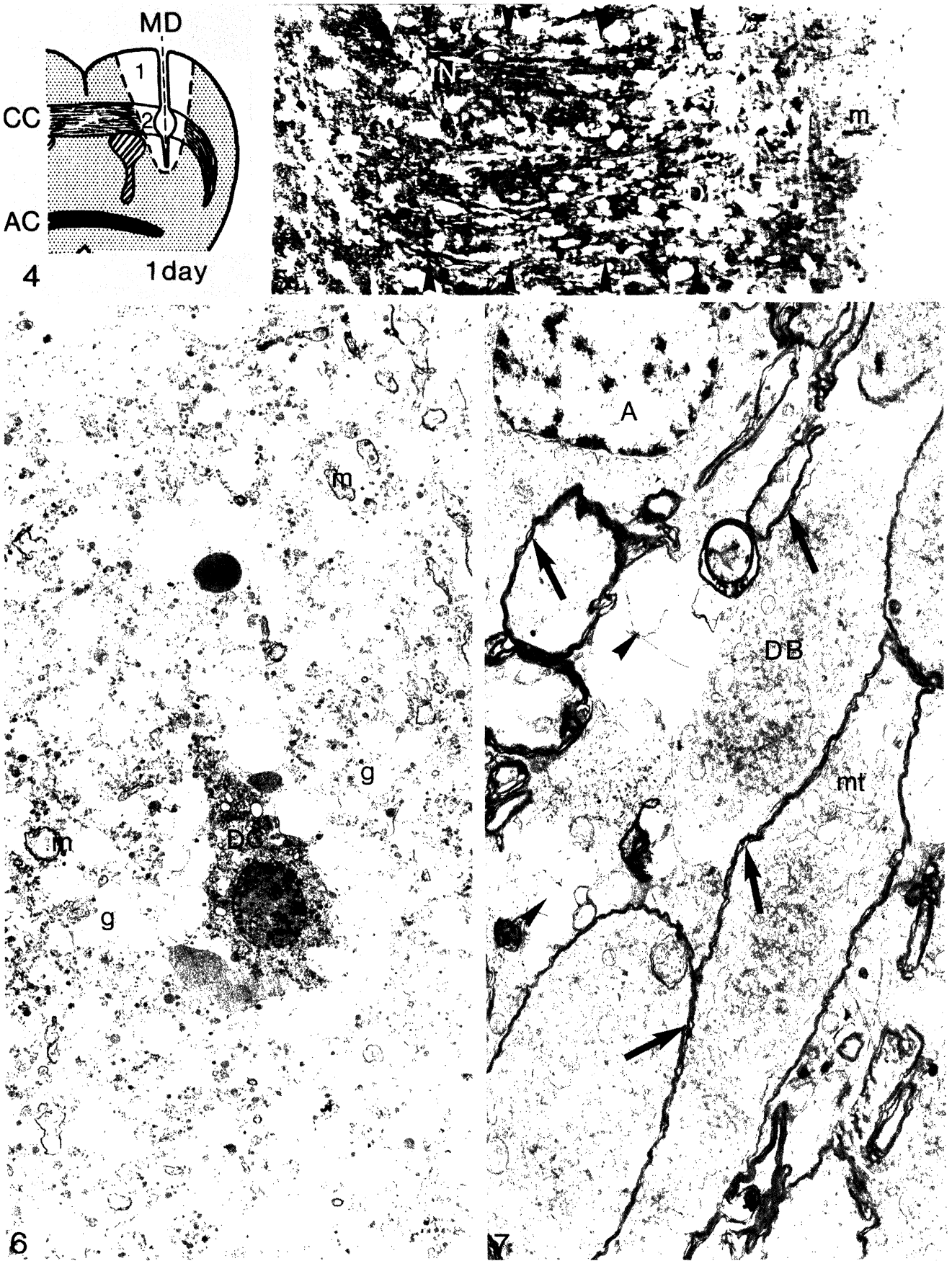

FIGURES 4–7. For description see opposite.

(*Facing p.* 486)

FIGURES 8–11. For description see facing plate 4.

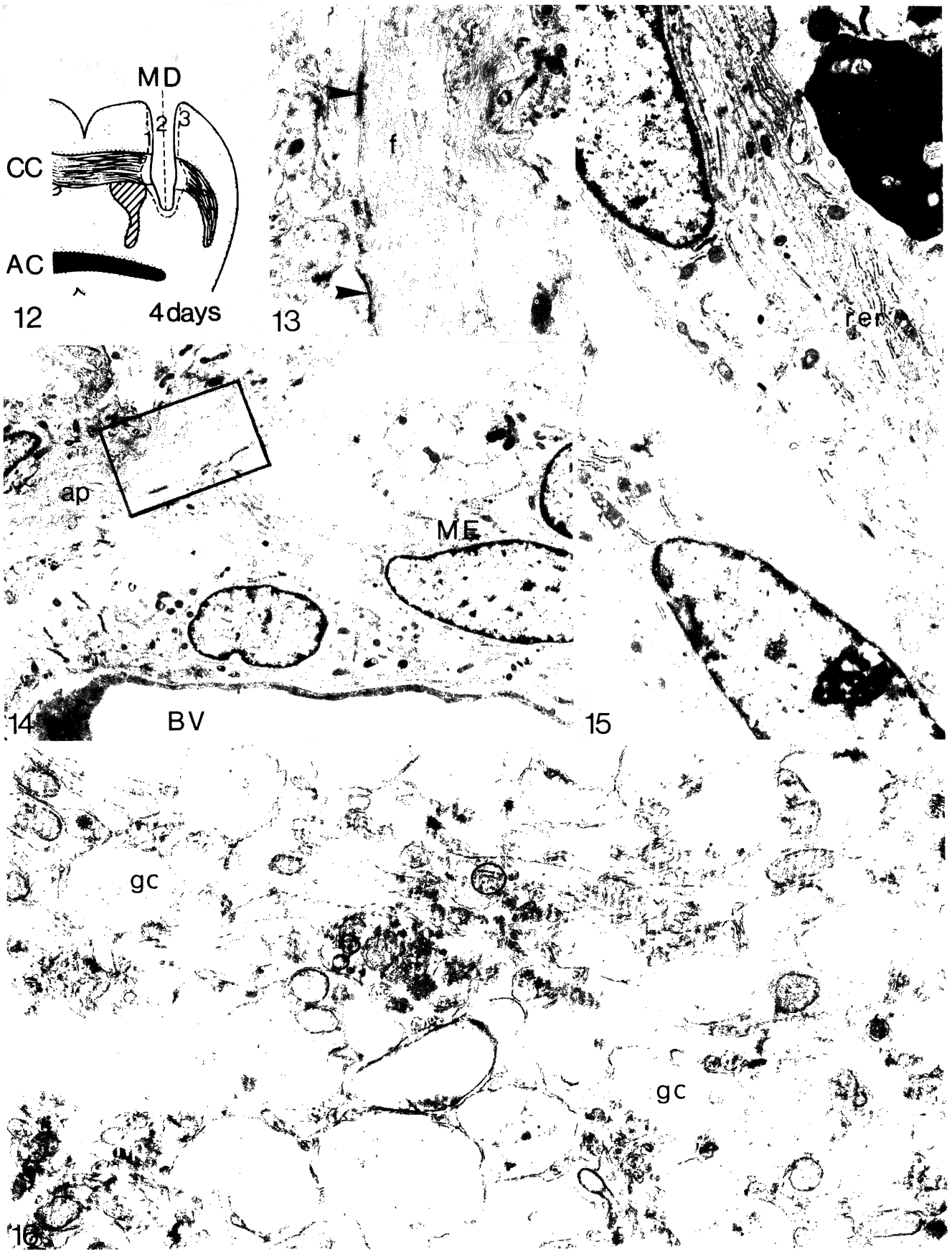

FIGURES 12–16. For description see facing plate 4.

Description of plate 2

Figure 8. A diagram of a 2 day lesion to show the location of the micrographs in figures 9 to 11. Key: 1, figures 9 and 10; 2, figure 11. The broken line delimits the area of damaged neuropile.

Figure 9. (Area 1, figure 8.) A high magnification electron micrograph of dense bodies to show their fibrous structure. (Magn. ×26300.)

Figure 10. (Area 1, figure 8.) An electron micrograph of two adjacent astrocytes (A) at the edge of the intact neuropile. In the upper astrocyte, the cytoplasm contains aggregations of rough endoplasmic reticulum (rer), whereas in the lower astrocyte it contains many glycogen granules (gl). The chromatin pattern in the lower astrocyte nucleus is suggestive of chromatin dispersal after a recent mitotic division. (Magn. ×6500.)

Figure 11. (Area 2, figure 8.) An electron micrograph of a reactive astrocyte (A) among the axons (ax) and degeneration bulbs (DB) containing dense bodies (arrowheads) (see figure 9) of the stump of the severed corpus callosum, at the junction of the intact and damaged neuropile. The astrocyte cytoplasm contains bundles of glial fibrils (f) and aggregations of glycogen granules (gl). Several processes extend from the cell body (arrow) into the enlarged extracellular space between the damaged axons and degeneration bulbs of the corpus callosum (Magn. ×6850.)

Description of plate 3

Figure 12. A diagram of a 4 day lesion to show the location of the micrographs in figures 13 to 16. Key: 1, figures 13 and 14; 2, figure 15; 3, figure 16. The broken line delimits the area of damaged neuropile.

Figure 13. (Area 1, figure 12.) A higher magnification electron micrograph of the area outlined in figure 14 to show the numerous fibrils (f) within the astrocyte processes and the gap junctions (arrowheads) between the apposed processes. (Magn. ×12000.)

Figure 14. (Area 1, figure 12.) An electron micrograph of the edge of the cicatrix in the cortex to illustrate the close apposition of mesenchymal cells (ME), blood vessels (BV) and astrocyte processes (ap) which extend from the neuropile into the body of the cicatrix. (Rectangle, figure 13; magn. ×5050.)

Figure 15. (Area 2, figure 12.) An electron micrograph of fibroblasts within the cicatrix. Their cytoplasm contains many cisternae of rough endoplasmic reticulum (rer). (Magn. ×6300.)

Figure 16. (Area 3, figure 12.) An electron micrograph to show growth cones (gc) among neurite processes (np) in the neuropile adjacent to the remaining area of cell swelling in the cortex. The growth cones contain small vesicles and a few small fibrils. Mitochondria (mt) occur in the proximal parts of the neurite processes. (Magn. ×20150.)

Description of plate 4

Figure 17. A diagram of an 8 day lesion to show the location of the micrographs in figures 18 to 21. Key: 1, figure 18: 2, figure 19; 3, figure 21; 4, figure 20. The broken line around the lesion indicates the area of damaged neuropile.

Figure 18. (Area 1, figure 17.) A low magnification electron micrograph of an area within the cicatrix in the cortex. Fibroblasts (F) and macrophages (M) are seen in a loose matrix containing collagen fibrils (cf) in different orientations. (Magn. ×5250.)

Figure 19. (Area 2, figure 17.) An electron micrograph of extraparenchymatous astrocytes (A), macrophages (M) and microglia (MI) in the cicatrix of the corpus callosum. Astrocyte processes form a network within the scar tissue; the adjacent cell processes, which contain glial filaments, are joined by gap junctions (arrows). There is no collagen in the extracellular space. (Magn. ×8100.)

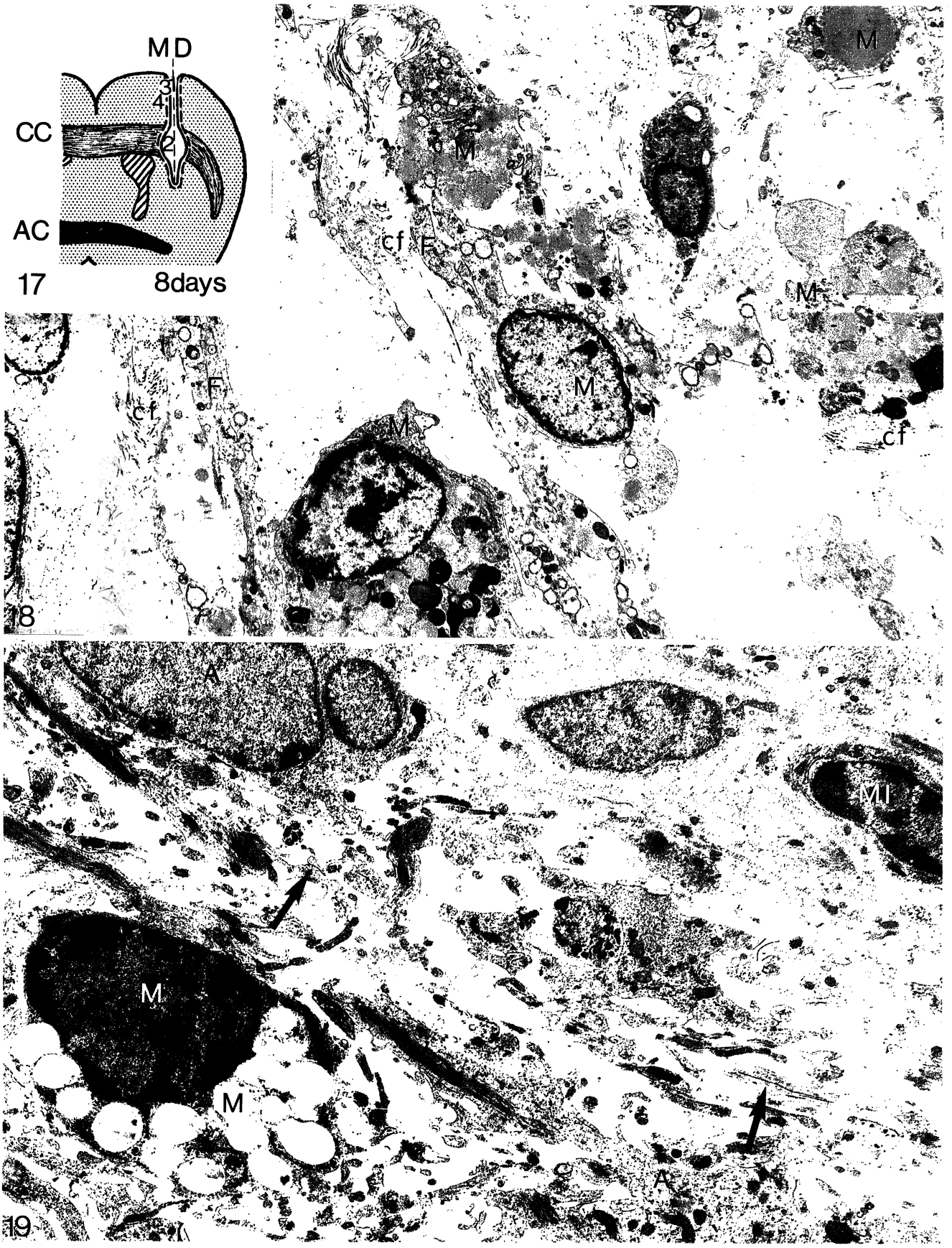

FIGURES 17–19. For description see opposite.

FIGURES 20 AND 21. For description see facing plate 7.

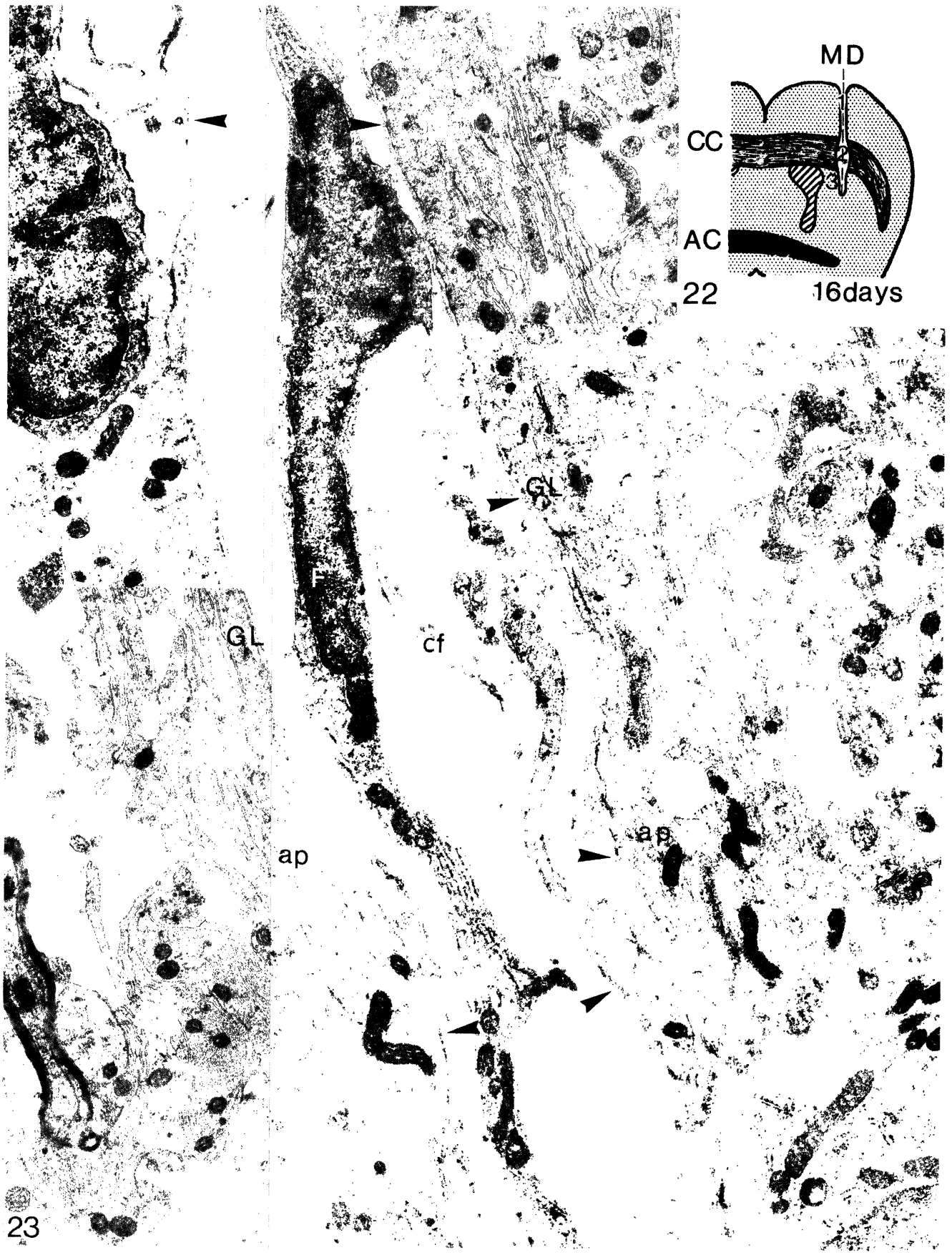

FIGURES 22 AND 23. For description see facing plate 7.

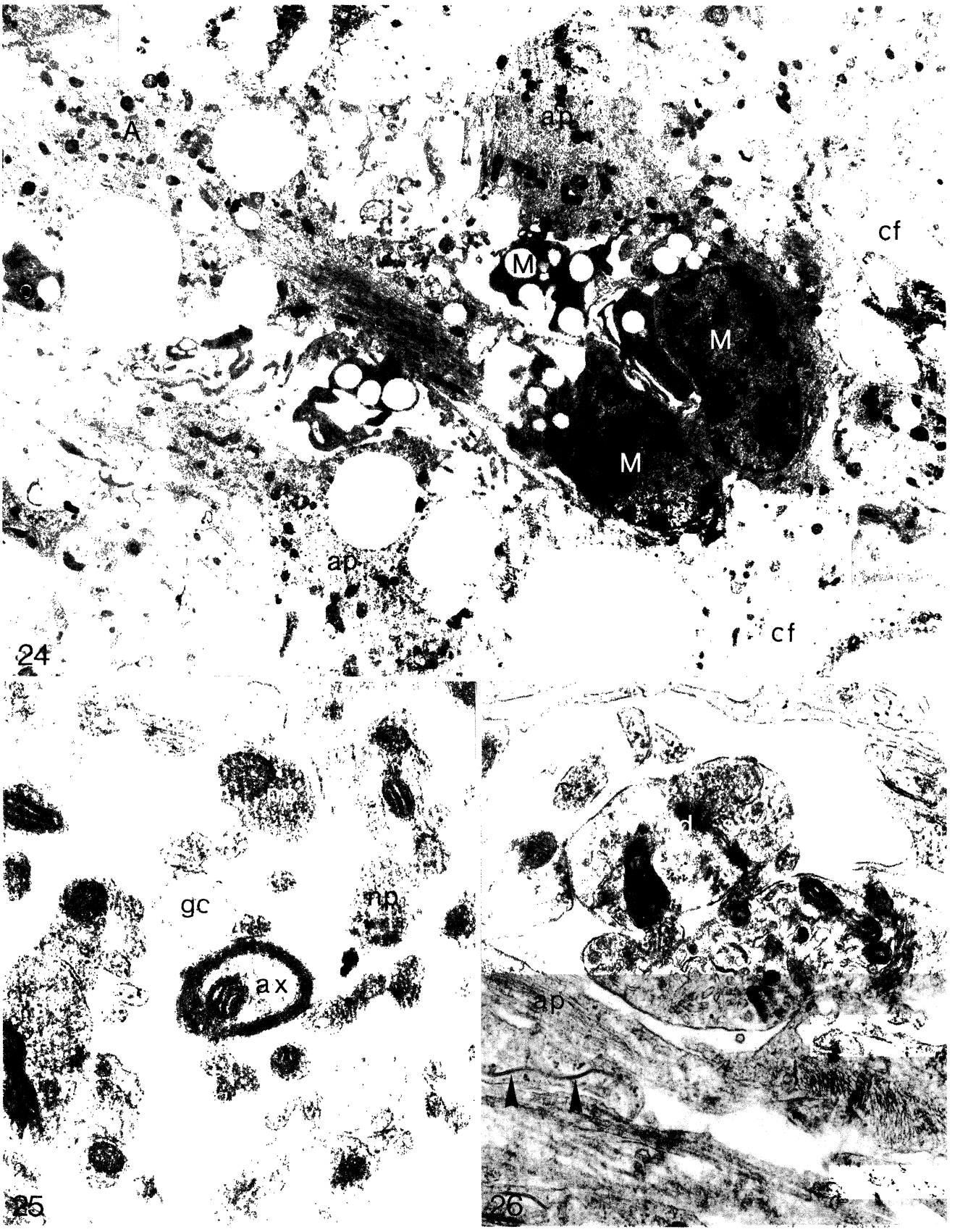

FIGURES 24–26. For description see opposite.

Description of plate 5

Figure 20. (Area 4, figure 17.) An electron micrograph of an astrocyte (A) at the margin of the neuropile bordering the scar tissue in the deep cortex. The astrocyte processes (ap) overlie groups of swollen neurite processes (np) which are the remnants of the area of cell swelling. A basement membrane covers the astrocyte layer (arrowheads). The astrocytes and basement membrane form the glia limitans. (Magn. × 8800.)

Figure 21. (Area 3, figure 17.) An electron micrograph of a growth cone (gc) in the cortical neuropile just deep to the glia limitans. The growth cone contains vesicles (v); microtubules and neurofilaments are found in its neurite process (np). Surrounding neurite processes (np) contain vesicles, mitochondria and microtubules. (Magn. × 35100.)

Description of plate 6

Figure 22. A diagram of a 16-day lesion to show the location of the micrographs in figures 23 to 26. Key: 1, figure 23; 2, figure 24; 3, figures 25 and 26.

Figure 23. (Area 1, figure 22.) An electron micrograph of the whole width of the lesion in the cortex. A fibroblast (F) in the scar tissue is surrounded by groups of collagen fibrils (cf). The glia limitans (GL) borders the lesion; it consists of astrocytes (A) and their processes (ap) containing glial fibrils, and a basement membrane (arrowheads). (Magn. × 15950.)

Description of plate 7

Figure 24. (Area 2, figure 22.) An electron micrograph of macrophages (M) and astrocyte cell processes (ap) near the midline within the lumen of the lesion in the corpus callosum. The astrocyte processes form a network throughout the lumen. A few collagen fibrils (cf) occur in the extracellular space. (Magn. × 6300.)

Figure 25. (Area 3, figure 22.) An electron micrograph of a growth cone (gc) adjacent to a myelinated axon (ax) in the corpus striatum. Neurite processes (np) are found in the extracellular space. A developing synapse (s), which lacks a post-synaptic density, but which contains spherical synaptic vesicles (sv), is present. (Magn. × 26000.)

Figure 26. (Area 3, figure 22.) An electron micrograph of neurite processes in the corpus striatum. A synapse (s) with a clear post synaptic density (d) is observed. Astrocyte processes (ap) joined by gap junctions (arrowheads), are present. (Magn. × 29500.)

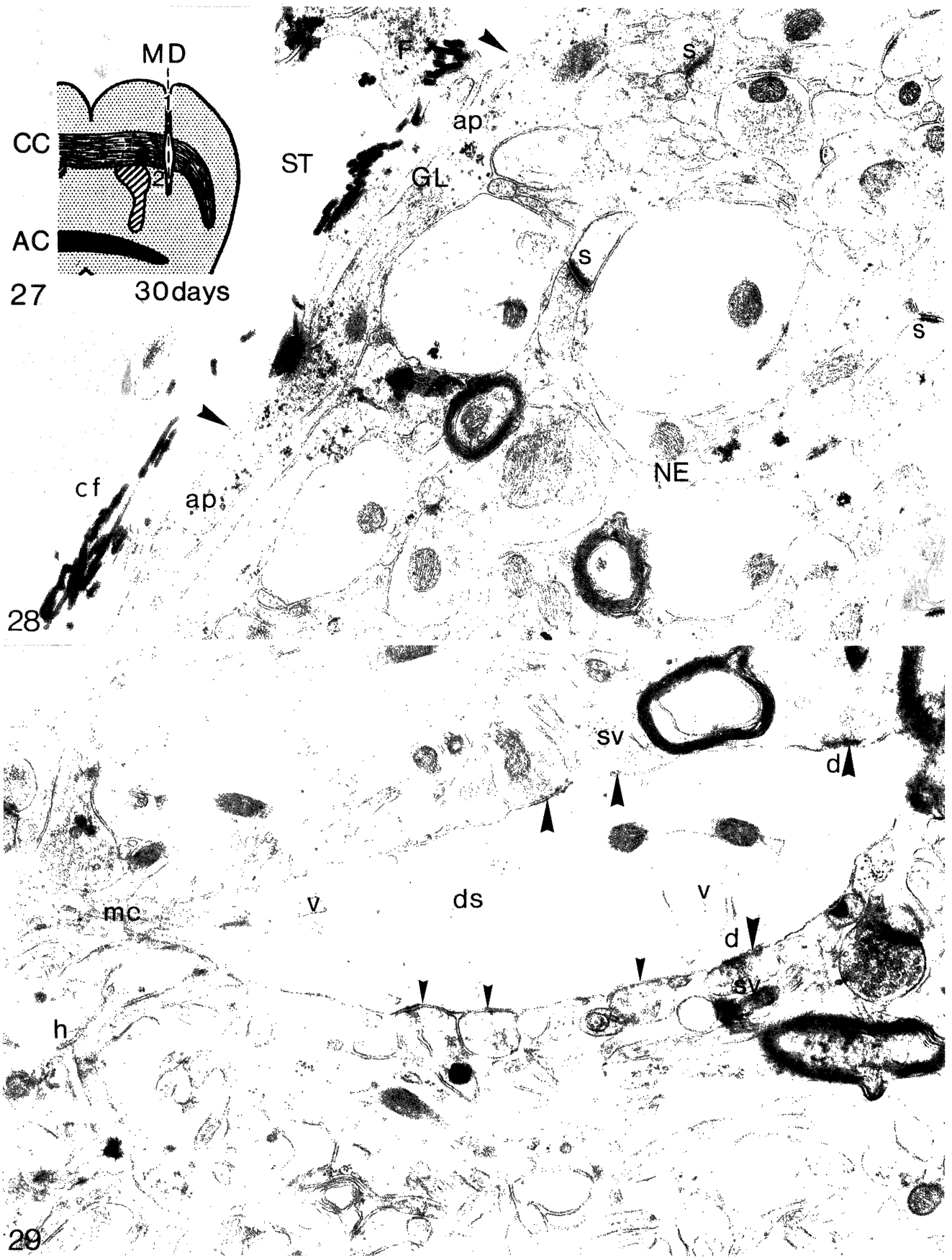

FIGURES 27–29. For description see opposite.

Description of plate 8

Figure 27. A diagram of the 30 day lesion to show the location of the micrographs in figures 28 and 29. Key: 1, figure 28; 2, figure 29.

Figure 28. (Area 1, figure 27.) An electron micrograph of the glia limitans in the cortex. The discrete glia limitans (GL) is formed by astrocyte processes (ap) and their basement membrane (arrowheads); this layer separates the scar tissue (ST) from the neuropile (NE). Fibroblasts (F) and collagen fibrils (cf) are present in the scar tissue. A large number of synapses (s) is found in the neuropile adjacent to the glia limitans. (Magn. $\times 13450$.)

Figure 29. (Area 2, figure 27.) An electron micrograph of a dendritic swelling (ds) in the neuropile near the lesion in the corpus striatum. A number of developing synapses (smaller arrowheads) can be seen on this growth cone; they contain spherical synaptic vesicles (sv), but only some (large arrowheads) possess a post-synaptic density (d). The dendritic shaft contains microtubules (mc), the swelling contains some vesicles (v). (Magn. $\times 24750$.)

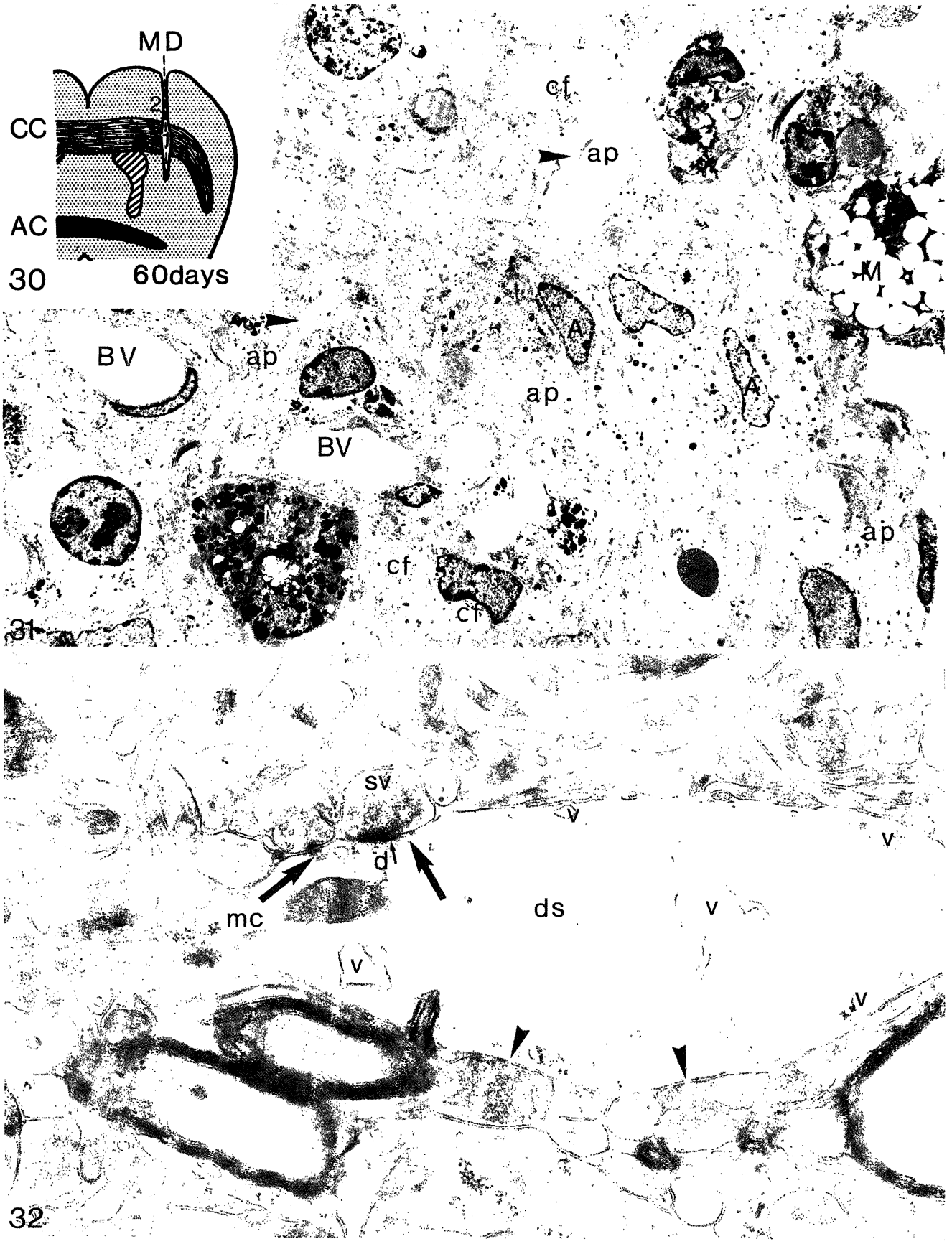

FIGURES 30–32. For description see opposite.

Description of plate 9

Figure 30. A diagram of a 60 day lesion to show the location of the micrographs in figures 31 and 32. Key: 1, figure 31; 2, figure 32.

Figure 31. (Area 1, figure 30.) A low magnification electron micrograph of the central region of the scar in the corpus callosum. Astrocytes and macrophages (M) fill this area. The astrocytes form an extensive network of cell processes (ap), which are packed with glial fibrils (arrowheads). Blood vessels (BV) permeate this network. Bundles of collagen fibrils (cf) are present in the extracellular spaces. (Magn. ×3150.)

Figure 32. (Area 2, figure 30.) An electron micrograph of a dendritic swelling (ds) in the cortical neuropile near the lesion. The dendritic shaft contains numerous microtubules (mc), but these do not extend into the swelling which contains a few vesicles (v). Different stages of synaptogenesis are seen; two synapses (arrows) have synaptic vesicles (sv) and postsynaptic densities (d), but other developing synapses (arrowheads), have synaptic vesicles, but no postsynaptic densities. (Magn. ×29350.)

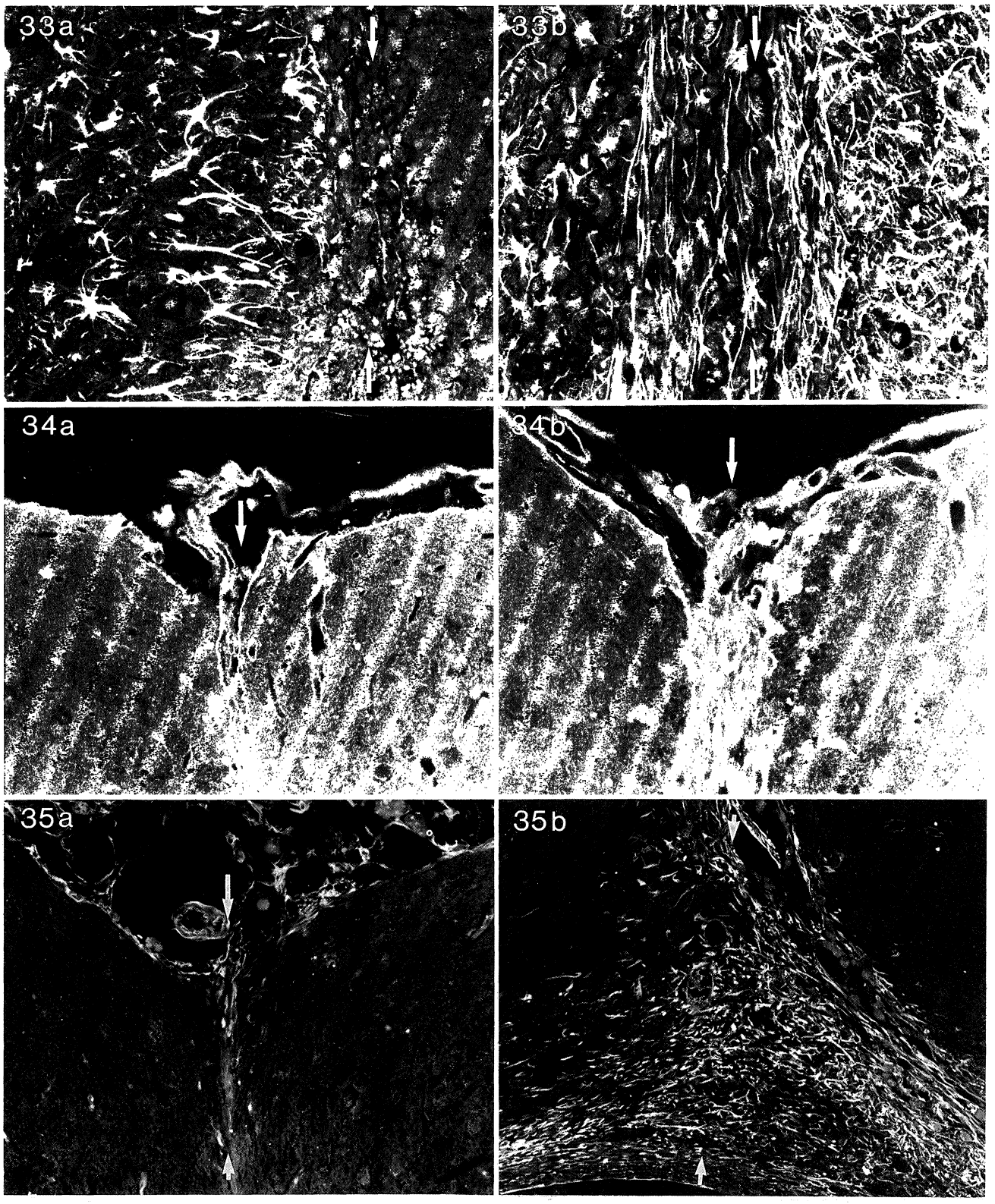

FIGURES 33*a*, *b*, 34*a*, *b* AND 35*a*, *b*. For description see p. 487.

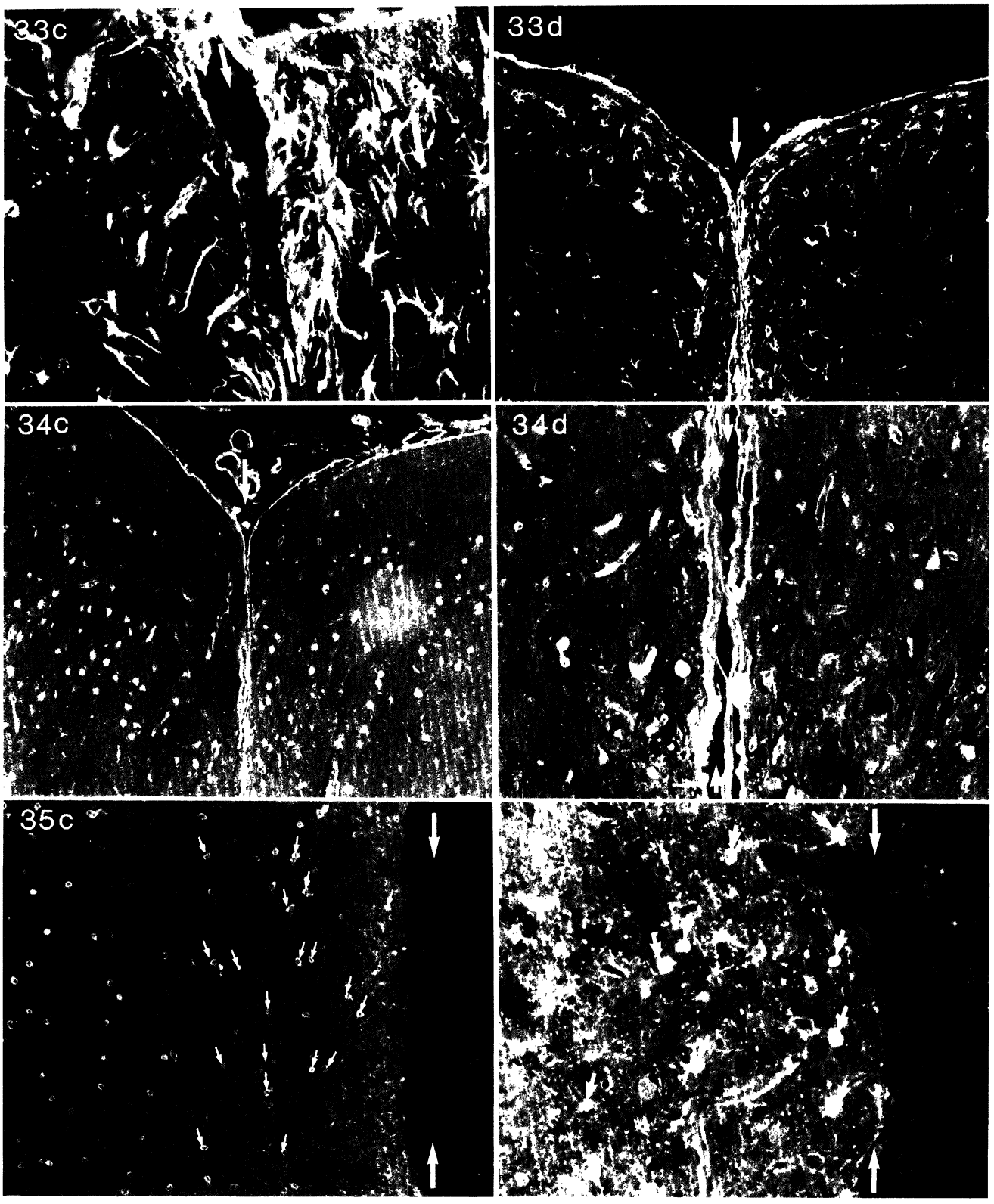

FIGURES 33*c*, *d*, 34*c*, *d* AND 35*c*, *d*. For description see p. 487.

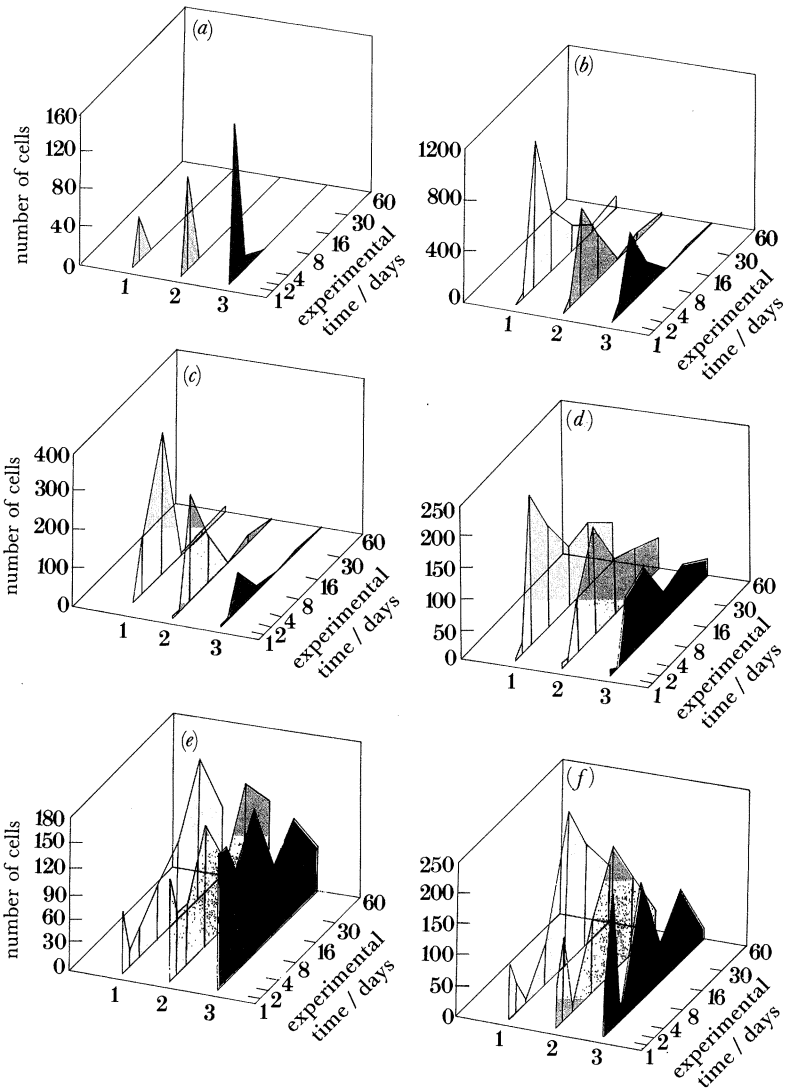

FIGURE 36. Graphs to show the numbers and distribution of the mesenchymal and glial cells associated with the lesion with increasing distance from the midline at the different experimental times. (*a*) monocytes; (*b*) macrophages; (*c*) fibroblasts; (*d*) astrocytes; (*e*) oligodendrocytes; (*f*) microglia. Key: 1, cells between midline and 100 μm on either side; 2, cells between 100 and 200 μm on either side; 3, cells between 2 and 300 μm on either side.

(iii) *Eight- to twelve-day lesions (figure* 17)

The edges of the lesion are closer together throughout the lesion; the oedema is confined to swollen neurite processes at the margins of the neuropile. Scar tissue now penetrates the full depth of the lesion (figure 3). Fibroblasts are found only within the scar tissue (figure 18). Monocytes are no longer present, but macrophages are numerous especially near the corpus callosum within loosely packed scar tissue. The collagenous extracellular matrix is extensive (figure 18). Many capillaries ramify through the scar tissue. A few extravascular erythrocytes are still seen.

Astrocytes are now found along the borders of the scar tissue in all parts of the lesion. The numbers of reactive astrocytes, demonstrated by their GFAP-binding is maximal (figure 33*b*, *c*) at this time. In the cortex, their processes extend towards the lumen and intermingle to form a compact layer that contains many processes within its thickness. A basement membrane, which is probably secreted by the astrocytes, has developed along their surface abutting the scar tissue (figure 20); this constitutes a glia limitans separating the viable neuropile from the scar tissue. That it is a true basement membrane is shown by its content of type IV collagen (Maxwell *et al.* 1984) and laminin (figure 34*a*, *b*). It is continuous with the glia limitans on the surface of the cortex. In the corpus callosum and corpus striatum, the glia limitans is not yet formed and astrocyte processes extend into the scar tissue (figure 19). The astrocytic cytoplasm contains many glial filaments and occasional lipid droplets. The glia limitans of the scar is established by 12 days, but a few astrocytes remain associated with the scar tissue to form a network of cell processes linked by gap junctions (figure 19). The cytoplasm of the extraparenchymatous astrocytes is packed with filaments; no basement membrane is found around their processes.

At 12 days, a fully developed glia limitans has been formed in the corpus callosum. The distribution of the reactive, anti-GFAP-binding cells is similar to that at 8 days.

Growth cones are most numerous at 8 days. They are seen frequently in the cortex and corpus striatum on the abluminal side of the developing glia limitans (figure 21). The neurites supporting the growth cones contain mitochondria, microtubules and neurofilaments.

Description of plates 10 and 11

Figure 33. Photomicrographs to show the binding of antibodies to GFAP by the reactive astrocytes in lesions (arrows) at different experimental times. (*a*) A 4 day lesion. The astrocyte processes are orientated towards the lesion. (*b*, *c*) An 8 day lesion. (*b*) The orientation of the astrocyte processes in the developing scar tissue in the deep cortex. (*c*) The developing glia limitans in the superficial cortex. The astrocyte reaction is maximal. (*d*) A 76 day lesion. The continuity of the glia limitans externa with that of the scar is clearly seen. There are now only a few 'reactive' astrocytes that bind anti-GFAP antibodies. (Magn. (*a–c*) ×238; (*d*) ×119.)

Figure 34. Photomicrographs to show the binding of antibodies to laminin by the basement membranes associated with lesions (arrows) at different experimental times. (*a*) An 8 day lesion. The basement membrane of the glia limitans is present only in the cortex. (*b*) A 12 day lesion. (*c*, *d*) A 76 day lesion. (Magn. (*a*, *c*) ×119; (*b*, *d*) ×238.)

Figure 35. Photomicrographs to show the binding of antibodies to vimentin and carbonic anhydrase by the cells in lesions (arrows) at different experimental times. (*a*, *b*) A 76 day lesion. Antibodies to vimentin are bound by fibroblasts in the meninges and in the lesion and also by the astrocyte processes at the pial surface. In the periventricular white matter (*b*), the astrocytes in the corpus callosum and adjacent lesion bind the antibody very strongly. (*c*) A 2-day lesion and (*d*) 16-day lesion to show the binding of antibodies to carbonic anhydrase by the oligodendrocyts (small arrows). (Magn. (*a–c*) ×119; (*d*) ×238.)

(iv) *Sixteen- to sixty-day lesions* (*figures* 22, 27 *and* 30)

By 16 days, most of the scar tissue has contracted, so bringing the borders of the neuropile close together except in the corpus callosum. In the cortex, the fibrous tissue contains a few fibroblasts and macrophages (figures 23 and 28). In the corpus callosum, the scar tissue is wider and contains extraparenchymatous astrocytes which intermingle with the mesenchymal cells (figures 24 and 31); these astrocytes do not form a basement membrane. Throughout the remainder of the experimental period, this organization of the scar is maintained, despite some reduction in width. Some macrophages are still present within the neuropile of the corpus callosum at 16 days.

A fully developed glia limitans is present in the corpus callosum at 16 days, whereas in the corpus striatum it is still incomplete. At 30 days, the scar tissue and neuropile are separated by a glia limitans throughout the depth of the lesion. The scar tissue contracts so that from 30 days onwards it consists of a thin layer of fibrous tissue with a few macrophages and fibroblasts, bounded by the basement membranes of the opposing layers of astrocytes. The continuity of the basement membrane throughout the lesion is shown by the anti-laminin antibody (figure 34*c*, *d*). GFAP-positive astrocytes are now restricted to the glia limitans (figure 33*d*), except in the corpus callosum where reactive cells are found along the fibre tract into the subcortical white matter.

None of the cells in the lesion binds the antibody to vimentin until 16 days. From this time onwards it is bound by the reactive astrocytes (figure 35*a*, *b*). Fibroblasts contain vimentin filaments, but the immunofluorescent results with the fibroblasts in the lesion were inconsistent.

Few growth cones are found in the neuropile of the cortex and corpus striatum during this experimental period, although many neurite processes are present in the neuropile adjacent to the glia limitans. Many of these processes contain empty vesicular inclusions and filaments, but others, in which post-synaptic densities have either not developed (figure 25), or are forming (figure 26), may represent stages in synaptogenesis. From 30 days onwards, both mature and developing synapses are numerous in the neuropile of the cortex bordering the lesion (figure 32), but in the corpus striatum, developing synapses predominate (figure 29). Post-synaptic densities are present in some of the synapses on dendritic swellings; in others, post-synaptic densities are absent (figures 29 and 32). These swellings may be either varicosities along the shafts of dendrites, or dendritic growth cones (see Discussion, *a*(ii)). In the corpus callosum, myelinated axons are now found juxtaposed to the scar tissue.

The distribution of oligodendrocytes, as shown by their binding of the antibody to carbonic anhydrase (CAII), is similar to that at 2 days (compare figure 35*c*, *d*).

(*c*) *Quantitative analysis of the distribution of the cells*

The total numbers of different cells within 0–100 μm, 100–200 μm and 200–300 μm from the midline of the lesion are shown graphically in figure 36*a–f*.

Monocytes and macrophages (figure 36*a*, *b*) appear at 2 days. By 4 days, the number of monocytes is reduced dramatically, whereas the number of macrophages has increased sixfold. Comparison of figure 36*a* with figure 3 shows that at 2 and 4 days most of the monocytes are found in the injured neuropile and not in the lumen; there are no monocytes at 8 days. Between 9 and 30 days, the total number of macrophages is reduced to less than 10% of that

at 4 days and remains at this level (figure 36*b*). Macrophages are least numerous near the midline at 2 days, but, in contrast, by 4 days and after, nearly half the total number is near the midline. At 60 days, most of the macrophages are found in the scar tissue formed by the meninges penetrating the superficial cortex (figure 36*b*).

The fibroblasts recorded at 1 and 2 days are those in the intact meninges; their number rises very rapidly to reach its maximum at 4 days as they invade the lesion (figure 36*c*). By 8 days, there is both a reduction in fibroblast number in the cortical area of the lesion, and a rise near the corpus callosum. By 16 days onwards, the few remaining fibroblasts are in the scar tissue near the midline of the lesion (figure 36*c*). Most of the original population of astrocytes has degenerated by 2 days, but by 4 days, is replaced by a larger population of reactive astrocytes. As the glia limitans forms and matures, the numbers of astrocytes drop. Most of the reactive astrocytes are found in the neuropile at the lesion edge (figure 36*d*).

Although there is both spatial and temporal variation in the number of oligodendrocytes (figure 36*e*), there is an overall reduction in their number by the end of the experimental period. The initial large population of microglia doubles by day 2. The reduction on day 4 is followed by a replenishment and subsequent slow reduction to 60 days (figure 36*f*).

Discussion

The purpose of this study was to investigate, qualitatively and quantitatively, the response of the cerebral hemisphere to a penetrant knife lesion. To quantify the cellular changes, the numbers of glial and mesenchymal cells at increasing distances from one lesion only at each experimental time were estimated; Illis (1973*b*) and Imamoto & Leblond (1977) used similarly small samples. The use of only one animal at each experimental time can clearly be criticized. We consider, however, that the results give an acceptable indication of the changes in the numbers of the different cells associated with the lesion during healing. Parnavelas *et al.* (1983) have shown that variation is small between animals of the same age that are within 15% of the mean mass of the litter. The masses of the rats used for the analysis were well within this range, because the litter size was reduced at birth to five animals.

(*a*) *The reactions of neurons to injury*

(i) *Perikarya*

Ultrastructural evidence for cell death is seen in the zone of cell swelling. No axonal reaction of 'dark' or 'light' neuronal degeneration is observed either in commissural, corticofugal or association neurons distant from the lesion (Barron *et al.* 1973; Blackwood 1976; Cox 1976; Torvik & Soreide 1972). The failure of many CNS neurons to exhibit an axotomy reaction is well recognized (see reviews by Barron (1983) and Lieberman (1971)) and has been attributed to an abundance of undamaged collateral axons which maintain the viability of the neurons (Startzl & Magoun 1951).

(ii) *Axons and dendrites*

Between 1 and 8 days, degeneration bulbs (also called retraction balls (Gennarelli *et al.* 1982) or reactive swellings (Povlishock 1986)) are found in the cerebrum on both proximal and distal axonal stumps; a similar observation was made in the spinal cord by Kao *et al.* (1977*a*).

The dendrites in the zone of cell swelling in the cortex are represented by empty membrane ghosts, which suggests that damaged dendrites do not form retraction or degeneration bulbs similar to those of severed axons.

Growth cones may be axonal or dendritic (Skoff & Hamburger 1974; Vaughn *et al.* 1974). Axonal growth cones are attenuated with thin filopodia. They contain a dense cytoplasmic matrix with numerous neurofilaments, but the few microtubules are confined to the proximal pole. Axonal growth cones are occasionally presynaptic, but rarely postsynaptic. In contrast, dendritic growth cones are bulbous structures that may be located either distally or interstitially (Bunge 1973; del Cerro & Snider 1968; Grainger & James 1970). The cytoplasm is electron lucent and contains vesicles of varying size, neurofilaments and occasional microtubules. Dendritic growth cones are frequently postsynaptic.

It is difficult to classify the growth cones seen before 16 days as axonal or dendritic. In the later stages of healing, dendritic swellings are observed, which could be either varicosities, or true interstitial or terminal growth cones; they are engaged by presynaptic swellings. A feature that favours their identification as growth cones is that the synapses proximal to the observed dendrites are more mature than those situated more distally (Skoff & Hamburger 1974; Vaughn *et al.* 1974).

Dendritic regeneration may, therefore, occur in the mature rat CNS, but the growing dendritic processes fail to cross the lesion. Bernstein & Bernstein (1973*b*, 1977*a*, *b*) observed dendritic sprouting and the re-establishment of dendritic fields and axo-dendritic synapses after spinal lesions in the rat.

(iii) *Synaptogenesis*

The formation of synapses on the growth cones of regenerating dendrites described here is similar to synaptogenesis on growing dendrites in the normally developing chick and mouse spinal cords observed by Skoff & Hamburger (1974) and Vaughn *et al.* (1974). They also reported that developing synaptic contacts first appear on the most distal parts of the growth cones and as the growing point of the cone advances through the neuropile, the maturing synapses are displaced to a more proximal position on the dendritic shaft. Synaptic plasticity is a recognized feature of the injury response of the nervous system, but its magnitude varies in different regions (Berry 1983, 1985; Field *et al.* 1980; Goldberger & Murray 1974; Guillery 1972; Hoff *et al.* 1981*a*, *b*; Kerr 1972; Lund & Lund 1971; Matthews *et al.* 1976; Raisman & Field 1973; Tripp & Wells 1978; Vaughan & Foundas 1982). The newly formed synapses observed in the lesions described here are all type I asymmetrical synapses containing round vesicles similar to those in the dentate gyrus (Matthews *et al.* 1976). No synapses containing abnormal proportions of oval vesicles were seen in the present study like those observed by Bernstein & Bernstein (1977*a*), Lund & Lund (1971) and Westrum & Black (1971). The presynaptic elements may be either collateral sprouts of uninjured axons (Bernstein 1970; Bernstein & Bernstein 1971; Illis 1973*a*; Raisman & Field 1973), or regenerating axons that invade the lesion edge during abortive growth (Bernstein 1970; Bernstein & Bernstein 1969, 1971, 1973*b*; Ramon y Cajal 1928). Bizarre synapses, such as those seen by Bernstein & Bernstein (1973*a*, *b*, 1977*a*, *b*) and Raisman & Field (1973) are not present in the injured cerebral cortex of the mature rat.

(*b*) *The reactions of the neuroglia*

(i) *Astrocytes*

Fibrous and protoplasmic astrocytes differ in their morphology, ontogeny, biochemistry and distribution (Miller & Raff 1984). The relationship between these astrocytes and type-1 and type-2 astrocytes in the optic nerve is uncertain (Raff *et al.* 1983), although in the optic nerve, it is suggested that type-1, but not type-2, astrocytes react to injury (Miller *et al.* 1986). In the cortex, however, both fibrous and protoplasmic astrocytes respond locally and within the entire hemisphere (Berry 1979; Colmant 1968; Krikorian *et al.* 1981; Latov *et al.* 1979; Mathewson & Berry 1985; Murabe & Sano 1981; Murabe *et al.* 1981; Takamiya *et al.* 1988). Our estimates of the numbers of astrocytes in the wound area show a rapid decline which could be due to perivascular astrocytic degeneration as observed in other types of brain injury (Allen *et al.* 1983; Maxwell *et al.* 1988). Near the site of the initial incision the astrocyte nuclei become pyknotic and their cytoplasmic processes break up into vesicles, which Alzheimer (1910) called 'filling bodies'. Many mitotic astrocytes are found near wounds in mature rat brains especially 2–3 days after injury (Al-Ali & Robinson 1982; Cavanagh 1970; Cavanagh & Lewis 1969; Fugita *et al.* 1981). Takamiya *et al.* (1988) have shown that mitoses of reactive astrocytes are confined to the molecular layer and subcortical white matter and that increases in their number in layers II to VI is by migration from these sources; this might explain the absence of mitotic figures in the cortex in this study. Migration of astrocytes has also been observed around neonatal hippocampal transplants in adult host brain (Lawrence *et al.* 1984). The astrocytes seen in the present experiments contain increased amounts of glycogen (Al-Ali & Robinson 1982; Bignami & Ralston 1969; Colmant 1968), and also of filamentous material, which is correlated with the presence of increased amounts of glial fibrillar acidic protein (Bignami & Dahl 1976; Mathewson & Berry 1985).

From 4 days onwards, thin astrocytic processes insinuate within the neuropile and scar tissue, to form a layer, or sheet, of cell processes held together by gap junctions; this 'cytoplasmic sheet' reaction (Cox 1976; Torvik & Soreide 1972) is maximal in the cortex at 8 days, and is complete in the corpus striatum by 30 days. This layer of linked astrocyte processes and their associated basement membranes comprise the glia limitans, which separates the mesenchymal from the neuroectodermal tissues. A few astrocytes, without a basement membrane, are isolated within the mesenchymal scar tissue.

(ii) *Oligodendroglia*

Although there are some reports that oligodendroglia have an active role after injury (Cook & Wisniewski 1973; Illis 1973*b*; Ludwin 1984, 1985; Ludwin & Bakker 1988), other authors report a lack of response (Bignami & Ralston 1969; Imamoto & Leblond 1977; Matthews & Kruger 1973; Murabe *et al.* 1981; Vaughn & Pease 1970). In this study, neither qualitative, nor quantitative, changes in the oligodendroglia were observed which suggests that a stable population survives intact in the injured CNS despite retrograde and anterograde degeneration of axons and perikarya. Caroni & Schwab (1988) and Schnell & Schwab (1990) have evidence that a protein which is extracted from myelin and which binds to the surface of oligodendrocytes, is a non-permissive substrate for neurite growth both *in vivo* and *in vitro* (see also review by Chiquet (1989)). The few unreactive oligodendrocytes in the injured unmyelinated cerebral cortex would be unlikely to provide a sufficient area of non-permissive

substrate to account for the total failure of axonal regeneration and neurite outgrowth observed in the present study. Axons presented with a choice between permissive and non-permissive substrates will continue to grow over the former, but not the latter (Carbonnetto *et al.* 1987; Caroni & Schwab 1988; Fawcett *et al.* 1989; Schwab & Thoenen 1985); this choice is present in the cerebral cortex yet axons fail to regenerate.

(*c*) *Cerebral necrosis*

The zone of cell swelling that develops in the first 24 h probably has a vasogenic and cytotoxic ischaemic aetiology (Klatzo 1985). The vasogenic oedema may be mediated primarily by the positive osmotic pressure of the extravasated blood (Aarabi & Long 1979). Both the capillary hydrostatic pressure and the hydraulic conductivity of the damaged tissue (Fenstermacher & Patlak 1976) are involved and may be accentuated by a transient rise in arterial pressure immediately after mechanical injury (Wei *et al.* 1980). The cytotoxic oedema, which is more pronounced in grey matter than in white matter, is caused by a disruption of osmoregulation in the cerebral microvasculature (Aarabi & Long 1979; DeWitt *et al.* 1986; Maxwell *et al.* 1988; Povlishock 1986; Wei *et al.* 1980). After 1–2 days, oedema appears in the white matter probably because of an influx of plasma and tissue fluid. Astrocytes initially respond within 30 min to extravasated material by swelling (Barron *et al.* 1988; Maxwell *et al.* 1988); later they become intensely GFAP-positive and migrate from the surrounding viable neuropile to the border of the necrotic tissue where they enter the developing scar tissue (Allen *et al.* 1983; Maxwell *et al.* 1988). After the removal of the necrotic tissue over the first 8 days after injury, astrocytes begin to form the glia limitans.

(*d*) *The reactions of the mesenchyme*

(i) *Monocytes*

Between 2 and 4 days monocytes migrate into the damaged brain tissue probably from the blood (Imamoto & Leblond 1977). Their disappearance between 4 and 8 days is correlated with an increase in the number of macrophages; this supports the evidence that monocytes may differentiate into macrophages (Kaur *et al.* 1987; Schelper & Adrian 1986; Volkman & Gowans 1965). This monocytic reaction is similar to that reported by Imamoto & Leblond (1977).

(ii) *Macrophages*

The proportion of macrophages in the total mesenchymal cell population of the lesion is estimated as 76% at 4 days, 47% at 8 days and 22% at 16 days; again these changes are similar to those reported by Imamoto & Leblond (1977). At least 50 secretory products of macrophages have been described and classified into functional groups (Nathan & Cohn 1980; Nathan *et al.* 1980). These include proteinases, such as collagenase and elastase, that may be implicated in CNS scarring, because they promote the further accumulation of macrophages (Nathan *et al.* 1980). Macrophages appear before fibroblasts in all areas of the lesion which suggests that the fibroblast growth factor produced by macrophages may be active (Leibovich & Ross 1975, 1976; Simpson & Ross 1972; Stein & Levenson 1966). There is no evidence for the secretion by macrophages of factors that directly stimulate or inhibit neurite outgrowth, but several enzymes secreted by macrophages may be inimical to neurite outgrowth and

account for the few axonal growth cones observed in the lesions. The neutral proteinases, for example, may disrupt the extracellular matrix and prevent axonal guidance, whereas acid hydrolases induce chronic inflammatory lesions *in vivo* (Davies & Allison 1976). The possible role of the matrix is discussed later.

(iii) *Microglia*

The percentage of microglia among the mesenchymal cell population is about 6% at 4 days, but it rises gradually to about 78% from 16 days onwards. These changes are similar to those described by Imamoto & Leblond (1977), although the size of the population in the present study is larger.

The three possible sources of microglia in the wound are migrating endogenous microglia, or transforming monocytes or macrophages (Imamoto & Leblond 1977; Perry *et al.* 1985; Streit & Kreutzberg 1987). Activation of microglia occurs more readily in closed than open wounds (Blakemore 1975; Kerns & Hinsman 1973; Skoff 1975; Torvik 1975; Vaughn & Skoff 1972). Although monocytes are rare in the area of the lesion when microglia become numerous, a few monocytes may, nevertheless, transform into microglia over the first few days after the lesion is made (Adrian & Williams 1973; Imamoto & Leblond 1977). Recently, a variety of immunocytochemical markers have been used to distinguish true microglia from haematogenous macrophages derived from the monocyte cell line (Kaur *et al.* 1987; Perry *et al.* 1985; Schelper & Adrian 1980, 1986). In the present study, specific antibody markers were not used to make this distinction. The decrease in the number of macrophages, reported here, occurs simultaneously with the rise in the number of microglia, which suggests that some macrophages may transform to become microglia-like (Kaur *et al.* 1987). The proposal that microglia react rapidly to injury by hyperplasia (Cammermeyer 1970) and are actively phagocytic in lesions, is not supported by our results or by those of other workers (Bignami & Ralston 1969; Imamoto & Leblond 1977; Kaur *et al.* 1987; Matthews & Kruger 1973; Murabe *et al.* 1981; Schelper & Adrian 1986).

(iv) *Fibroblasts*

Fibroblasts are not normally present in the CNS. The fibroblasts associated with the lesion described in this paper appear to migrate from the superficial to the deep parts of the lesion and this supports the suggestion that they originate in the meninges (Carbonell & Boya 1988). Krikorian *et al.* (1981) suggest that in lesions of the spinal cord fibroblasts arise from mesenchymal cells in the overlying bone and muscle, but their evidence is equivocal. The migration of the fibroblasts into the lesion may be under the influence of brain and macrophage-derived fibroblast-growth-factors released in the wound (Berry *et al.* 1983; Gospodarowicz 1974; Logan *et al.* 1985; Nathan & Cohn 1980). It has been suggested that wound closure is effected by a force generated by modified fibroblasts or myofibroblasts within granulation tissue (Madden *et al.* 1974). More recent evidence, however, suggests that contraction occurs before fibroblasts develop stress fibres and become myofibroblasts, and that a matrix rich in type III collagen contracts more readily than one with little type III collagen (Ehrlich 1988).

(v) *Extracellular matrix*

That an extracellular matrix is essential for morphogenetic movements is well established (Hay 1981; Toole 1981). The directional growth of neurites in the developing eye and peripheral nervous system may be determined by similar interactions between the growth cones and matrices (Ebendal 1977; Krayanek & Goldberg 1981; Lofberg *et al.* 1980).

The only extracellular matrices containing fibrous collagen present within the uninjured brain and spinal cord are those associated with the blood vessels (Shellswell *et al.* 1979). Thus the development of scar tissue along the line of the lesion is an intrusion of collagenous connective tissue into the brain. The scar tissue matrix contains both type I and type III collagen fibrils (Maxwell *et al.* 1984). Attempts to characterize the glycosaminoglycans in the fibrous tissue of the scar yielded inconclusive results, because histochemical methods using the dye, Alcian Blue, proved insufficiently sensitive to characterize the small amounts of glycosaminoglycans present unequivocally (W. L. Maxwell & D. E. Ashhurst, unpublished observations). The results obtained, however, suggest that a sulphated glycosaminoglycan, probably chondroitin sulphate, and hyaluronan are present.

The mature scar tissue is separated from the nervous tissue by a basement membrane that is secreted by the astrocytes of the new glia limitans. This basement membrane contains laminin and type IV collagen; some type V collagen is also associated with it (Maxwell *et al.* 1984). Astrocytes can synthesize type IV collagen, glycosaminoglycans and laminin (Bernstein *et al.* 1985; Blakemore 1976; Dayan *et al.* 1982; Lewis & Lampert 1977; Liesi *et al.* 1984; Sandback *et al.* 1980). The cellular interactions that influence the synthesis of extracellular matrix macromolecules in the CNS are still unclear. Fibroblasts may induce astrocytes to produce basement membranes as at other epithelial–mesenchymal interfaces (Bernfield & Banerjee 1978; Banerjee *et al.* 1977; Bluemink *et al.* 1976; Lyser 1972; Sievers *et al.* 1981; Watson 1976).

Recently, attention has focused on the role of laminin in the injury response because neurite outgrowth from chick and mouse retinal cells, and both peripheral and central neurons *in vitro*, is greatly enhanced if the cells are cultured on a substratum containing laminin or poly-L-lysine, in contrast to fibronectin or type IV collagen (Adler *et al.* 1985; Johnson *et al.* 1988; Rogers *et al.* 1983; Smalheiser *et al.* 1984). Punctate deposits of laminin were detected in the optic fibre pathway during pioneering axonal growth (Cohen *et al.* 1986, 1987; Letourneau *et al.* 1988; McLoon *et al.* 1988). Laminin, other than that in the basement membranes, was not detected in the healing adult cerebrum. Laminin is not essential, however, for the growth of adult mammalian ganglion cell axons *in vitro* and *in vivo* (Giftochristos & David 1988; Johnson *et al.* 1988).

The mature scar, with its dense connective tissue bordered by the glia limitans, is an obvious barrier to axonal growth. Because this barrier matures after the peak time period of growth cone development, it may be that deficiencies in the extracellular environment of the growing neurites restrict their growth so that they reach the scar tissue after the barrier is formed.

(*e*) *Conclusions*

The acute haemorrhagic response to injury of the cerebrum is accompanied by ischaemic necrosis along the boundaries of the wound which become oedematous. By 4 days, large numbers of macrophages have invaded the necrotic tissue, most of which is removed by 8 days.

Fibroblasts also appear in the core of the lesion by 4 days, replacing thrombus and depositing collagen fibrils. Initial fibroblast invasion is into the most superficial subpial regions of the wound and organization of the scar proceeds, with time, reaching the depths of the lesion by 8 days. The development of a glia limitans starts at 8 days, and by 16 days it separates the fibroblasts and macrophages occupying the centre of the lesion from the surrounding neuropile. Some astrocytes are trapped in this mesenchymal tissue, where they are still seen at 60 days; these cells do not produce a basement membrane. Subsequent changes in the scar after the eighth day are those of wound contraction and reductions in the numbers of mesenchymal cells.

Degenerating neural elements are plentiful in the neuropile about the wound in the acute period, but have largely disappeared by 8 days. The appearance of growth cones at 4 days heralds the first sign of neural regeneration. Growth cones become more abundant at 8 days. By 16 days synaptogenesis on dendritic swellings is observed. Thus the reorganization of the damaged neuropile involves the growth of neurites which ultimately form new synaptic contacts.

This research was supported by a grant from the Nuffield Foundation. We are grateful to Mrs M. Coulton for her patience in the preparation of the manuscript, to Mr M. N'Jai for technical assistance, and to Miss Y. S. Bland, Mr K. Fitzpatrick and Miss S. Smith, for help in the preparation of the figures.

References

Aarabi, B. & Long, D. M. 1979 Dynamics of cerebral edema. The role of an intact vascular bed in the production and propagation of vasogenic brain edema. *J. Neurosurg.* **51**, 779–784.

Abercrombie, M. 1946 Estimation of nuclear populations from microtomic sections. *Anat. Rec.* **94**, 239–247.

Adler, R., Jerdan, J. & Hewitt, A. T. 1985 Responses of cultured neural retinal cells to substratum-bound laminin and other extracellular matrix molecules. *Devl Biol.* **112**, 100–114.

Adrian, E. K. & Williams, M. G. 1973 Cell proliferation in injured spinal cord. An electron microscope study. *J. Comp. Neurol.* **151**, 1–24.

Al-Ali, S. Y. A. & Robinson, N. 1982 Brain phagocytes: source of high acid phosphatase activity. *Am. J. Path.* **107**, 51–58.

Allen, I. V., Kirk, J., Maynard, R. L., Cooper, G. K., Scott, R. & Crockard, A. 1983 An ultrastructural study of experimental high velocity penetrating head injury. *Acta Neuropathol.* **59**, 277–282.

Alzheimer, A. 1910 Beiträge zur Kenntnis der pathologischen Neuroglia und ihrer Beziehungen zu den Abbauvorgängen. *Nervengewebe* **3**, 401–554.

Bakay, L. 1968 Changes in barrier effect in pathological states. *Prog. Brain Res.* **29**, 315–339.

Banerjee, S. D., Cohn, R. H. & Bernfield, M. R. 1977 Basal lamina of embryonic salivary epithelia. Production by the epithelium and role in maintaining lobular morphology. *J. Cell Biol.* **73**, 445–463.

Barber, P. C. 1981 Axonal growth by newly-formed vomeronasal neurosensory cells in the normal adult mouse. *Brain Res.* **216**, 229–237.

Barron, K. D. 1983 Comparative observations on the cytologic reactions of central and peripheral nerve cells to axotomy. In *Spinal cord reconstruction* (ed. C. C. Kao, R. P. Bunge & P. J. Reier), pp. 7–40, New York: Raven Press.

Barron, K. D., Means, E. D. & Larsen, E. 1973 Ultrastructure of retrograde degeneration in thalamus of rat. I. Neuronal soma and dendrites. *J. Neuropath. exp. Neurol.* **32**, 218–244.

Barron, K. D., Dentinger, M. P., Kimelberg, H. K., Nelson, L. R., Bourke, R. S., Keegan, S., Mankes, R. & Cragoe, E. J. 1988 Ultrastructural features of a brain injury model in cat. 1) Vascular and neuroglial changes and the prevention of astroglial swelling by a fluorenyl(aryloxy)alkanoic acid derivative (L-644, 711). *Acta Neuropathol., Berl.* **75**, 295–307.

Bernfield, M. R. & Banerjee, S. D. 1978 The basal lamina of epithelial-mesenchymal morphogenetic interactions. In *Biology and chemistry of basement membranes* (ed. N. A. Kefalides), pp. 137–148. New York: Academic Press.

Bernstein, J. J. 1970 The relation of collateral sprouting to CNS regeneration. *Exp. Neurol. Suppl.* **5**, 8–19.

Bernstein, J. J. & Bernstein, M. E. 1969 Ultrastructure of normal regeneration and loss of regenerative capacity following teflon blockage in goldfish spinal cord. *Exp. Neurol.* **24**, 538–557.

Bernstein, J. J. & Bernstein, M. E. 1971 Axonal regeneration and formation of synapses proximal to the site of lesion following hemisection of the rat spinal cord. *Exp. Neurol.* **30**, 336–351.

Bernstein, J. J. & Bernstein, M. E. 1973*a* Neuronal alteration and reinnervation following axonal regeneration and sprouting in mammalian spinal cord. *Brain Behav. Evol.* **8**, 135–161.

Bernstein, M. E. & Bernstein, J. J. 1973*b* Regeneration of axons and synaptic complex formation rostral to the site of hemisection in the spinal cord of the monkey. *Int. J. Neurosci.* **5**, 15–26.

Bernstein, M. E. & Bernstein, J. J. 1977*a* Synaptic frequency alteration on rat ventral horn neurons in the first segment proximal to spinal cord hemisection: an ultrastructural statistical study of regenerative capacity. *J. Neurocytol.* **6**, 85–102.

Bernstein, M. E. & Bernstein, J. J. 1977*b* Dendritic growth cone and filopodia formation as a mechanism of spinal cord regeneration. *Exp. Neurol.* **57**, 419–425.

Bernstein, J. J., Jetz, R., Jefferson, M. & Keleman, M. 1985 Astrocytes secrete basal lamina after hemisection of rat spinal cord. *Brain Res.* **327**, 135–141.

Berry, M. 1979 Regeneration in the central nervous system. *Rec. Adv. Neuropath.* **1**, 67–111.

Berry, M. 1982 Post-injury myelin-breakdown products inhibit axonal growth; an hypothesis to explain the failure of axonal regeneration in the mammalian central nervous system. *Bibliotheca Anatomica* **23**, 1–11.

Berry, M. 1983 Regeneration of axons in the central nervous system. *Prog. Anat.* **3**, 213–233.

Berry, M. 1985 Regeneration and plasticity in the C.N.S. In *Scientific basis of clinical neurology* (ed. M. Swash & C. Kennard), pp. 658–679. London: Churchill Livingston.

Berry, M. & Riches, A. C. 1974 An immunological approach to regeneration in the central nervous system. *Br. Med. Bull.* **30**, 135–140.

Berry, M., Maxwell, W. L., Logan, A., Mathewson, A., McConnell, P., Ashhurst, D. E. & Thomas, G. H. 1983 Deposition of scar tissue in the central nervous system. *Acta Neurochirurgica Suppl.* **32**, 31–53.

Bignami, A. & Dahl, D. 1976 The astroglial response to stabbing. Immunofluorescence studies with antibodies to astrocyte specific protein (GFA) in mammalian and submammalian vertebrates. *Neuropath. App. Neurobiol.* **2**, 99–110.

Bignami, A. & Ralston, H. J. 1969 The cellular reaction to Wallerian degeneration in the central nervous system of the cat. *Brain Res.* **31**, 444–461.

Björklund, A., Katzman, R., Stenevi, U. & West, K. A. 1971 Development and growth of axonal sprouts from noradrenalin and 5-hydroxytryptamine neurones in the rat spinal cord. *Brain Res.* **31**, 21–33.

Björklund, A. & Stenevi, V. 1971 Growth of central catecholamine neurons into smooth muscle grafts in the rat mesencephalon. *Brain Res.* **31**, 1–20.

Björklund, A. & Stenevi, V. 1979 Regeneration of monoaminergic and cholinergic neurons in the mammalian central nervous system. *Physiol. Rev.* **59**, 62–100.

Blackwood, W. 1976 Normal structure and general pathology of the nerve cell and neuroglia. In *Greenfield's Neuropathology* (ed. W. Blackwood & J. A. N. Corellis), pp. 1–42, London: Edward Arnold.

Blakemore, W. F. 1975 The ultrastructure of normal and reactive microglia. *Acta Neuropath. Suppl.* **6**, 273–278.

Blakemore, W. F. 1976 Invasion of Schwann cells into the spinal cord of the rat following local injection of lysolecithin. *Neuropath. App. Neurobiol.* **2**, 21–39.

Bluemink, J. G., Maurik, Van P. & Lawson, K. A. 1976 Intimate cell contacts at the epithelial/mesenchymal interface in embryonic mouse lung. *J. Ultrastruct. Res.* **55**, 257–270.

Bunge, M. B. 1973 Fine structure of nerve fibers and growth cones of isolated sympathetic neurons in culture. *J. Cell Biol.* **56**, 713–735.

Bunge, M. B. 1977 Initial endocytosis of peroxidase or ferritin by growth cones of cultured nerve cells. *J. Neurocytol.* **6**, 407–439.

Cammermeyer, J. 1970 The life history of the microglial cell: a light microscopic study. In *Neurosciences Research* (ed. S. Ehrenpreis & O. C. Solnitzky), vol. 3, pp. 44–129. New York: Academic Press.

Carbonnetto, S., Evans, D. & Cochard, P. 1987 Nerve fibre growth in culture on tissue substrata from central and peripheral nervous system. *J. Neurosci.* **7**, 610–620.

Carbonell, A. L. & Boya, J. 1988 Ultrastructural study on meningeal regeneration and meningo-glial relationships after cerebral stab wound in the adult rat. *Brain Res.* **439**, 337–344.

Caroni, P. & Schwab, M. 1988 Antibody against myelin-associated inhibitor of neurite growth neutralizes non-permissive substrate properties of CNS white matter. *Neuron* **1**, 85–96.

Carter, D., Bray, G. M. & Aguayo, A. J. 1988 Normal ultrastructural characteristics of regenerated retino-colicular synapses in adult hamsters. *Neurosci. Lett. Suppl.* **32**, S75.

Cavanagh, J. B. 1970 The proliferation of astrocytes around a needle wound in the rat's brain. *J. Anat.* **106**, 471–487.

Cavanagh, J. B. & Lewis, P. D. 1969 Perfusion-fixation, colchicine and mitotic activity in the adult rat brain. *J. Anat.* **104**, 341–350.

Chiquet, M. 1989 Neurite growth inhibition by CNS myelin proteins: a mechanism to confine fiber tracts? *Trends Genet.* **12**, 1–3.

Cohen, J., Burne, J. F., Winter, J. & Bartlett, P. 1986 Retinal ganglion cells lose their response to laminin. *Nature, Lond.* **322**, 465–467.

Cohen, J., Burne, J. F., McKinlay, C. & Winter, J. 1987 The role of laminin and the laminin/fibronectin receptor complex in the outgrowth of retinal ganglion cell axons. *Devl Biol.* **122**, 407–418.

Colmant, H. J. 1968 Allgemeine Histopathologie der Glia. *Acta Neuropath. Berlin Suppl.* **4**, 61–76.

Cook, R. D. & Wisniewski, H. M. 1973 The role of oligodendroglia and astroglia in Wallerian degeneration of the optic nerve. *Brain Res.* **61**, 191–206.

Cox, V. S. 1976 Ultrastructure of the axon reaction in the immature rat thalamus. *J. Neuropath. exp. Neurol.* **35**, 191–203.

Davies, P. & Allison, A. C. 1976 Secretion of macrophage enzymes in relation to the pathogenesis of chronic inflammation. In *Immunobiology of the macrophages* (ed. D. S. Nelson), pp. 427–461. New York: Academic Press.

Dayan, D., Binderman, I., Abramovici, A. & Sandbank, U. 1982 Collagen types in CNS tumours. Abstracts of VIIIth meeting of Federation of European Connective Tissue Societies, Copenhagen, August 1982, pp. 131.

del Cerro, M. P. & Snider, R. S. 1968 Studies on the developing cerebellum. Ultrastructure of the growth cones. *J. comp. Neurol.* **133**, 341–362.

Dellman, H.-D. 1973 Degeneration and regeneration of neurosecretory systems. *Int. Rev. Cytol.* **36**, 215–315.

DeWitt, D. S., Jenkins, L. W., Wei, E. P., Lutz, H., Becker, D. P. & Kontos, H. A. 1986 Effects of fluid-percussion brain injury on regional cerebral blood flow and pial arteriolar diameter. *J. Neurosurg.* **64**, 787–794.

Ebendal, T. 1977 Extracellular matrix fibrils and cell contacts in the chick embryo. *Cell Tissue Res.* **175**, 439–458.

Ehrlich, H. P. 1988 Wound closure: evidence of cooperation between fibroblasts and collagen matrix. *Eye* **2**, 149–157.

Fawcett, J. W., Rokos, J. & Bakst, I. 1989 Oligodendrocytes repel axons and cause axonal growth cone collapse. *J. Cell. Sci.* **92**, 93–100.

Feeney, D. M., Boyeson, M. G., Linn, R. T., Murray, H. M. & Dail, W. G. 1981 Responses to cortical injury. I. Methodology and local effects of contusion in the rat. *Brain Res.* **211**, 67–77.

Fenstermacher, J. D. & Patlak, C. S. 1976 The movements of water and solutes in the brains of mammals. In *Dynamics of brain edema* (ed. H. M. Pappius & W. Feindel), pp. 87–94, Berlin, Heidelberg and New York: Springer Verlag.

Field, P. M., Coldham, D. E. & Raisman, G. 1980 Synapse formation after injury in the adult rat brain: preferential reinnervation of denervated fimbrial sites by axons of the contralateral fimbria. *Brain Res.* **189**, 103–113.

Fugita, S., Tsuchihashi, Y. & Kitamura, T. 1981 Origin, morphology and function of microglia. In *Glial and neuronal cell biology* (ed. E. Acosta Vidrio & S. Fedoroff), pp. 141–169. New York: A. R. Liss.

Gennarelli, T. A., Thibault, L. E., Adams, J. H., Graham, D. I., Thompson, C. J. & Marcincin, R. P. 1982 Diffuse axonal injury and traumatic coma in the primate. *Annal. Neurol.* **12**, 564–574.

Giftochristos, N. & David, S. 1988 Laminin and heparan sulphate proteoglycan in the lesioned adult mammalian central nervous system and their possible relationship to axonal sprouting. *J. Neurocytol.* **17**, 385–397.

Goldberger, M. E. & Murray, M. 1974 Restitution of function and collateral sprouting in the cat spinal cord: the deafferented animal. *J. comp. Neurol.* **158**, 37–53.

Gospodarowicz, D. 1974 Localization of a fibroblast growth factor and its effect alone and with hydrocortisone on 3T3 cell growth. *Nature, Lond.* **249**, 123–127.

Grainger, F. & James, D. W. 1970 Association of glial cells with the terminal parts of neurite bundles extending from chick spinal cord *in vitro*. *Z. Zellforsch Mikrosk. Anat.* **108**, 93–104.

Guillery, R. W. 1972 Experiments to determine whether retinogeniculate axons can form collateral sprouts in the dorsal lateral geniculate nucleus of the cat. *J. comp. Neurol.* **146**, 407–420.

Hay, E. D. 1981 Collagen and embryonic development. In *Cell biology of extracellular matrix* (ed. E. D. Hay), pp. 379–409. New York and London: Plenum Press.

Hoff, S. F., Scheff, S. W., Kwan, A. Y. & Cotman, C. W. 1981*a* A new type of lesion-induced synaptogenesis: I. Synaptic turnover in non-denervated zones of the dentate gyrus in young adult rats. *Brain Res.* **222**, 1–13.

Hoff, S. F., Scheff, S. W., Kwan, A. Y. & Cotman, C. W. 1981*b* A new type of lesion-induced synaptogenesis: II. The effect of aging on synaptic turnover in non-denervated zones. *Brain Res.* **222**, 15–27.

Hortega, P. del Rio & Penfield, W. 1928 Cerebral cicatrix: the reaction of neuroglia to brain wounds. *Arch. Neurol. Psychiat.* **19**, 180–189.

Houtoff, H. J., Go, K. G. & Huitema, S. 1981 The permeability of cerebral capillary endothelium in cold injury: comparison of an endogenous and exogenous protein tracer. In *Cerebral microcirculation and metabolism* (ed. J. Cerves-Navarro & E. Fritschka), pp. 331–336. New York: Raven Press.

Illis, L. S. 1973*a* Experimental model of regeneration in the central nervous system. I. Synaptic changes. *Brain* **96**, 47–60.

Illis, L. S. 1973*b* Experimental model of regeneration in the central nervous system. II. The reaction of glia in the synaptic zone. *Brain* **96**, 61–68.

Imamoto, K. & Leblond, C. P. 1977 Presence of labeled monocytes, macrophages and microglia in a stab wound of the brain after an injection of bone marrow cells labeled with ^{3}H-uridine into rats. *J. comp. Neurol.* **174**, 255–280.

Johnson, A. R., Wigley, C. B., Gregson, N. A., Cohen, J. & Berry, M. 1988 Neither laminin nor prior optic nerve section are essential for the regeneration of adult mammalian retinal ganglion cell axons *in vitro*. *J. Neurocytol.* **17**, 95–104.

Kalil, K. & Reh, T. 1979 Regrowth of severed axons in the neonatal central nervous system: establishment of normal connections. *Science, Wash.* **205**, 1158–1161.

Kao, C. C., Chang, L. W. & Bloodworth, J. M. B. 1977*a* Electron microscopic observations of the mechanisms of terminal club formation in transected spinal cord axons. *J. Neuropath. Exp. Neurol.* **36**, 140–156.

Kao, C. C., Chang, L. W. & Bloodworth, J. M. B. 1977*b* Axonal regeneration across transected mammalian spinal cords: an electron microscopic study of delayed microsurgical nerve grafting. *Exp. Neurol.* **54**, 591–615.

Kaur, C., Ling, E. A. & Wong, W. C. 1987 Origin and fate of neural macrophages in a stab wound of the brain of the young rat. *J. Anat.* **154**, 215–227.

Kawana, E., Sandri, C. & Akert, K. 1971 Ultrastructure of growth cones in the cerebellar cortex of the neonatal rat and cat. *Z. Zellforsch. Mikrosk. Anat.* **115**, 284–298.

Kerns, J. M. & Hinsman, E. T. 1973 Neuroglial response to sciatic neurectomy. I. Light microscopy and autoradiography. *J. comp. Neurol.* **151**, 237–254.

Kerr, F. W. L. 1972 The potential of cervical primary afferents to sprout in the spinal nucleus of V following long term trigeminal denervation. *Brain Res.* **43**, 547–560.

Kiernan, J. A. 1979 Hypotheses concerned with axonal regeneration in the mammalian nervous system. *Biol. Rev.* **54**, 155–197.

Klatzo, I. 1985 Brain oedema following brain ischaemia and the influence of therapy. *Br. J. Anaesth.* **57**, 18–22.

Klatzo, I., Li, C. L., Long, D. M., Bak, A. F., Mossakowski, M. J., Parker, L. O. & Rasmussen, L. E. 1968 The effects of hypothermia on electrical impedance and penetration of substances from CSF into pervascular brain tissue. *Progr. Brain Res.* **29**, 385–399.

Krayanek, S. & Goldberg, S. 1981 Orientated extracellular channels and axonal guidance in the embryonic chick retina. *Devl Biol.* **84**, 41–50.

Krikorian, J. G., Guth, L. & Donati, E. J. 1981 Origin of the connective tissue scar in the transected rat spinal cord. *Exp. Neurol.* **72**, 678–707.

Latov, N., Nilaver, G., Zimmerman, E. A., Johnson, W. G., Silverman, A. J., Defendini, R. & Cote, L. 1979 Fibrillary astrocytes proliferate in response to brain injury: a study combining immunoperoxidase technique for glial fibrillary acidic protein and radioautoradiography of tritiated thymidine. *Devl Biol.* **72**, 381–384.

Lawrence, J. M., Huang, S. K. & Raisman, G. 1984 Vascular and astrocyte reactions during establishment of hippocampal transplants in adult host brain. *Neuroscience* **12**, 745–760.

Leibovich, S. J. & Ross, R. 1975 The role of the macrophage in wound repair. A study with hydrocortisone and antimacrophage serum. *Am. J. Pathol.* **78**, 71–100.

Leibovich, S. J. & Ross, R. 1976 A macrophage-dependent factor that stimulates the proliferation of fibroblasts *in vitro*. *Am. J. Pathol.* **84**, 501–514.

Letourneau, P. C., Madsen, A. M., Palm, S. L. & Furcht, L. T. 1988 Immunoreactivity for laminin in the developing ventral longitudinal pathway of the brain. *Devl Biol.* **125**, 135–144.

Lewis, P. D. & Lampert, I. A. 1977 Glycosaminoglycans in astrocytes. *Neuropath. appl. Neurobiol.* **3**, 57–64.

Lieberman, A. R. 1971 The axon reaction: a review of the principal features of perikaryal responses to axon injury. *Int. Rev. Neurobiol.* **14**, 49–124.

Liesi, P., Kaakkola, S., Dahl, D. & Vaheri, A. 1984 Laminin is induced in astrocytes of adult brain by injury. *EMBO J.* **3**, 683–686.

Ling, E. A., Paterson, J. A., Privat, A., Mori, S. & Leblond, C. P. 1973 Investigation of glial cells in semithin sections. I. Identification of glial cells in the brain of young rats. *J. comp. Neurol.* **149**, 43–71.

Lofberg, J., Ahlfors, K. & Fallstrom, C. 1980 Neural crest cell migration in relation to extracellular matrix organization in the embryonic axolotl trunk. *Devl Biol.* **75**, 148–167.

Logan, A., Berry, M., Thomas, G. H., Gregson, N. A. & Logan, S. D. 1985 Identification and partial purification of fibroblast growth factor from the brains of developing rats and leucodystrophic mice. *Neuroscience* **15**, 1239–1246.

Ludwin, S. K. 1984 Proliferation of mature oligodendrocytes after trauma to the central nervous system. *Nature, Lond.* **308**, 274–275.

Ludwin, S. K. 1985 The reaction of oligodendrocytes and astrocytes in trauma and implantation: a combined autoradiographic and immunohistochemical study. *Lab. Invest.* **52**, 20–30.

Ludwin, S. K. & Bakker, D. A. 1988 Can oligodendrocytes attached to myelin proliferate? *J. Neurosci.* **8**, 1239–1244.

Lund, R. D. & Lund, J. S. 1971 Synaptic adjustments after deafferentation of the superior colliculus of the rat. *Science, Wash.* **171**, 804–807.

Lyser, K. M. 1972 The differentiation of glial cells and glia limitans in organ culture of chick spinal cord. *In Vitro*, **8**, 77–84.

Madden, J. W., Morton, D. & Peacock, F. E. 1974 Contraction of experimental wounds. I. Inhibiting wound contraction by using a topical smooth muscle antagonist. *Surgery* **76**, 8–15.

Matthews, D. A., Cotman, C. & Lynch, G. 1976 An electron microscopic study of lesion-induced synaptogenesis in the dentate gyrus of the adult rat. I. Magnitude and time course of degeneration. *Brain Res.* **115**, 1–21.

Matthews, M. A. & Kruger, L. 1973 Electron microscopy of non-neuronal cellular changes accompanying neural degeneration in thalamic nuclei of the rabbit. II. Reactive elements within the neuropile. *J. comp. Neurol.* **148**, 313–346.

Mathewson, A. J. & Berry, M. 1985 Observations on the astrocyte response to a cerebral stab wound in adult rats. *Brain Res.* **327**, 61–69.

Maxwell, W. L., Duance, V. C., Lehto, M., Ashhurst, D. E. & Berry, M. 1984 The distribution of types I, III, IV and V collagens in penetrant lesions of the rat central nervous system. *Histochem. J.* **16**, 1219–1229.

Maxwell, W. L., Irvine, A., Adams, J. H., Graham, D. I. & Gennarelli, T. A. 1988 Response of cerebral microvasculature to brain injury. *J. Pathol.* **155**, 327–335.

McConnell, P. & Berry, M. 1982*a* Regeneration of axons in the mouse retina after injury. In *Bibliotheca Anatomica* (ed. M. Berry), vol. 23 (*Growth and regeneration of axons in the nervous system*), pp. 26–37. Basel and London: S. Karger.

McConnell, P. & Berry, M. 1982*b* Regeneration of ganglion cell axons in the adult mouse retina. *Brain Res.* **241**, 362–365.

McLoon, S. C., McLoon, L. K., Palm, S. L. & Furcht, L. T. 1988 Transient expression of laminin in the optic nerve of the developing rat. *J. Neurosci.* **8**, 1981–1990.

Miller, R. H., Abney, E. R., David, S., ffrench-Constant, C., Lindsay, R., Patel, R., Stone, J. & Raff, M. C. 1986 Is reactive gliosis a property of a distinct subpopulation of astrocytes? *J. Neurosci.* **6**, 22–29.

Miller, R. H. & Raff, M. C. 1984 Fibrous and protoplasmic astrocytes are biochemically and developmentally distinct. *J. Neurosci.* **4**, 584–592.

Murabe, Y., Ibata, Y. & Sano, Y. 1981 Morphological studies on neuroglia. III. Macrophage response and 'microgliocytosis' in kianic acid-induced lesions. *Cell Tissue Res.* **218**, 75–86.

Murabe, Y. & Sano, Y. 1981 Morphological studies on neuroglia. I. Electron microscopic identification of silver-impregnated glial cells. *Cell Tissue Res.* **216**, 557–568.

Nathan, C. F. & Cohn, Z. A. 1980 Monocytes and macrophages. In *Textbook of rheumatology* (ed. W. N. Kelley, E. D. Harris, Jr, S. Ruddy & C. B. Sledge), pp. 136–162. Philadelphia: W. B. Saunders.

Nathan, C. F., Murray, H. W. & Cohn, Z. A. 1980 The macrophage as an effector cell. *New Engl. J. Med.* **303**, 622–626.

Parnavelas, J. G., Luder, R., Pollard, S. G., Sullivan, K. & Lieberman, A. R. 1983 A qualitative and quantitative ultrastructural study of glial cells in the developing visual cortex of the rat. *Phil. Trans. R. Soc. Lond.* B **301**, 55–84.

Penfield, W. 1927 The mechanism of cicatricial contraction in the brain. *Brain* **50**, 499–517.

Penfield, W. & Buckley, R. C. 1928 Punctures of the brain. The factors concerned in gliosis and cicatricial reaction. *Arch. Neurol. Psychiat.* **20**, 1–13.

Perry, V. H., Hume, D. A. & Gordon, S. 1985 Immunohistochemical localisation of macrophages and microglia in the adult and developing mouse brain. *Neuroscience* **15**, 313–326.

Povlishock, J. T. 1986 The morphopathologic responses to experimental head injuries of varying severity. In *Central nervous system trauma status report* (ed. D. P. Becker & J. T. Povlishock), pp. 443–452. Bethesda: National Institutes of Health.

Raff, M. C., Miller, R. H. & Noble, M. 1983 A glial progenitor cell that develops *in vitro* into an astrocyte or an oligodendrocyte depending on culture medium. *Nature, Lond.* **303**, 390–396.

Raisman, G. & Field, P. M. 1973 A quantitative investigation of the development of collateral reinnervation after partial deafferentation of the septal nuclei. *Brain Res.* **50**, 241–264.

Ramon y Cajal, S. 1928 *Degeneration and regeneration in the nervous system.* London: Oxford University Press.

Rogers, S. L., Letourneau, P. C., Palm, S. L., McCarthy, J. & Furcht, L. T. 1983 Neurite extension by peripheral and central nervous system neurons in response to substratum-bound fibronectin and laminin. *Devl Biol.* **98**, 212–220.

Sandback, U., Bubis, J. J., Barton, I., Dror, I., Budowski, P. & Wolman, M. 1980 Basal membrane labyrinths in the healing stages of chick nutritional encephalopathy. *Neuropath. Appl. Neurobiol.* **6**, 3–8.

Schelper, R. L. & Adrian, E. K. 1980 Non-specific esterase activity in reactive cells in injured nervous tissue labelled with ^{3}H-thymidine or 125-iododeoxyuridine injected before injury. *J. comp. Neurol.* **194**, 829–844.

Schelper, R. L. & Adrian, E. K. 1986 Monocytes become macrophages; they do not become microglia: a light and electron microscopic autoradiographic study using 125-iododeoxyuridine. *J. Neuropathol. exp. Neurol.* **45**, 1–19.

Schnell, L. & Schwab, M. E. 1990 Axonal regeneration in the rat spinal cord produced by an antibody against myelin-associated neurite outgrowth inhibitors. *Nature, Lond.* **343**, 269–272.

Schwab, M. E. & Thoenen, H. 1985 Dissociated neurons regenerate into sciatic but not optic nerve explants in culture irrespective of neurotrophic factors. *J. Neurosci.* **5**, 2415–2423.

Shellswell, G. B., Restall, D. J., Duance, V. C. & Bailey, A. J. 1979 Identification and differential distribution of collagen types in the central and peripheral nervous system. *FEBS Lett.* **106**, 305–308.

Sievers, J., Mangold, U., Berry, M., Allen, C. & Schlossberger, H. G. 1981 Experimental studies on cerebellar foliation. I. A qualitative morphological analysis of cerebellar fissuration defects after neonatal treatment with 6-OHDA in the rat. *J. comp. Neurol.* **203**, 751–769.

Simpson, D. M. & Ross, R. 1972 The neutrophil leukocyte in wound repair: a study with antineutrophil serum. *J. clin. Invest.* **51**, 2009–2023.

Skoff, R. P. 1975 The fine structure of pulse labelled (^{3}H-thymidine) cells in degenerating rat optic nerve. *J. comp. Neurol.* **161**, 595–611.

Skoff, R. P. & Hamburger, V. 1974 Fine structure of dendritic and axonal growth cones in embryonic chick spinal cord. *J. comp. Neurol.* **153**, 107–148.

Smalheiser, N. R., Crain, S. M. & Reid, L. M. 1984 Laminin as a substrate for retinal axons *in vitro*. *Devl Brain Res.* **12**, 136–140.

Startzl, T. E. & Magoun, H. W. 1951 Organisation of diffuse thalamic projection system. *J. Neuro. Physiol.* **14**, 133–146.

Steedman, H. F. 1957 Polyester wax. A new ribboning embedding medium for histology. *Nature, Lond.* **179**, 1345.

Stein, J. M. & Levenson, S. M. 1966 Effect of the inflammatory reaction on subsequent wound healing. *Surg. Forum* **17**, 484–485.

Streit, W. J. & Kreutzberg, G. W. 1987 Lectin binding by resting and reactive microglia. *J. Neurocytol.* **16**, 249–260.

Takamiya, Y., Kohsaka, S., Toya, S., Otani, M. & Tsukada, Y. 1988 Immunohistochemical studies on the proliferation of reactive astrocytes and the expression of cytoskeletal proteins following brain injury in rats. *Devl Brain Res.* **38**, 201–210.

Toole, B. P. 1981 Glycosaminoglycans in morphogenesis. In *Cell biology of extracellular matrix* (ed. E. Hay), pp. 259–294. New York and London: Plenum Press.

Torvik, A. 1975 The relationship between microglia and brain macrophages. Experimental investigations. *Acta Neuropath., Berl. Suppl.* **4**, 297–300.

Torvik, A. & Soreide, A. J. 1972 Nerve cell regeneration after axon lesions in newborn rabbits. Light and electron microscopic study. *J. Neuropath. exp. Neurol.* **31**, 683–695.

Tripp, L. N. & Wells, J. 1978 Formation of new synaptic terminals in the somatosensory thalamus of the rat after lesions of the dorsal column nuclei. *Brain Res.* **155**, 362–367.

Vaughan, D. W. & Foundas, S. 1982 Synaptic proliferation in the auditory cortex of the young adult rat following callosal lesions. *J. Neurocytol.* **11**, 29–51.

Vaughn, J. E. & Pease, D. C. 1970 Electron microscopic studies of Wallerian degeneration in rat optic nerves. II. Astrocytes, oligodendrocytes and adventitial cells. *J. comp. Neurol.* **140**, 207–226.

Vaughn, J. E. & Skoff, R. P. 1972 Neuroglia in experimentally altered central nervous system. In *The structure and function of nervous tissue* (ed. G. H. Bourne), pp. 39–72. New York: Academic Press.

Vaughn, J. E., Henrikson, C. K. & Grieshaber, J. A. 1974 A quantitative study of synapses on motor neurone dendritic growth cones in developing mouse spinal cord. *J. Cell Biol.* **60**, 664–672.

Vera, R. P. & Grafstein, B. 1981 Cellular mechanisms for recovery from nervous system injury: A conference report. *Exp. Neurol.* **71**, 6–75.

Volkman, A. & Gowans, J. L. 1965 The origin of macrophages from bone marrow in the rat. *Brit. J. exp. Path.* **46**, 62–70.

Watson, W. E. 1976 *Cell biology of brain*, pp. 6–15. London: Chapman & Hall.

Wei, E. P., Dietrich, W. D., Povlishock, J. T., Navari, R. M. & Kontos, H. A. 1980 Functional, morphological and metabolic abnormalities of the cerebral microcirculation after concussive brain injury in cats. *Circ. Res.* **46**, 37–47.

Westrum, L. E. & Black, R. G. 1971 Fine structural aspects of the synaptic organisation of the spinal trigeminal nucleus (pars interpolaris) of the cat. *Brain Res.* **25**, 265–287.

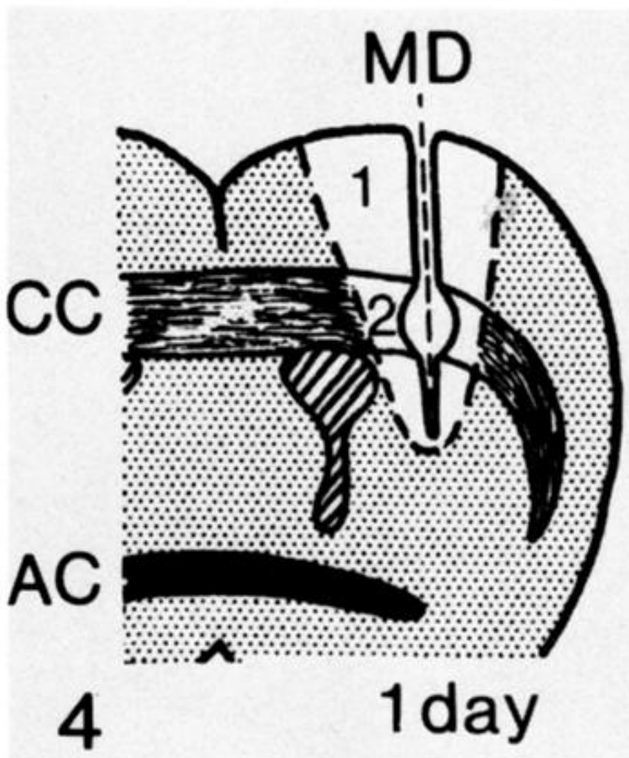

4

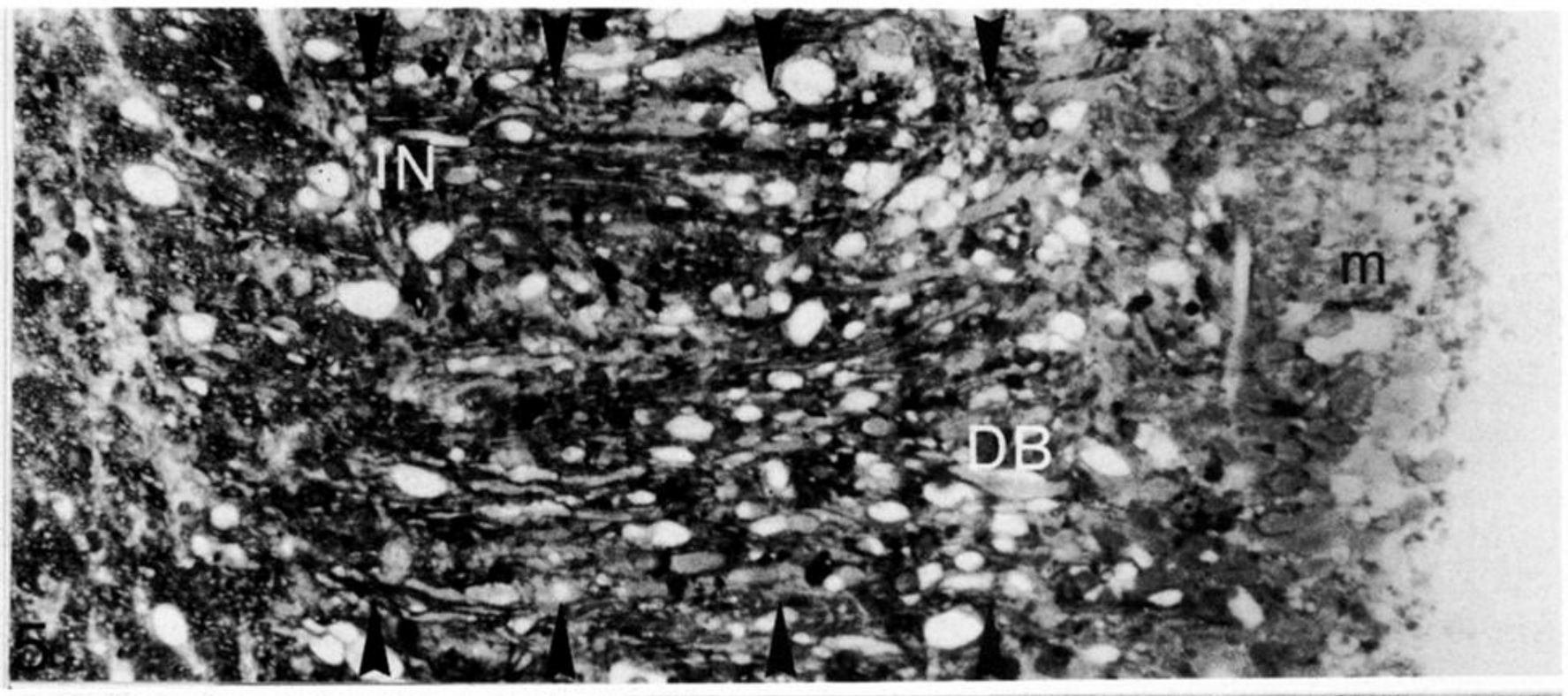

5

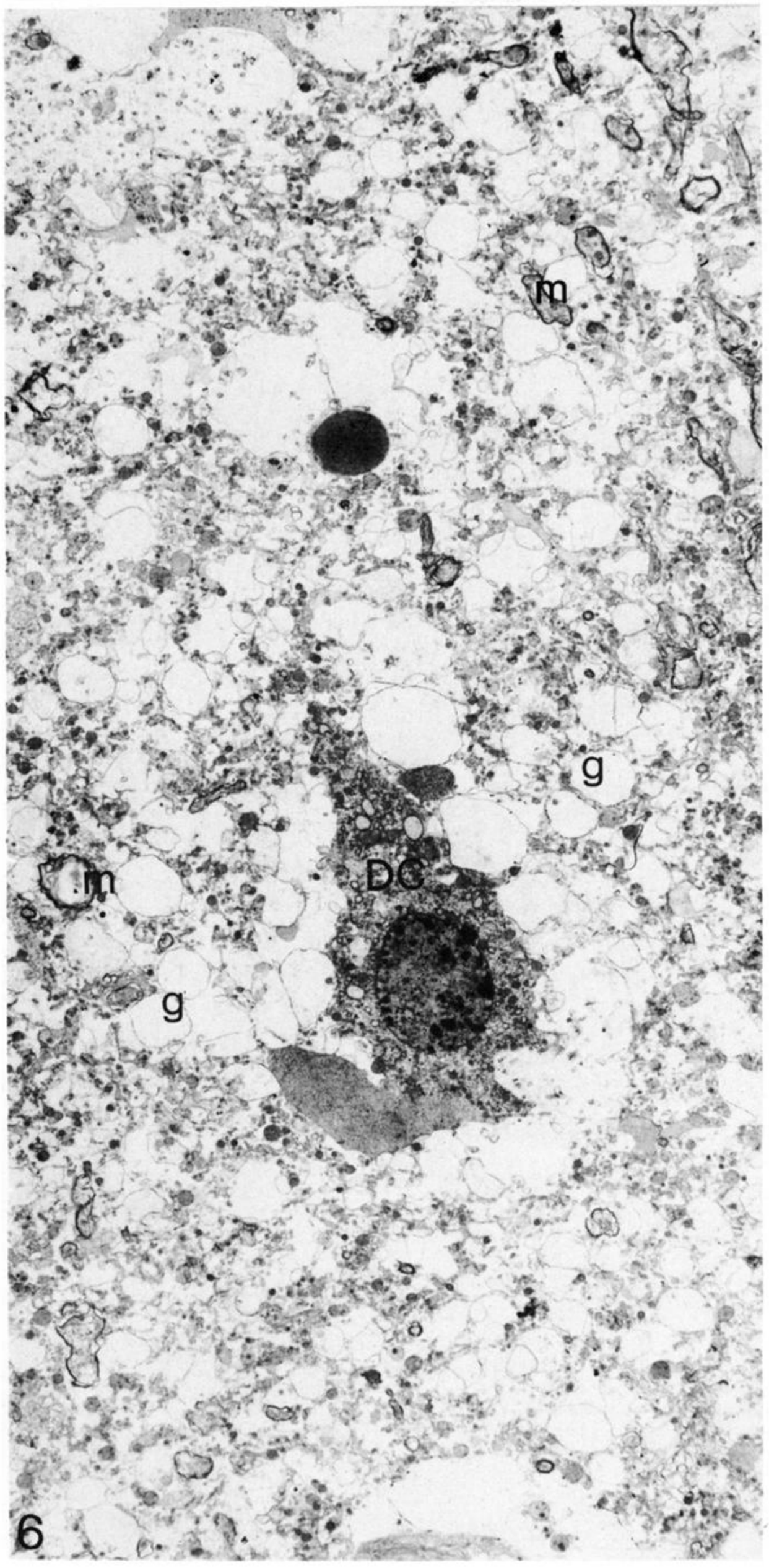

6

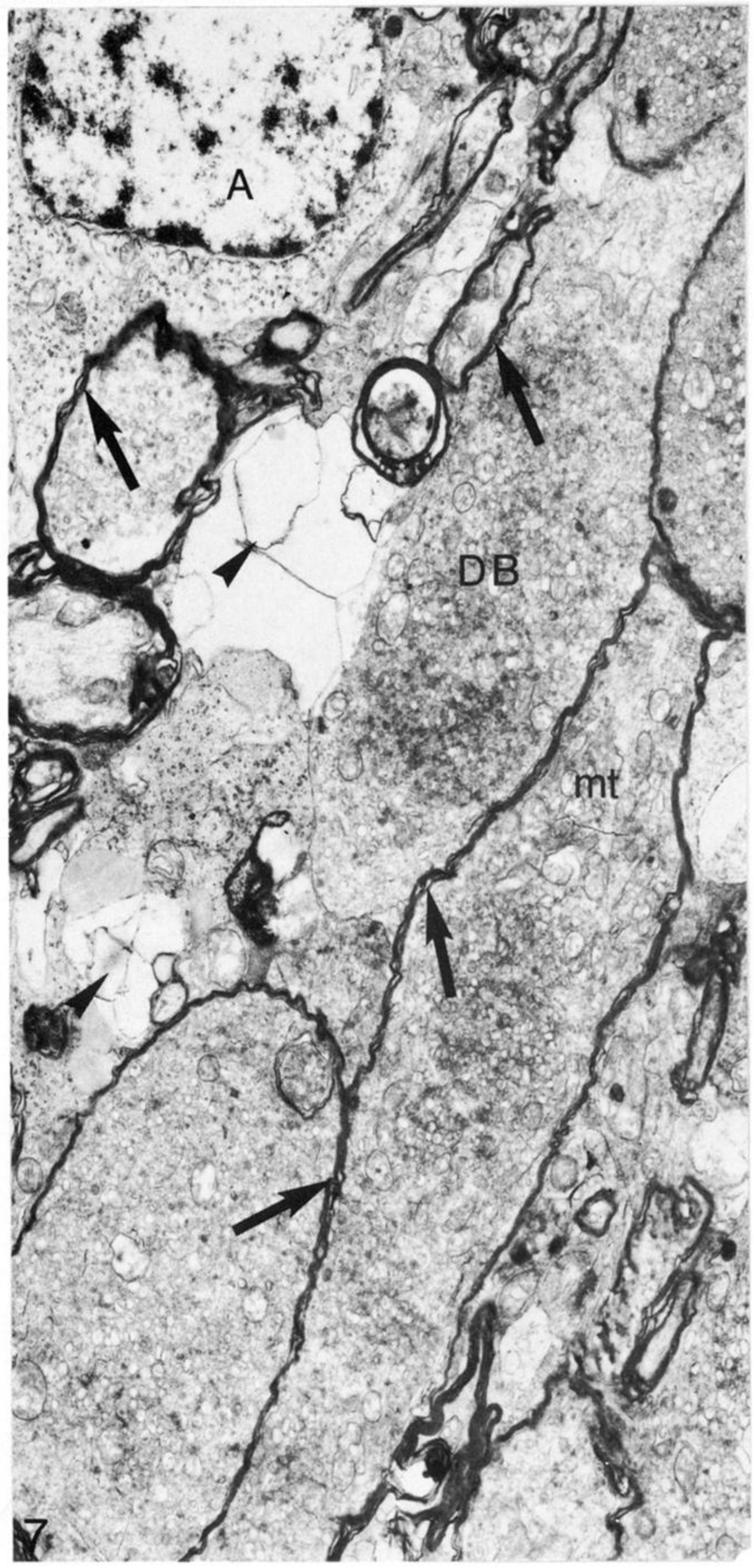

7

FIGURES 4–7. For description see opposite.

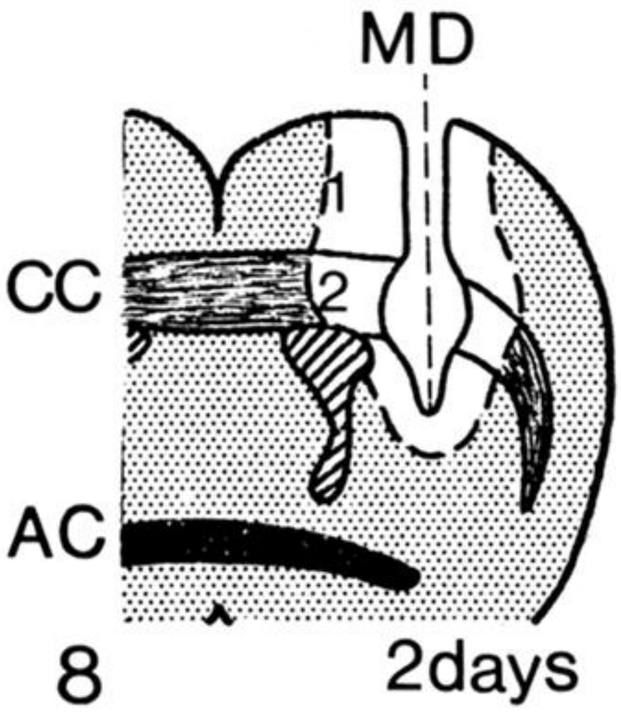

8

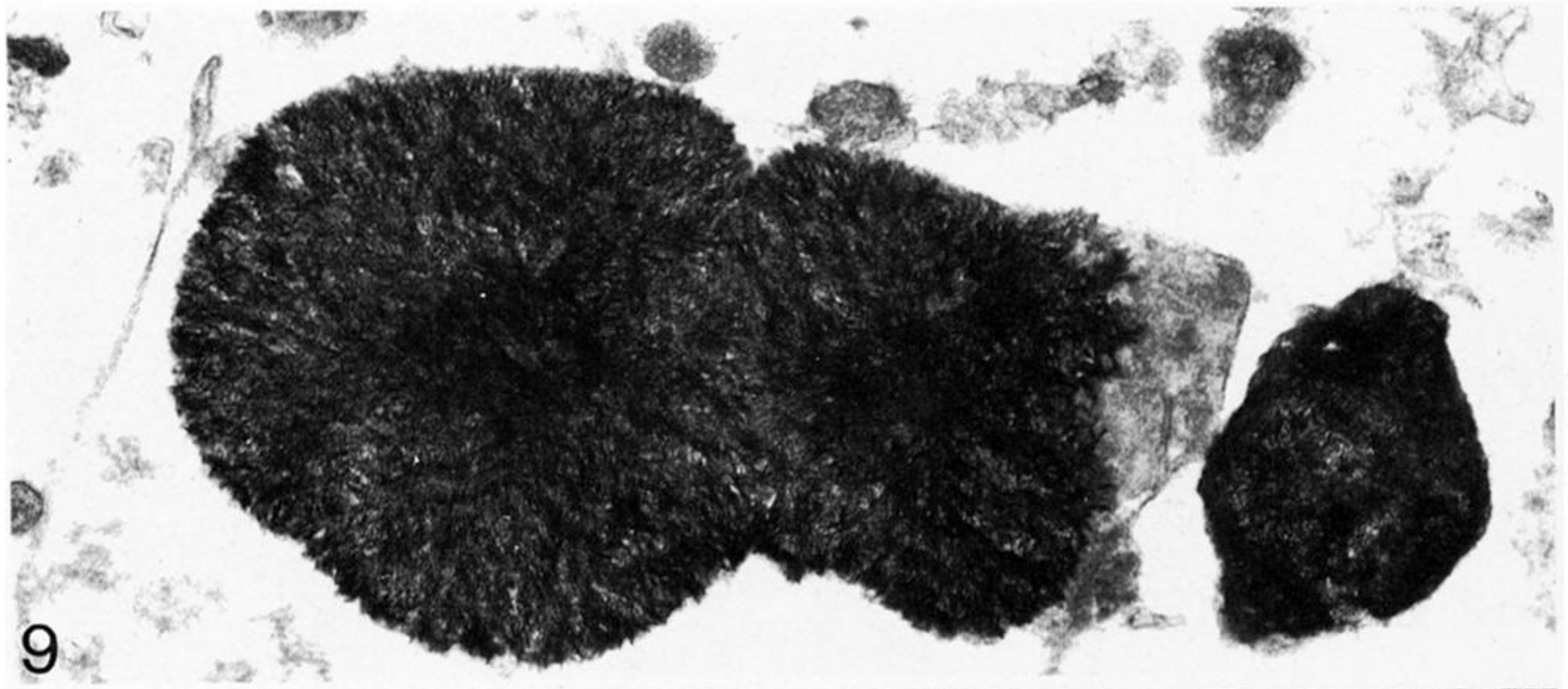

9

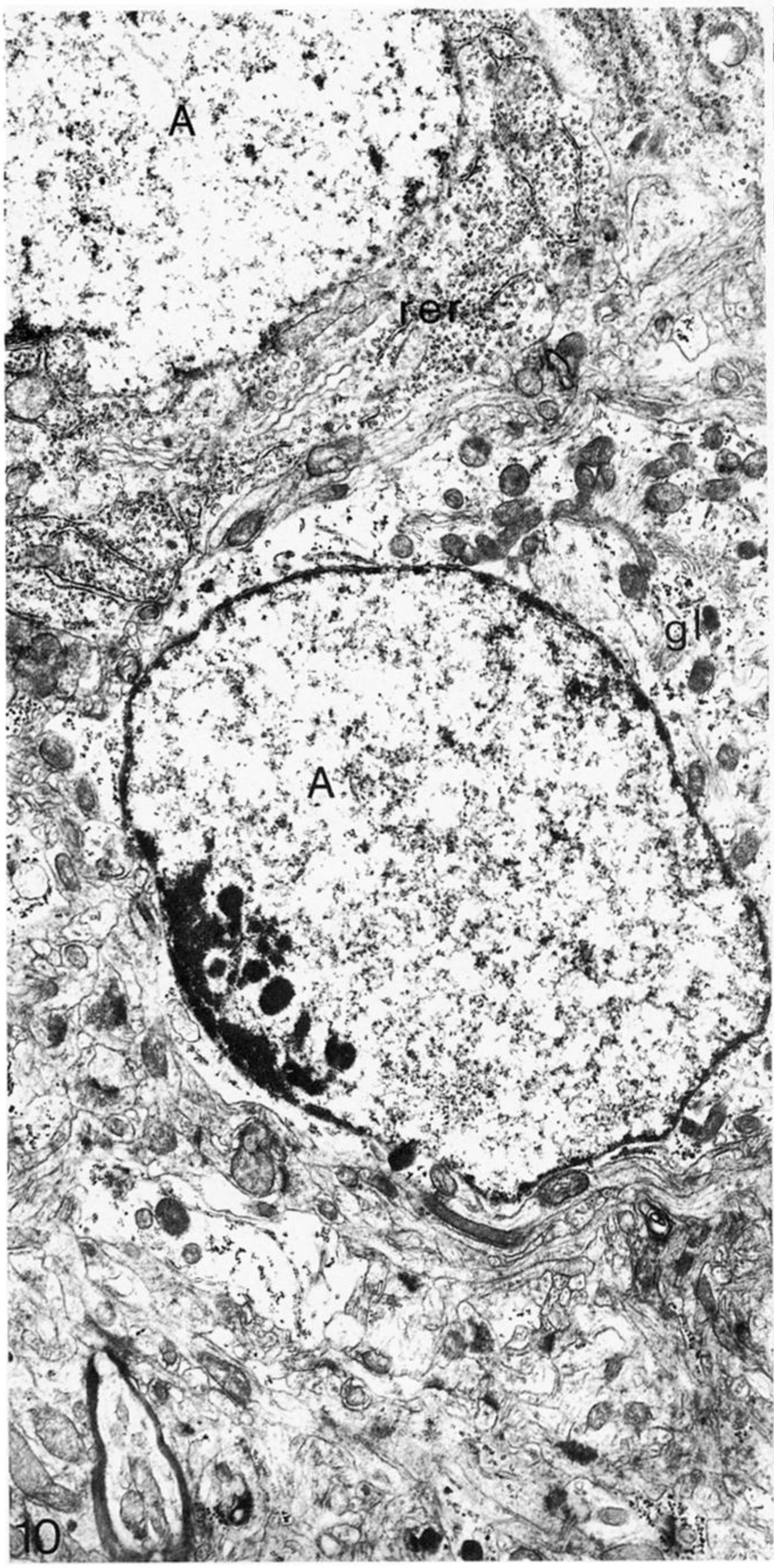

10

11

FIGURES 8–11. For description see facing plate 4.

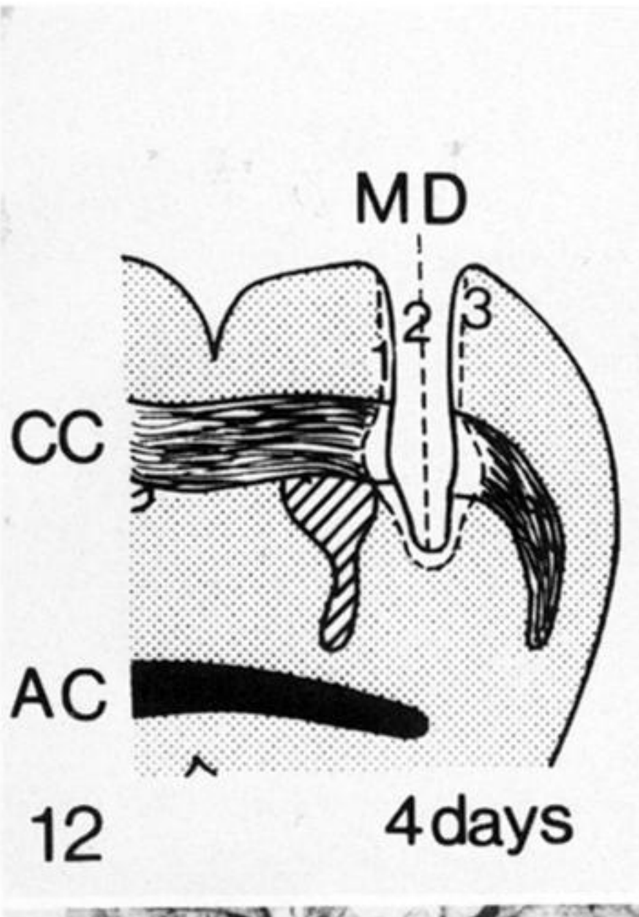

12

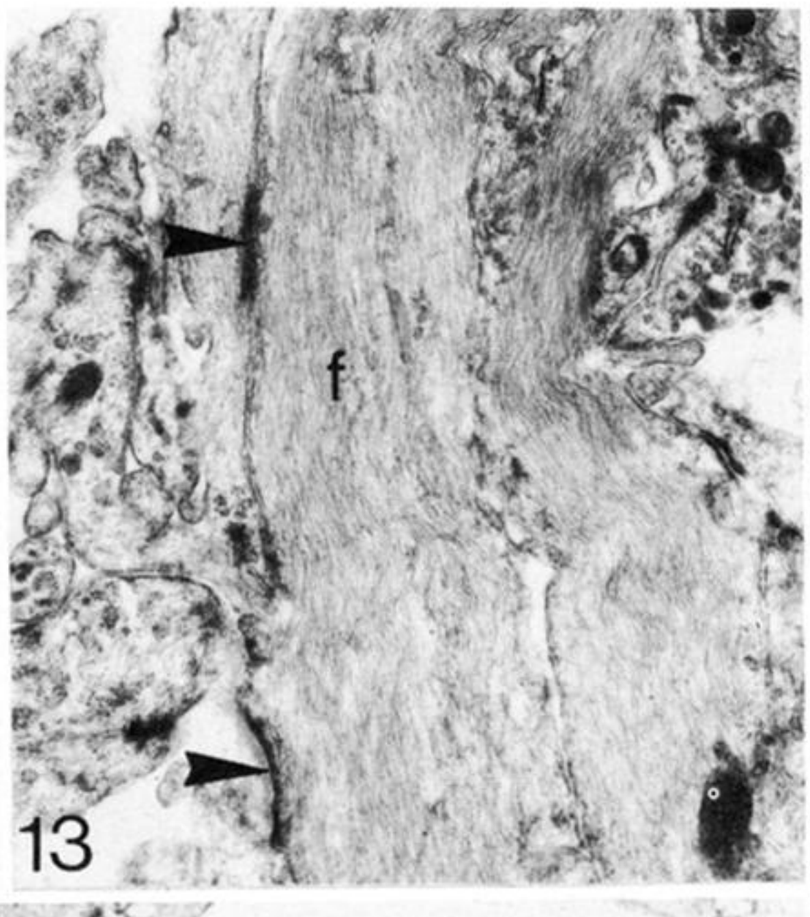

13

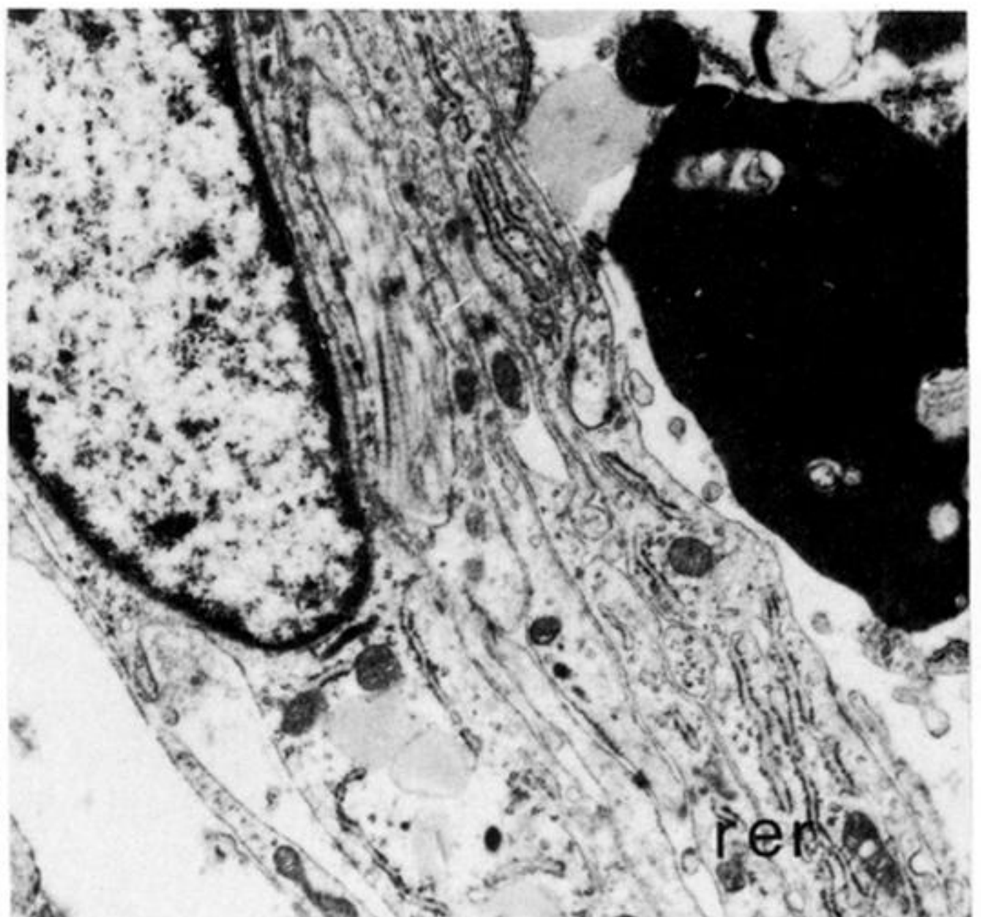

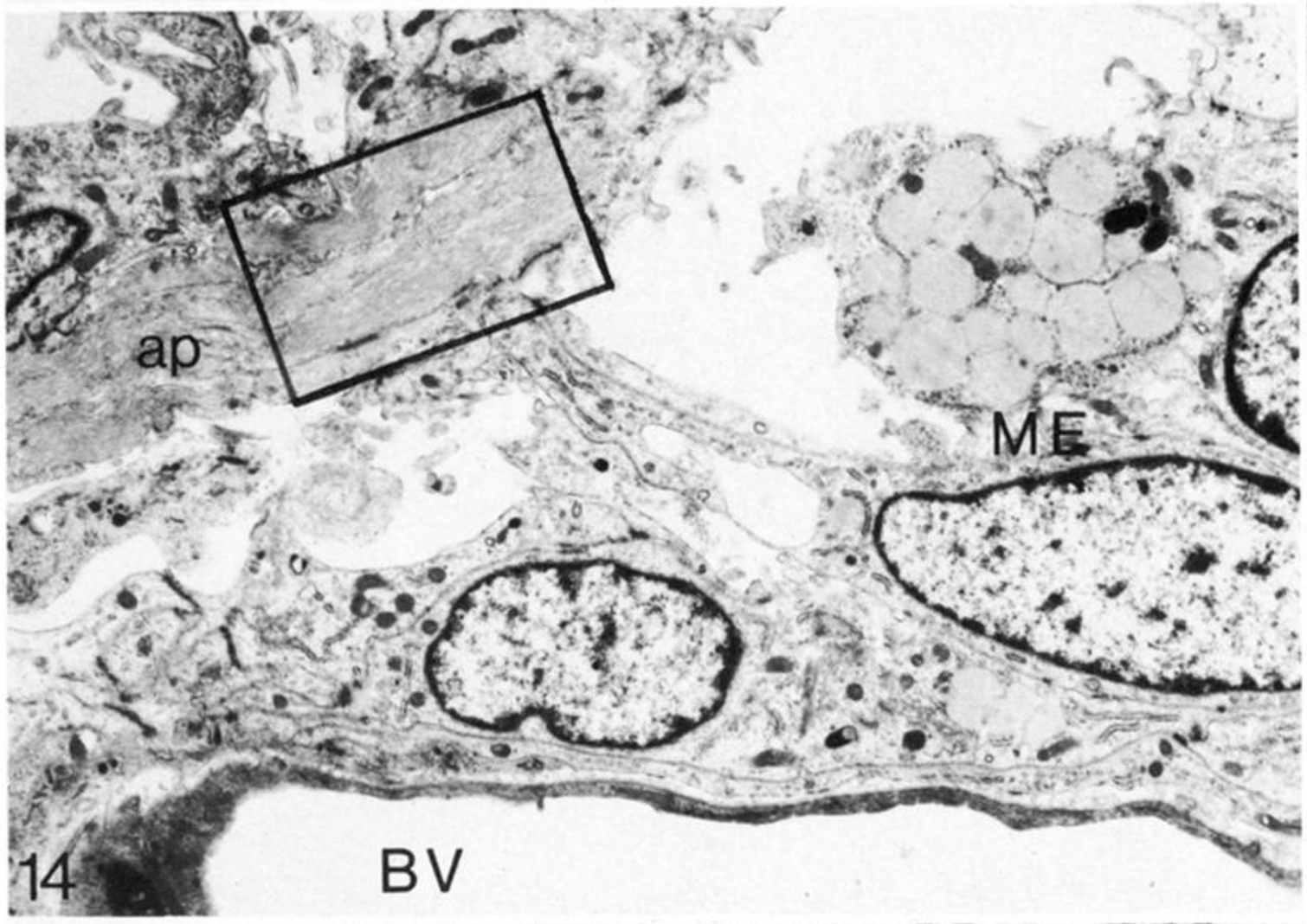

14

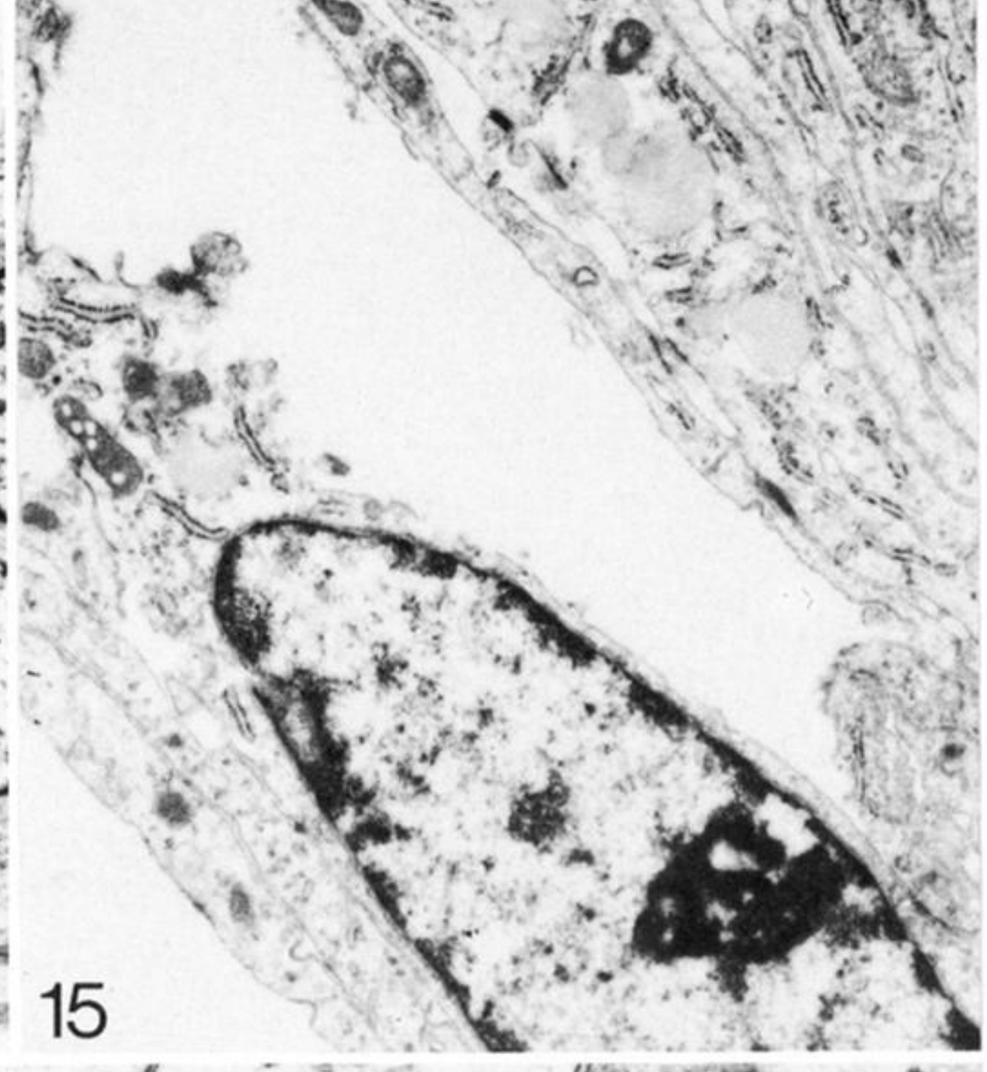

15

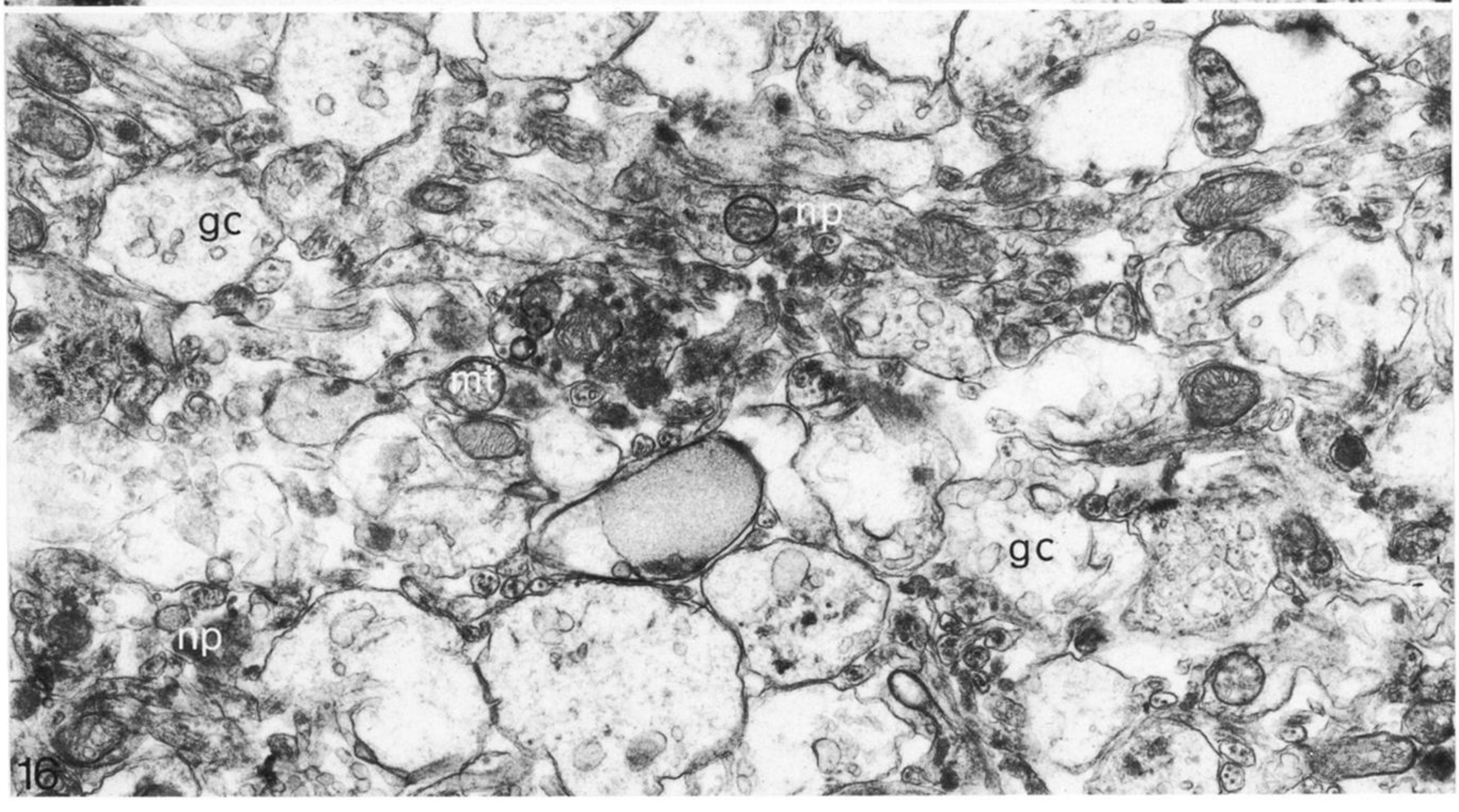

16

FIGURES 12–16. For description see facing plate 4.

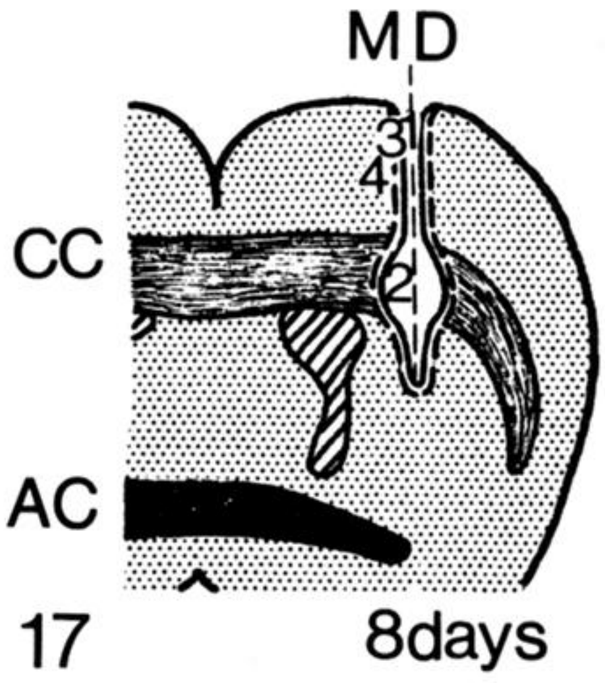

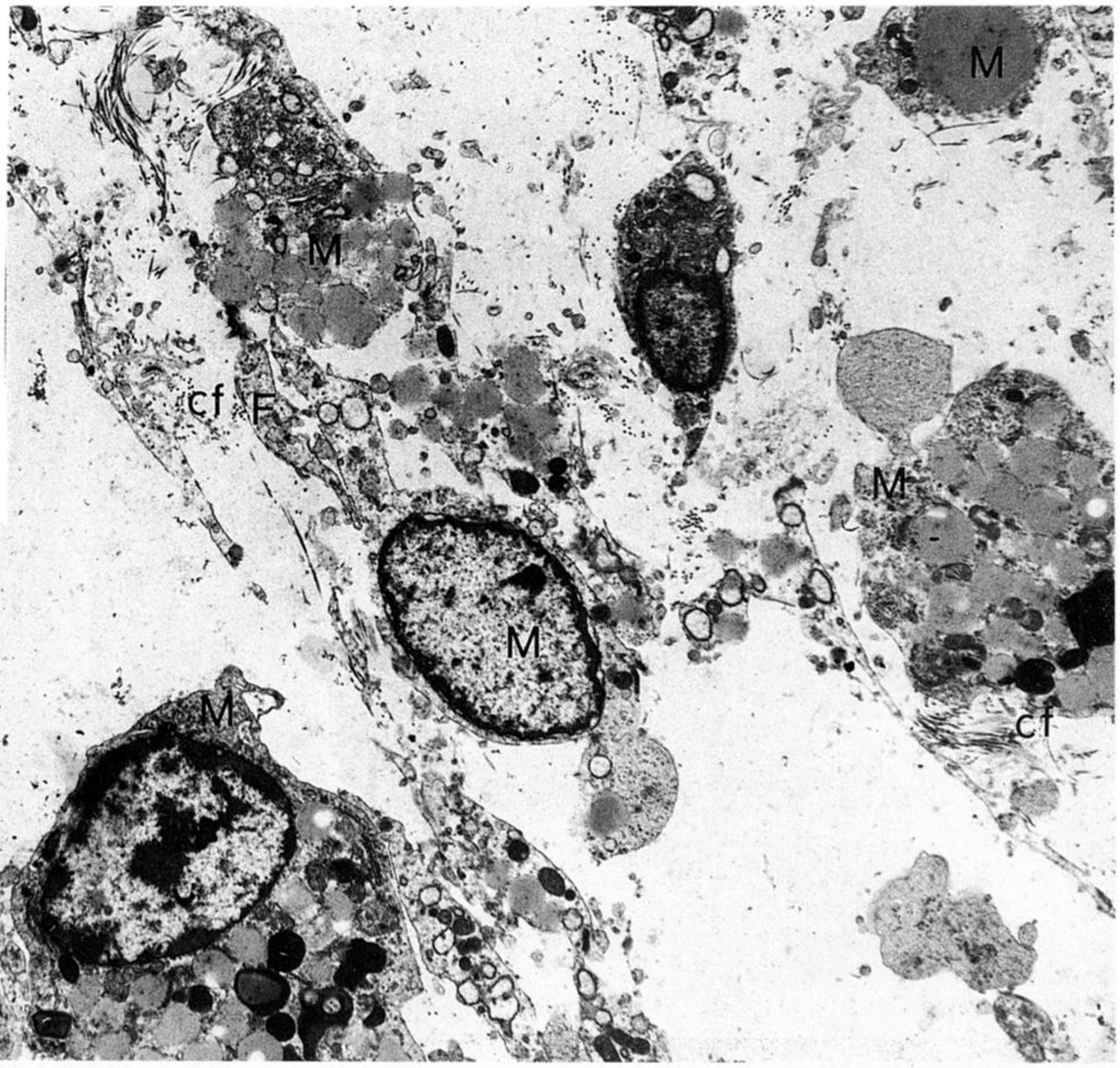

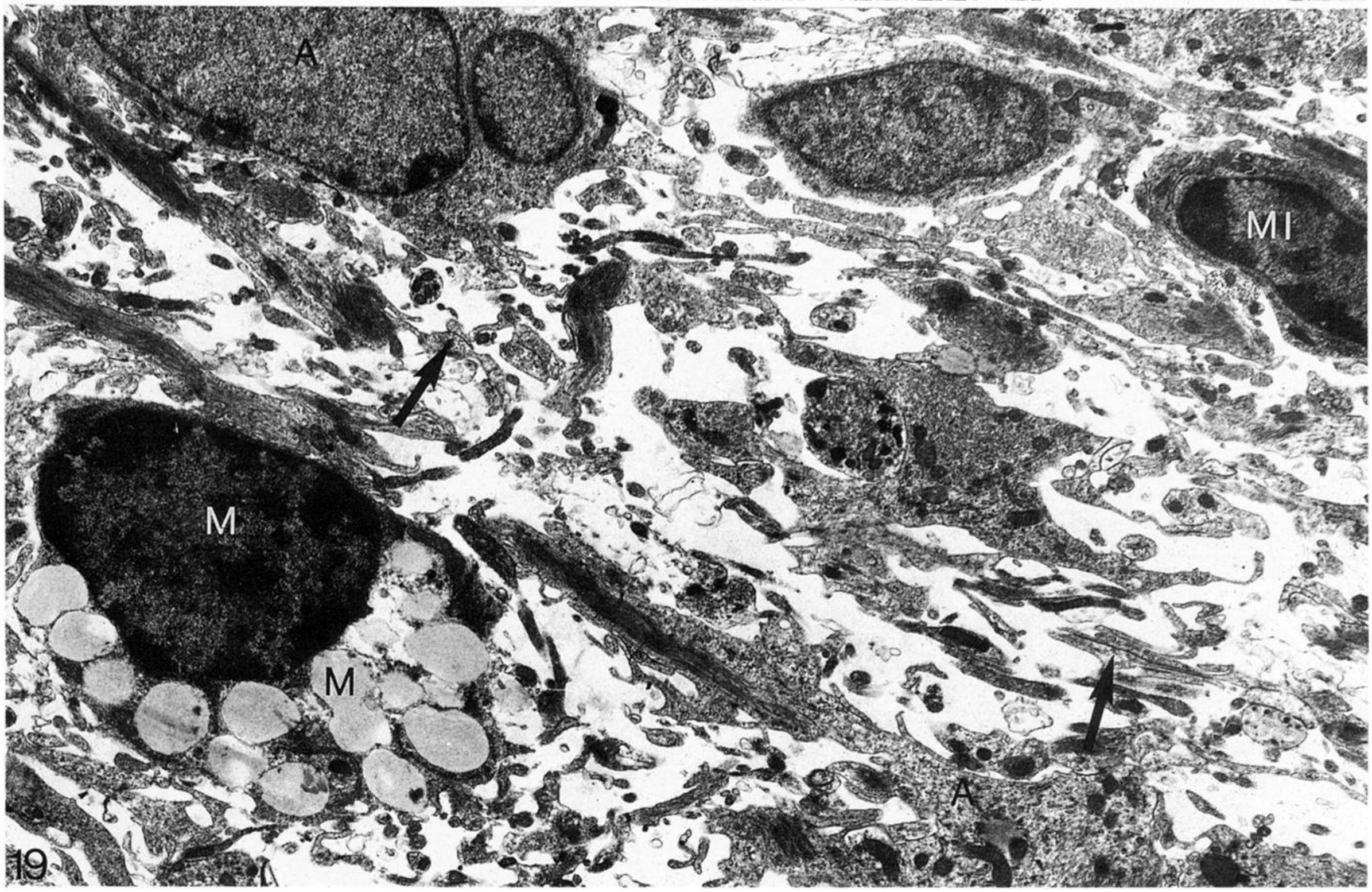

FIGURES 17–19. For description see opposite.

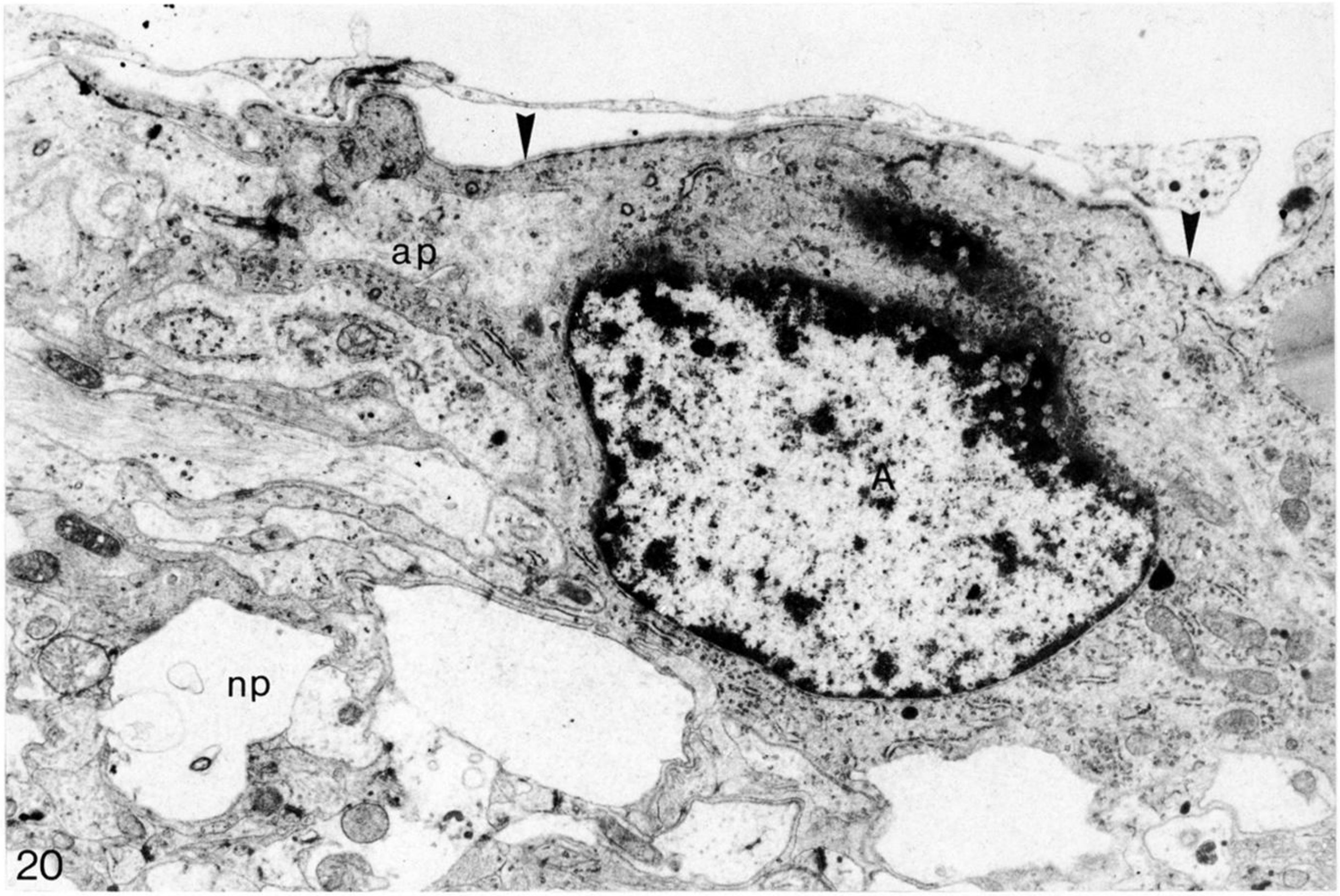

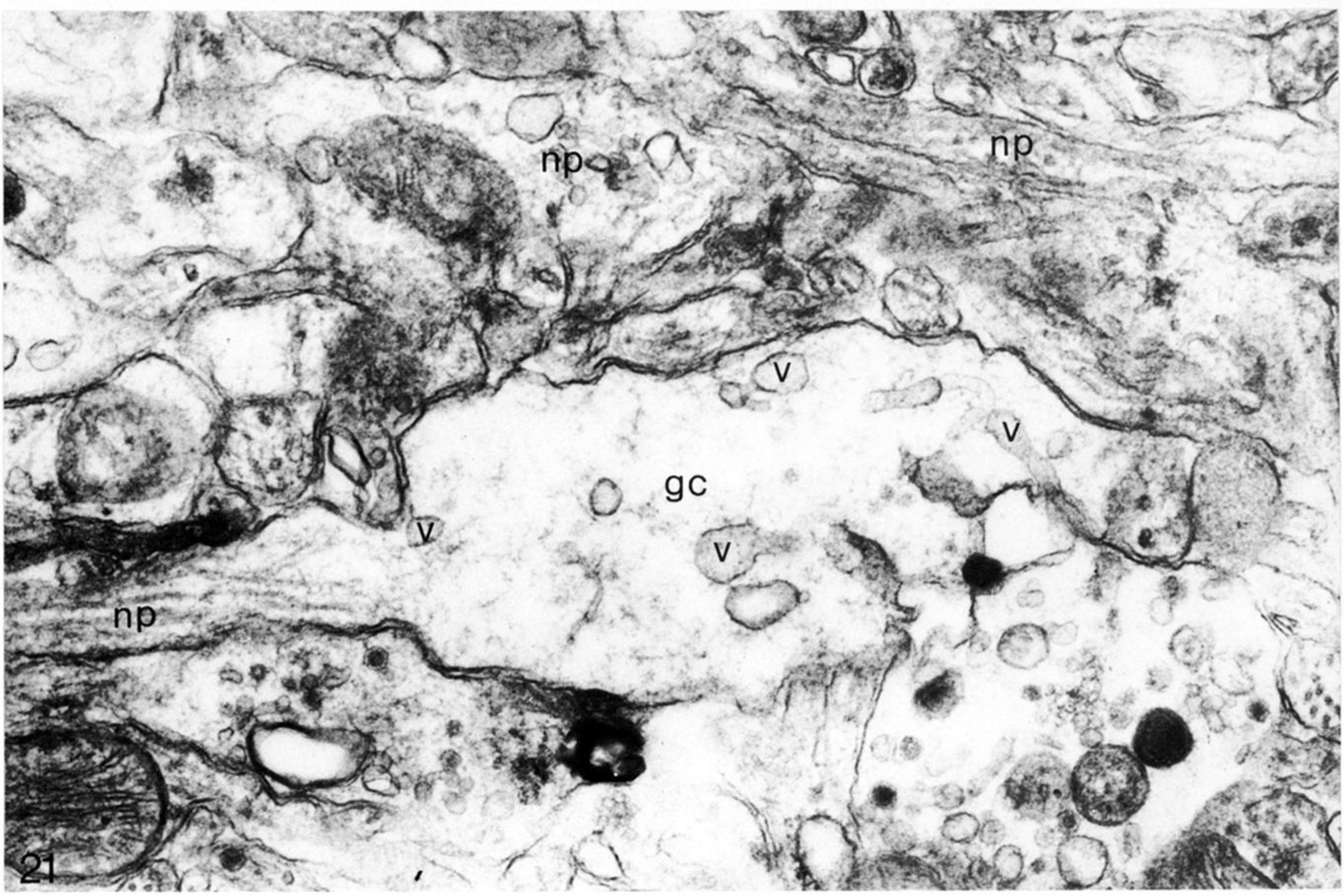

FIGURES 20 AND 21. For description see facing plate 7.

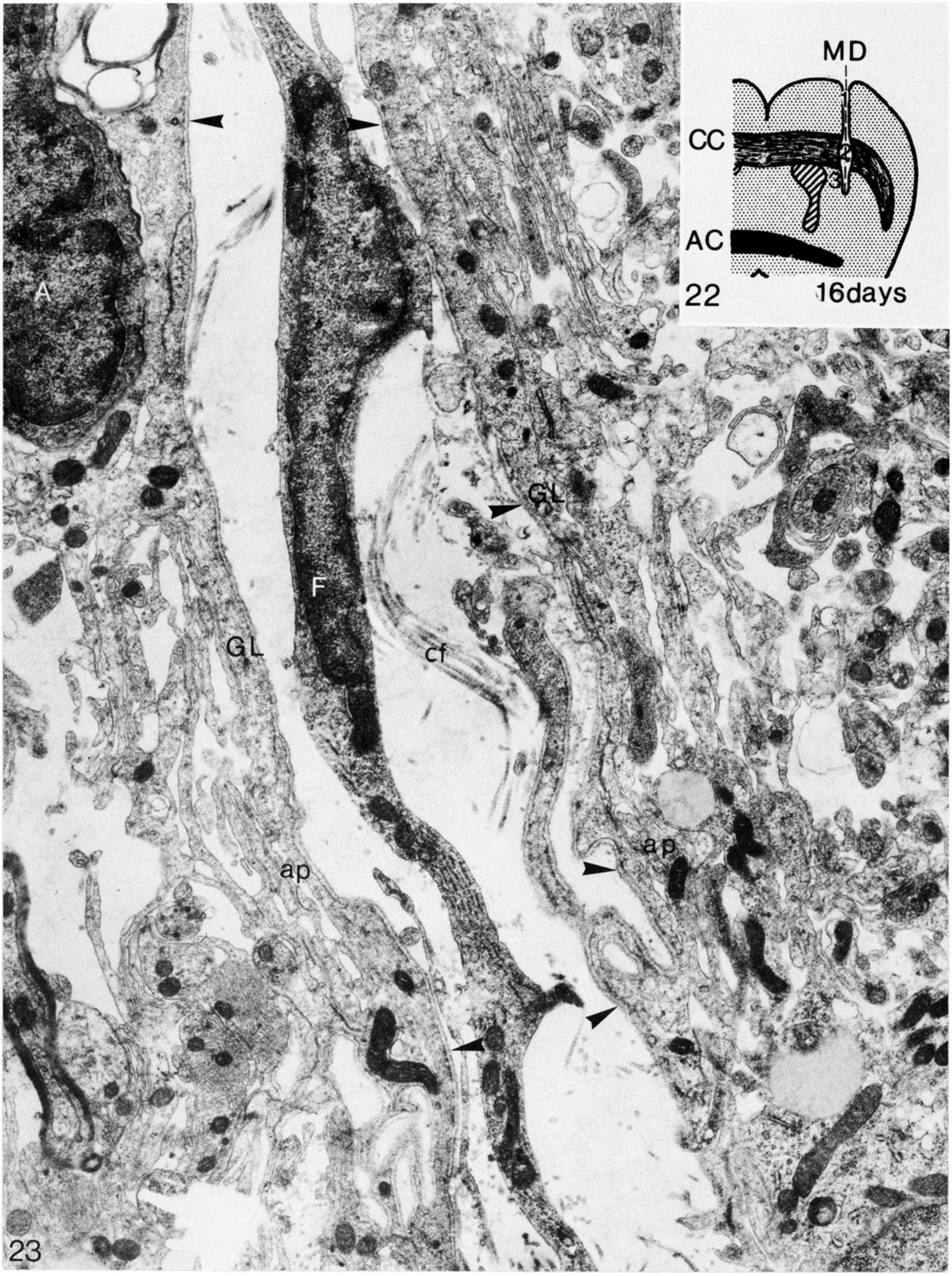

FIGURES 22 AND 23. For description see facing plate 7.

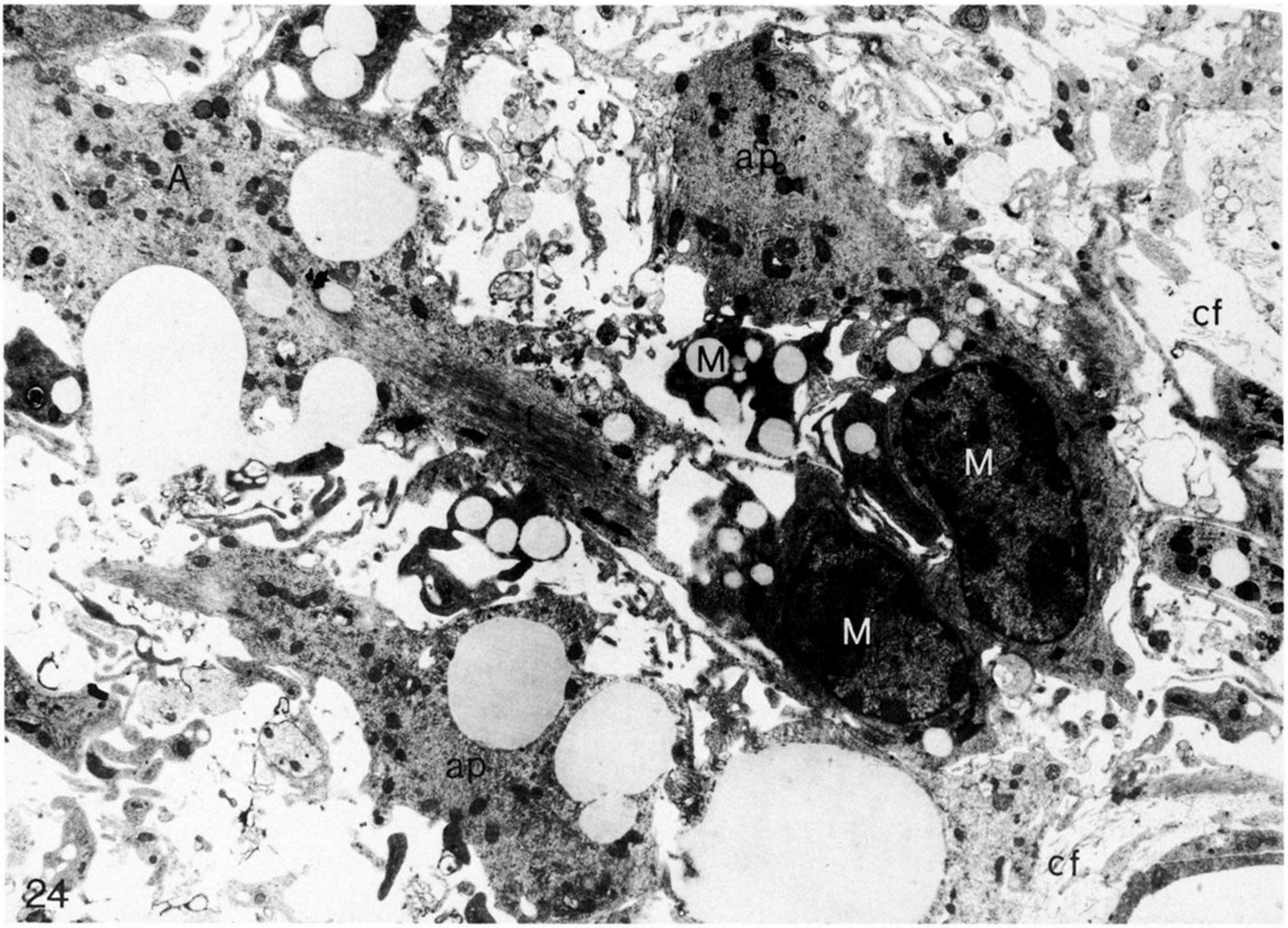

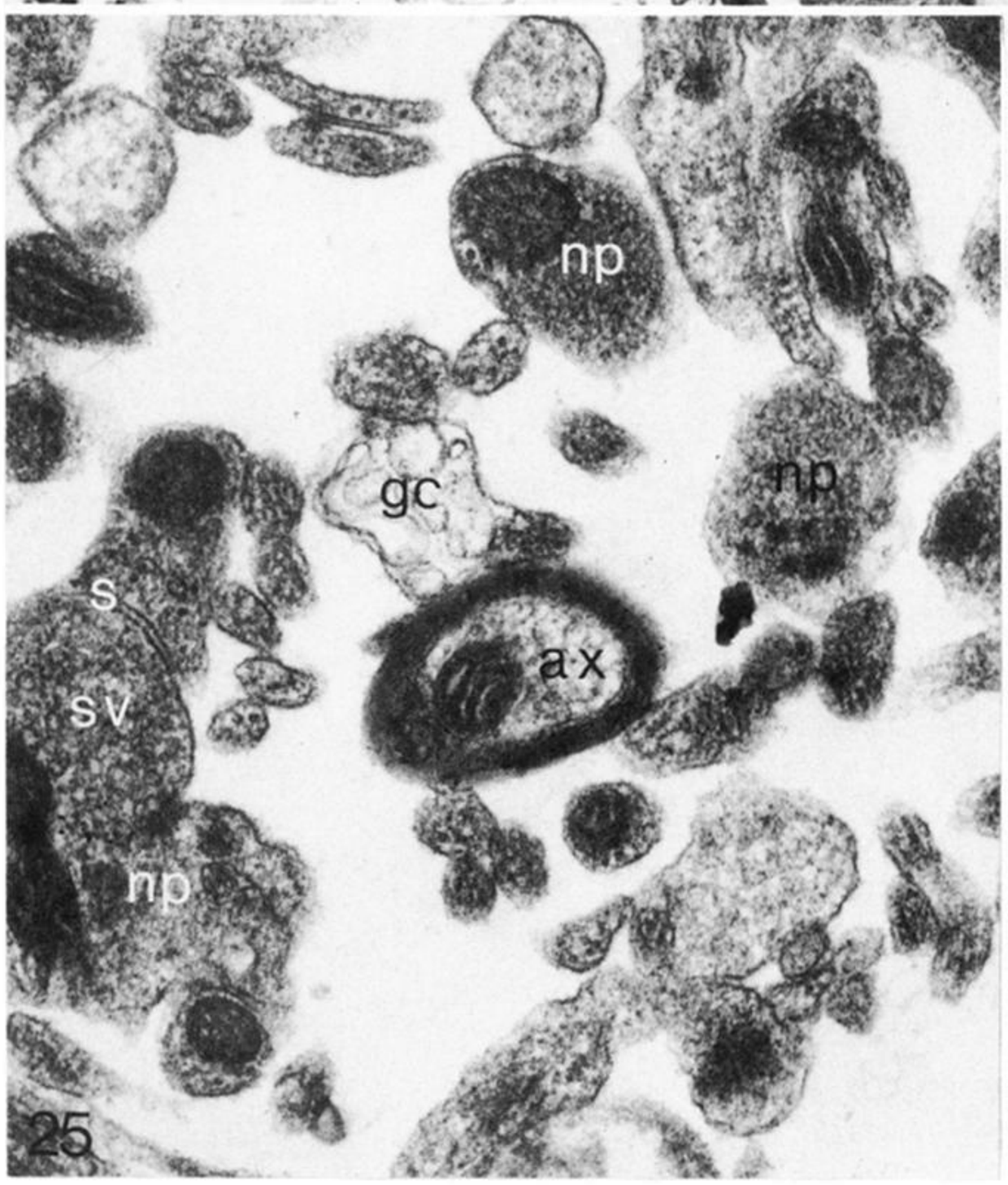

FIGURES 24–26. For description see opposite.

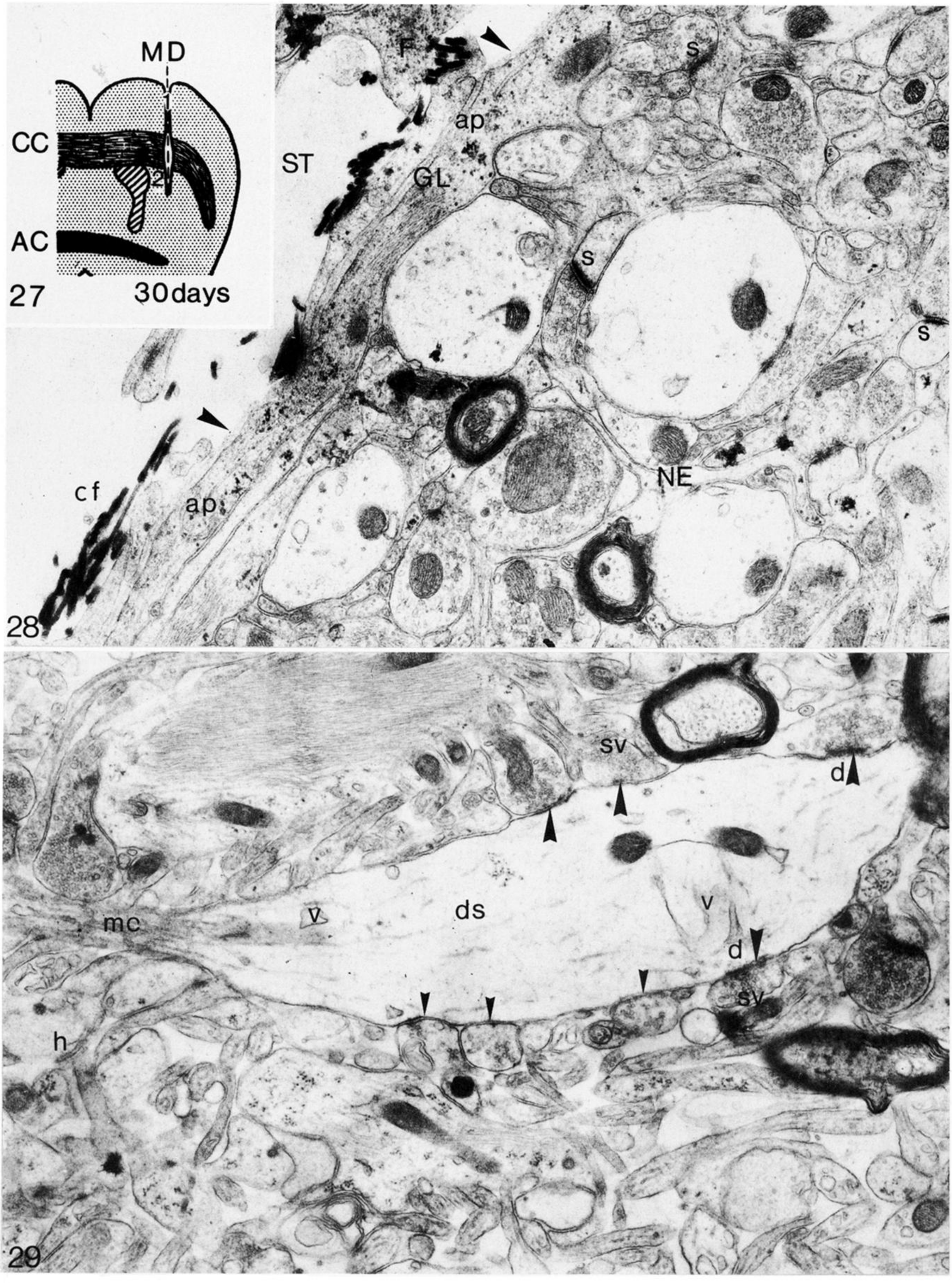

FIGURES 27–29. For description see opposite.

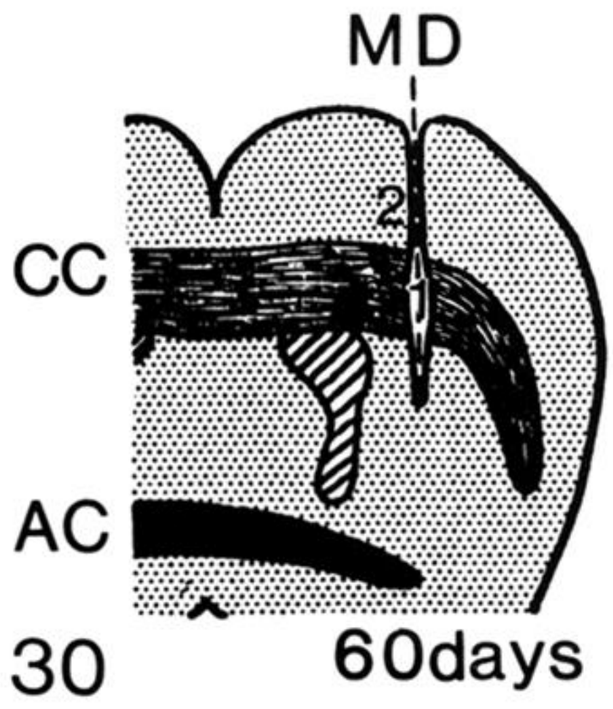

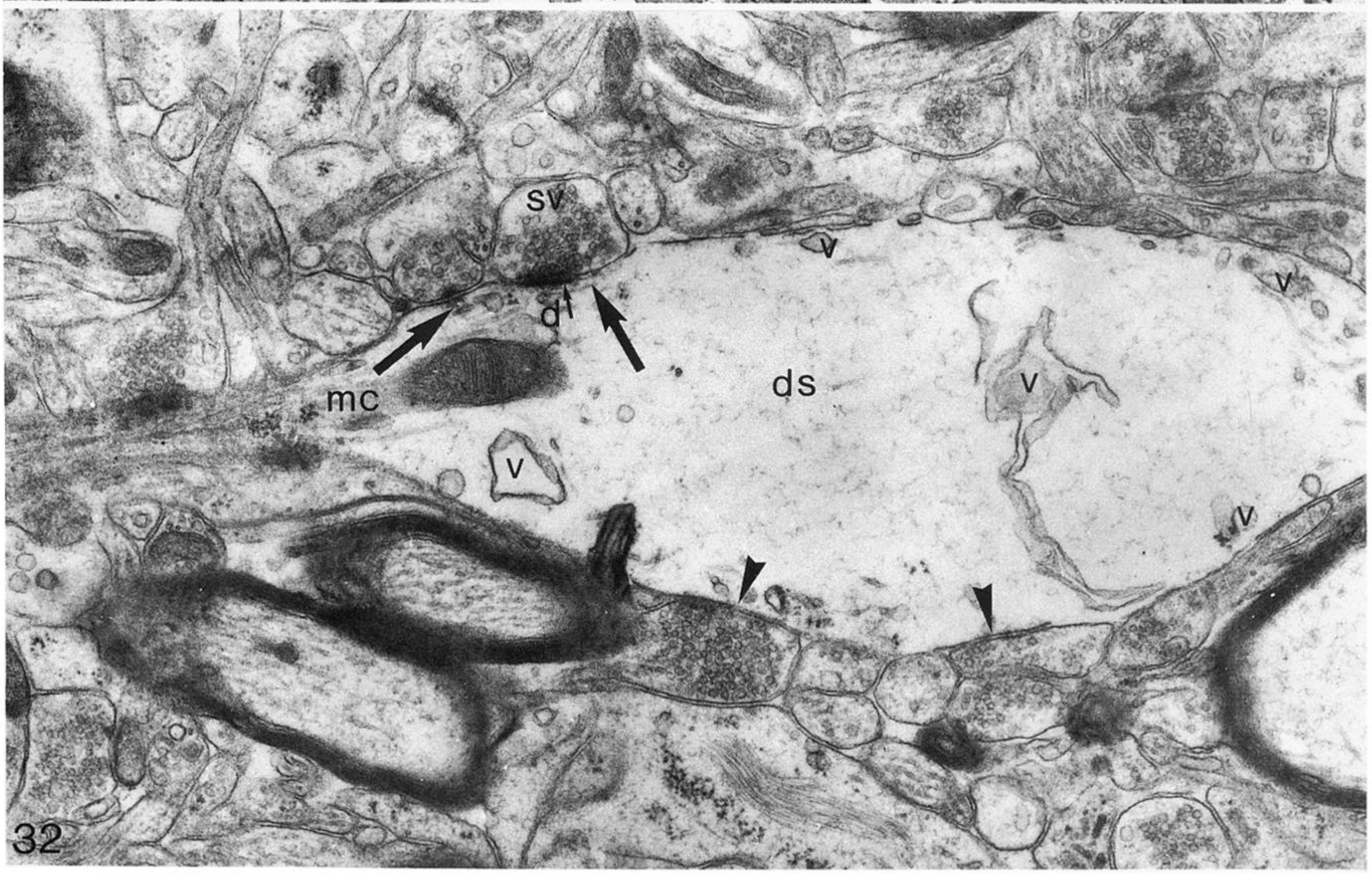

FIGURES 30–32. For description see opposite.

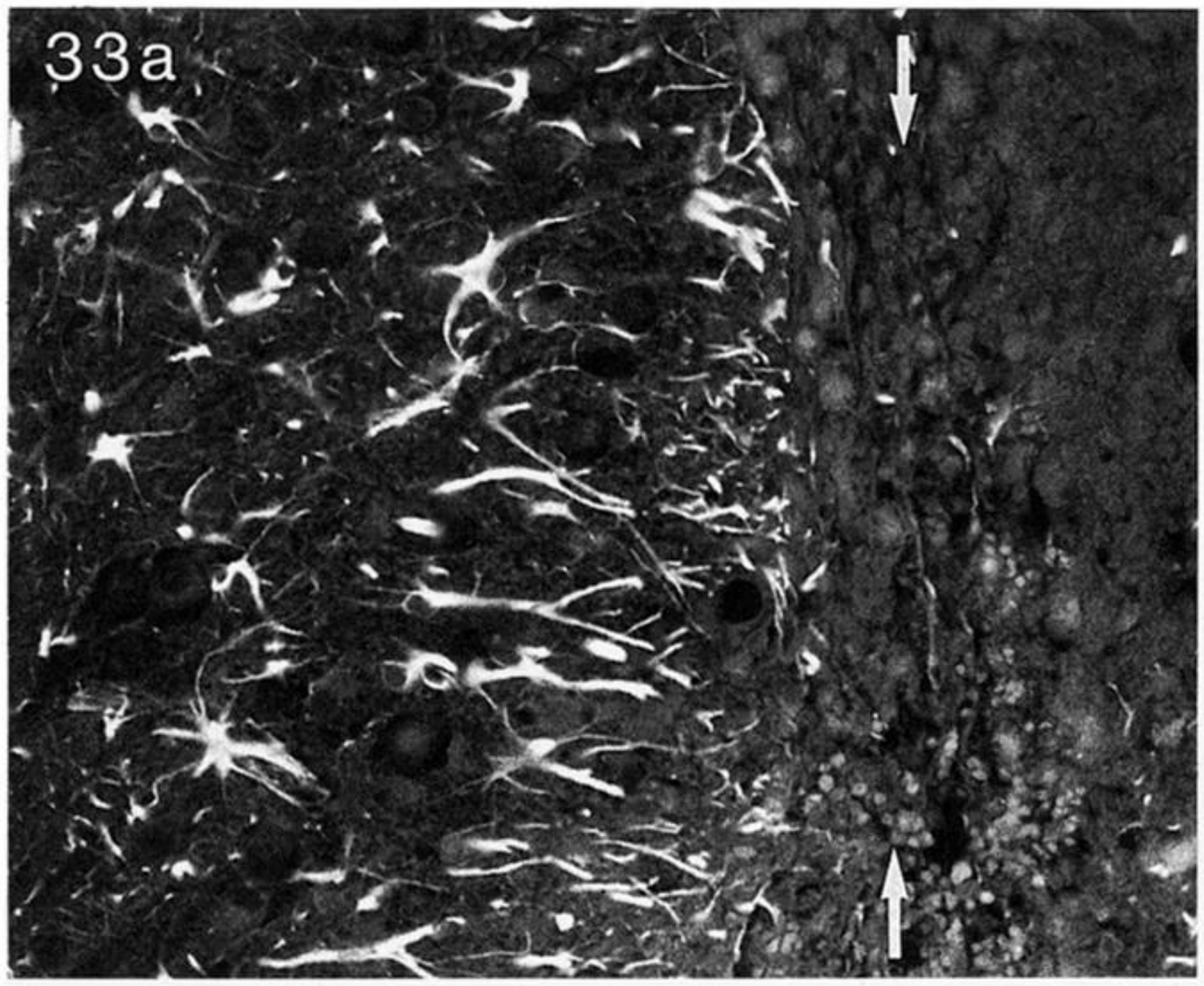

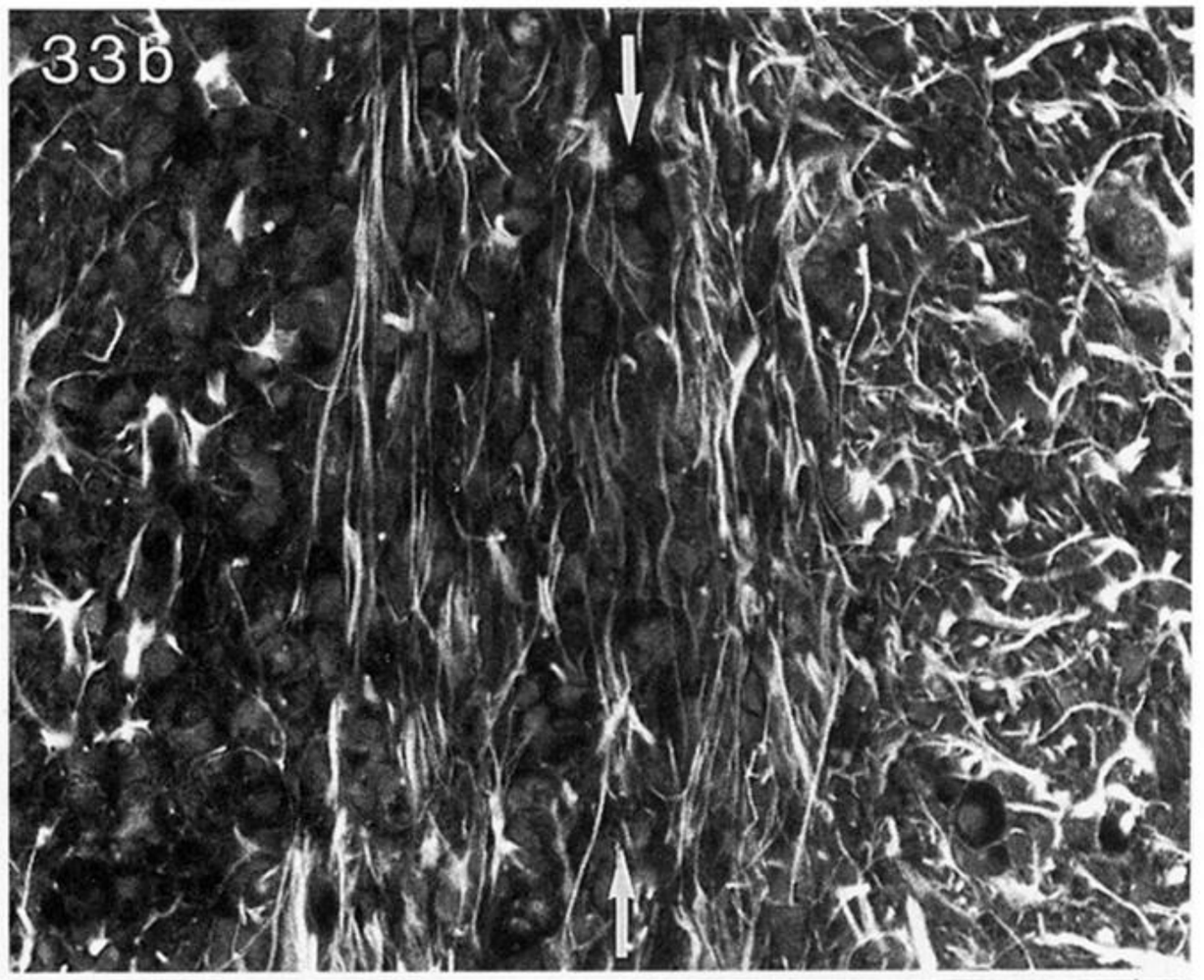

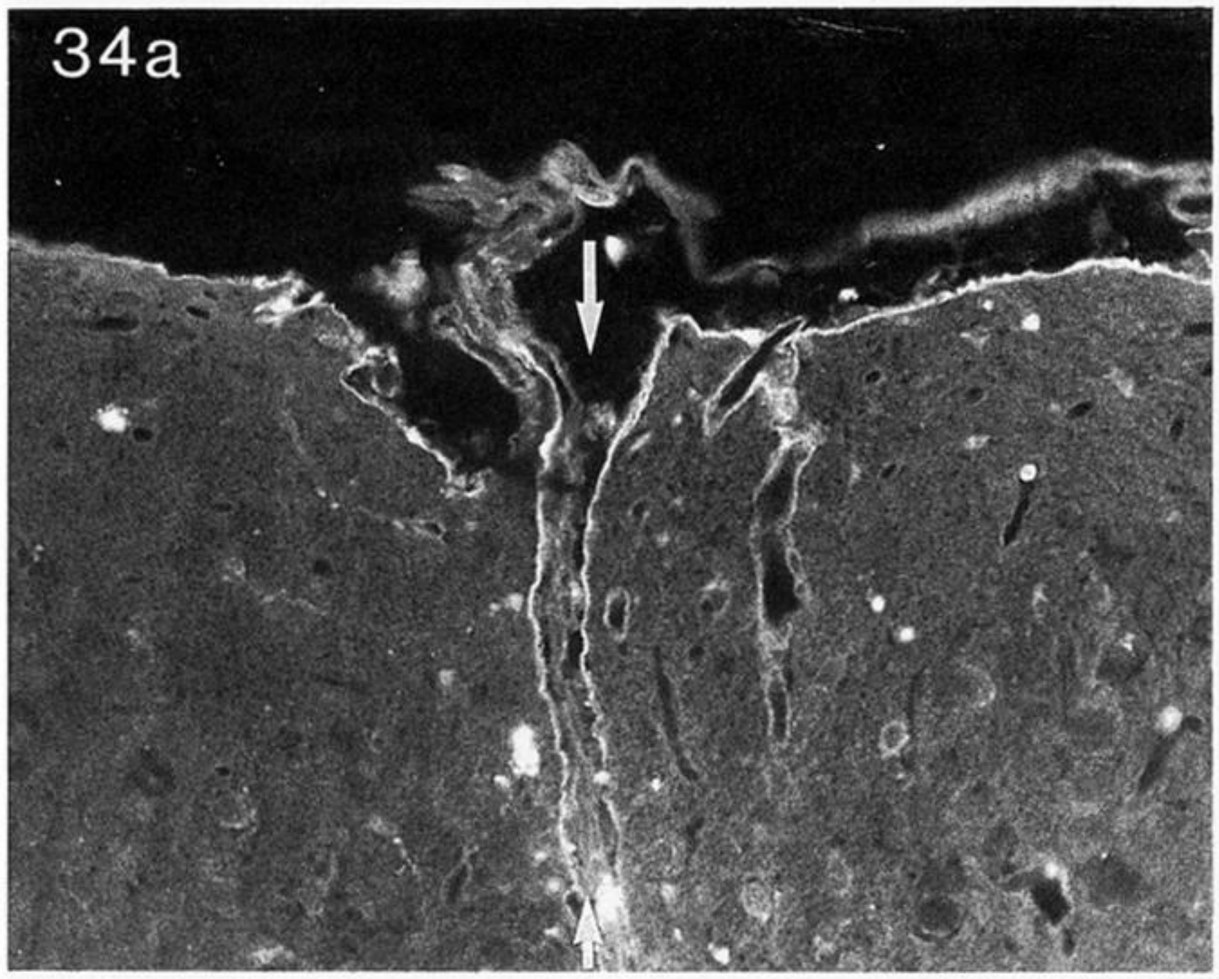

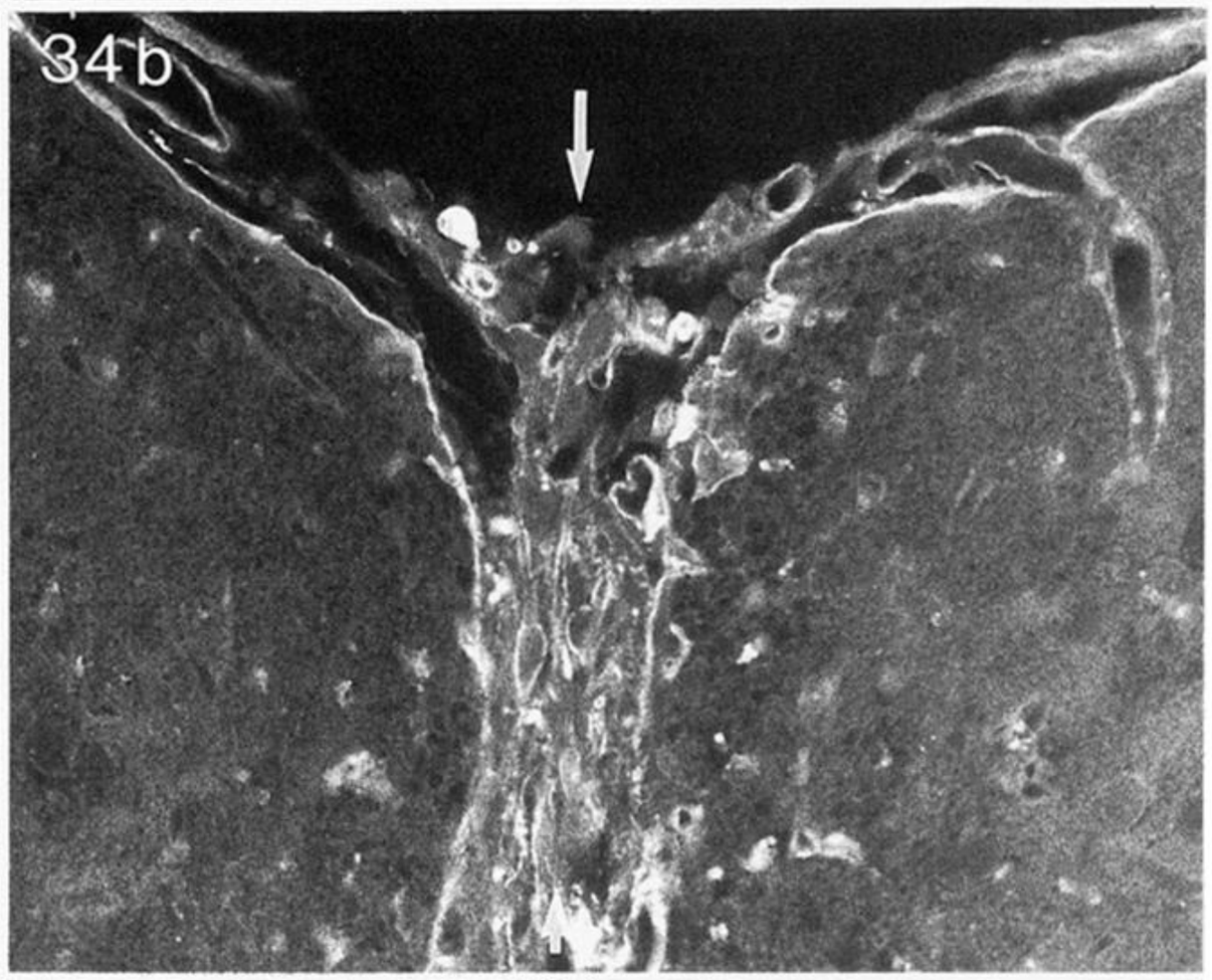

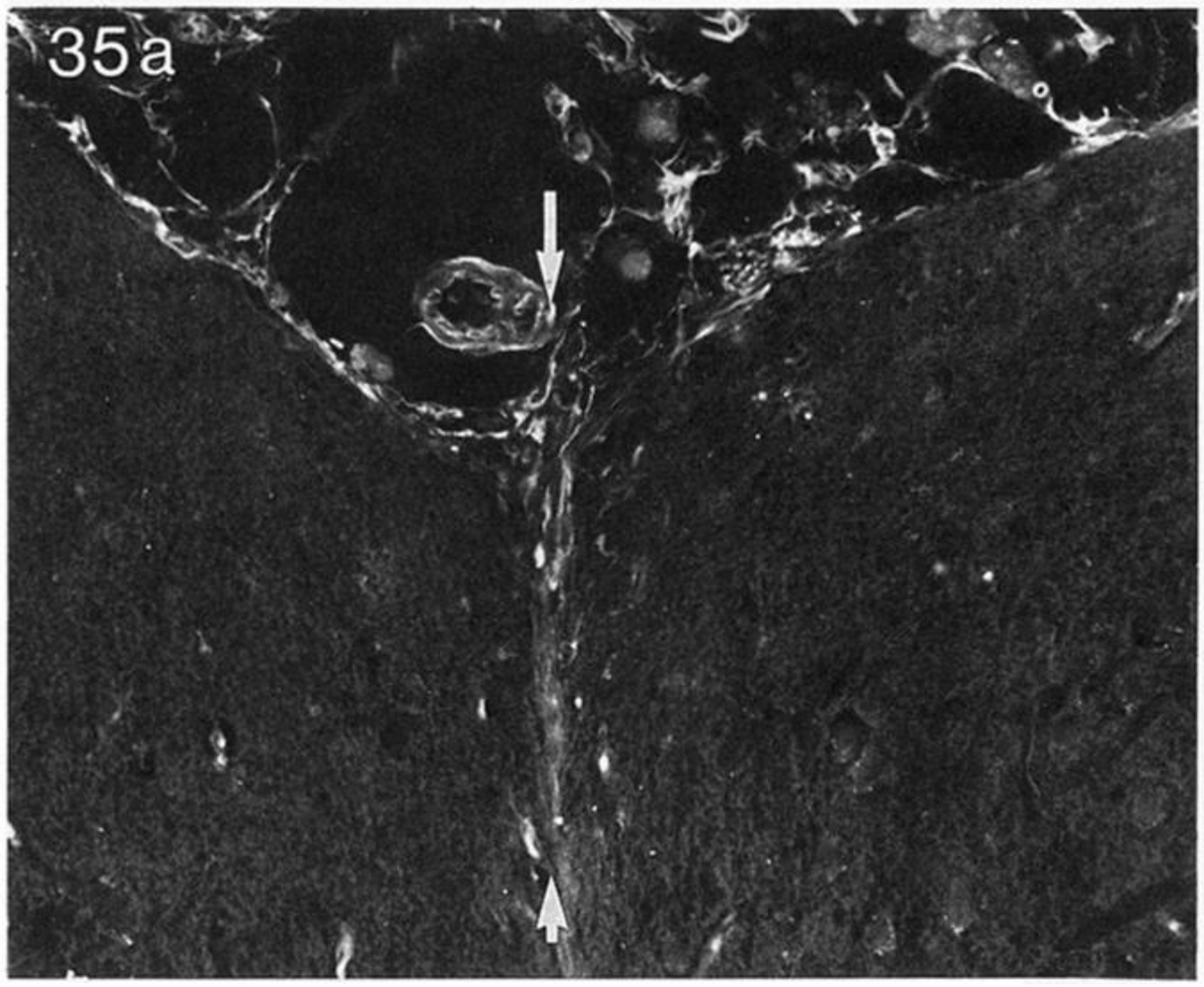

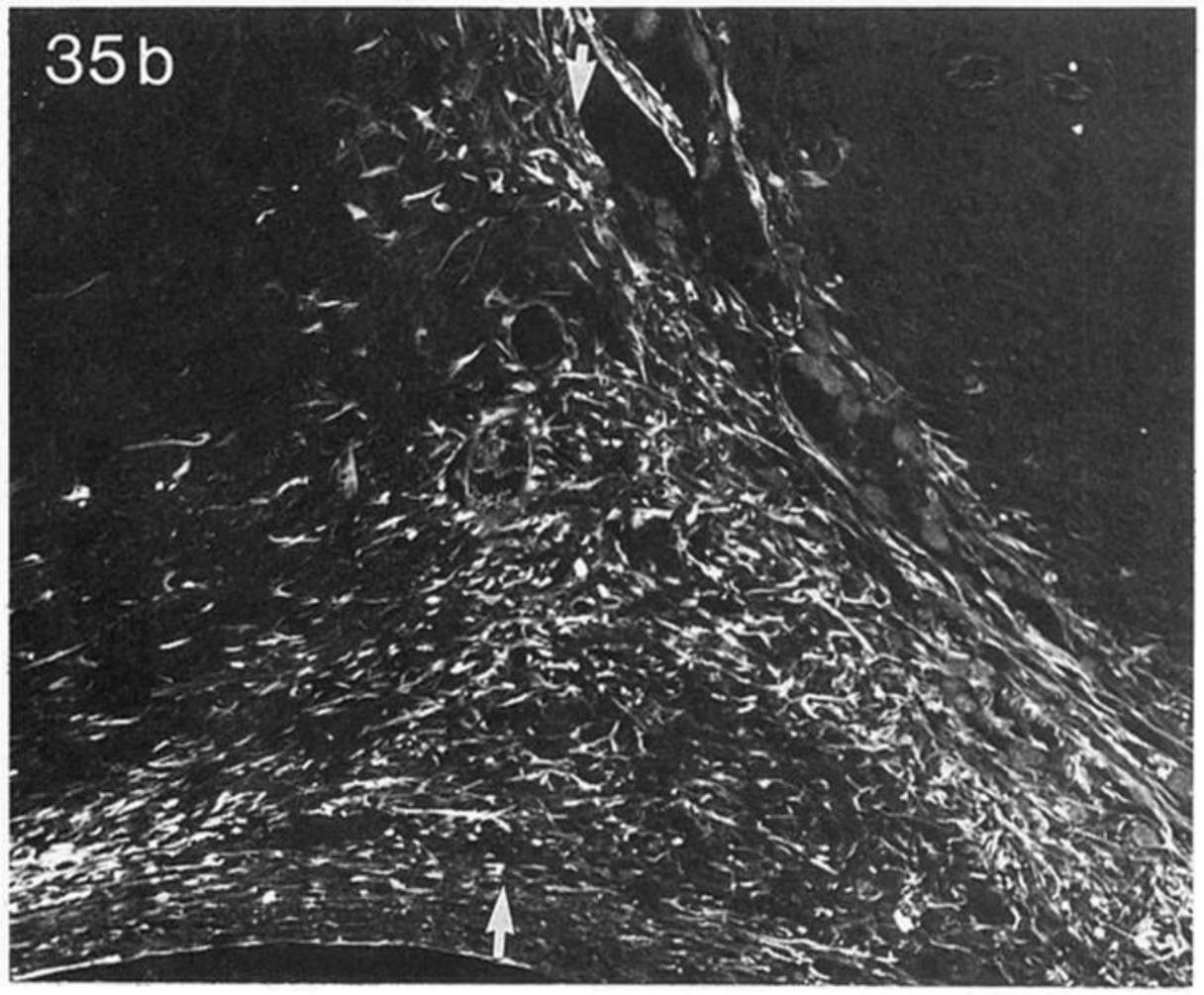

FIGURES 33*a*, *b*, 34*a*, *b* AND 35*a*, *b*. For description see p. 487.

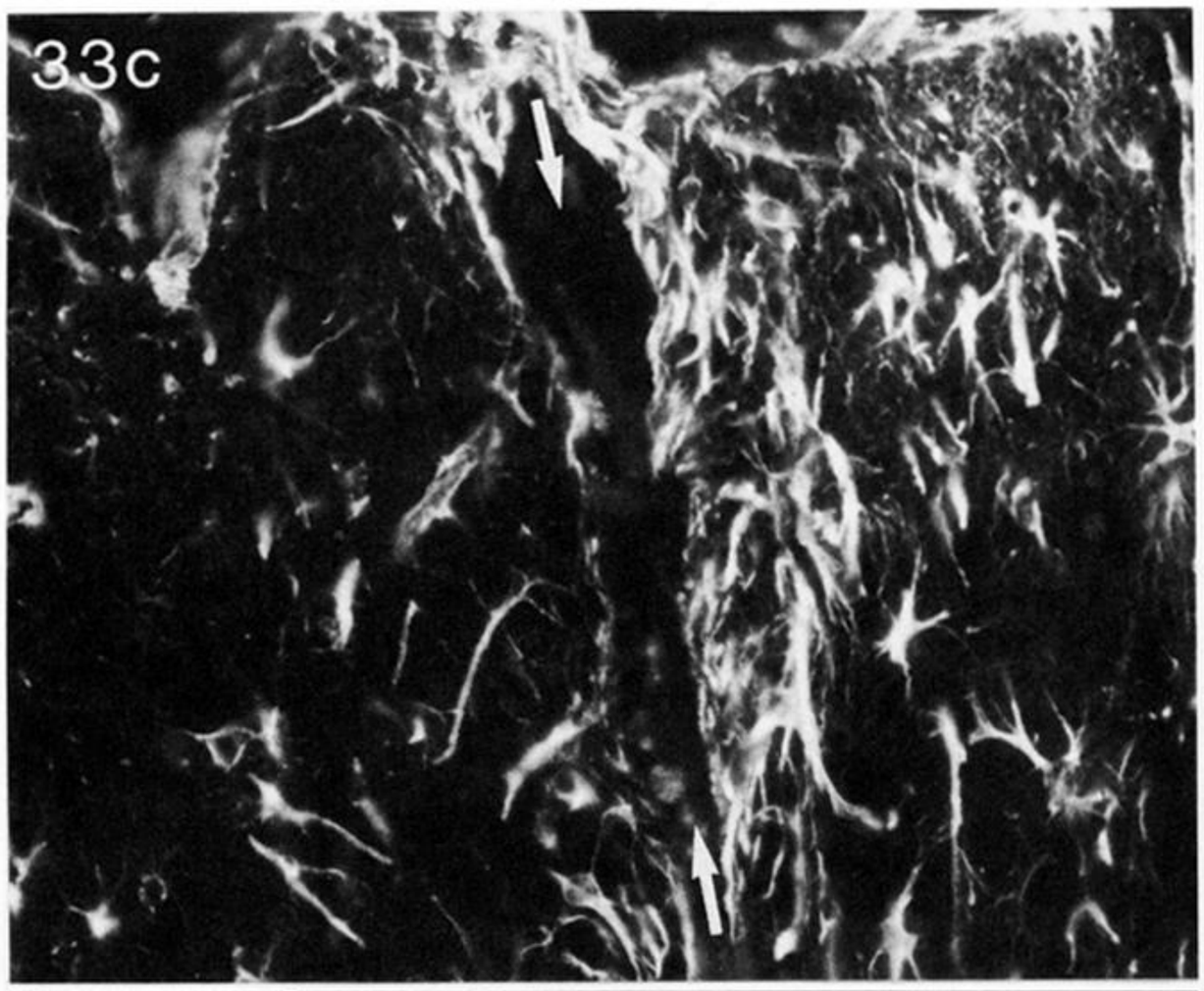

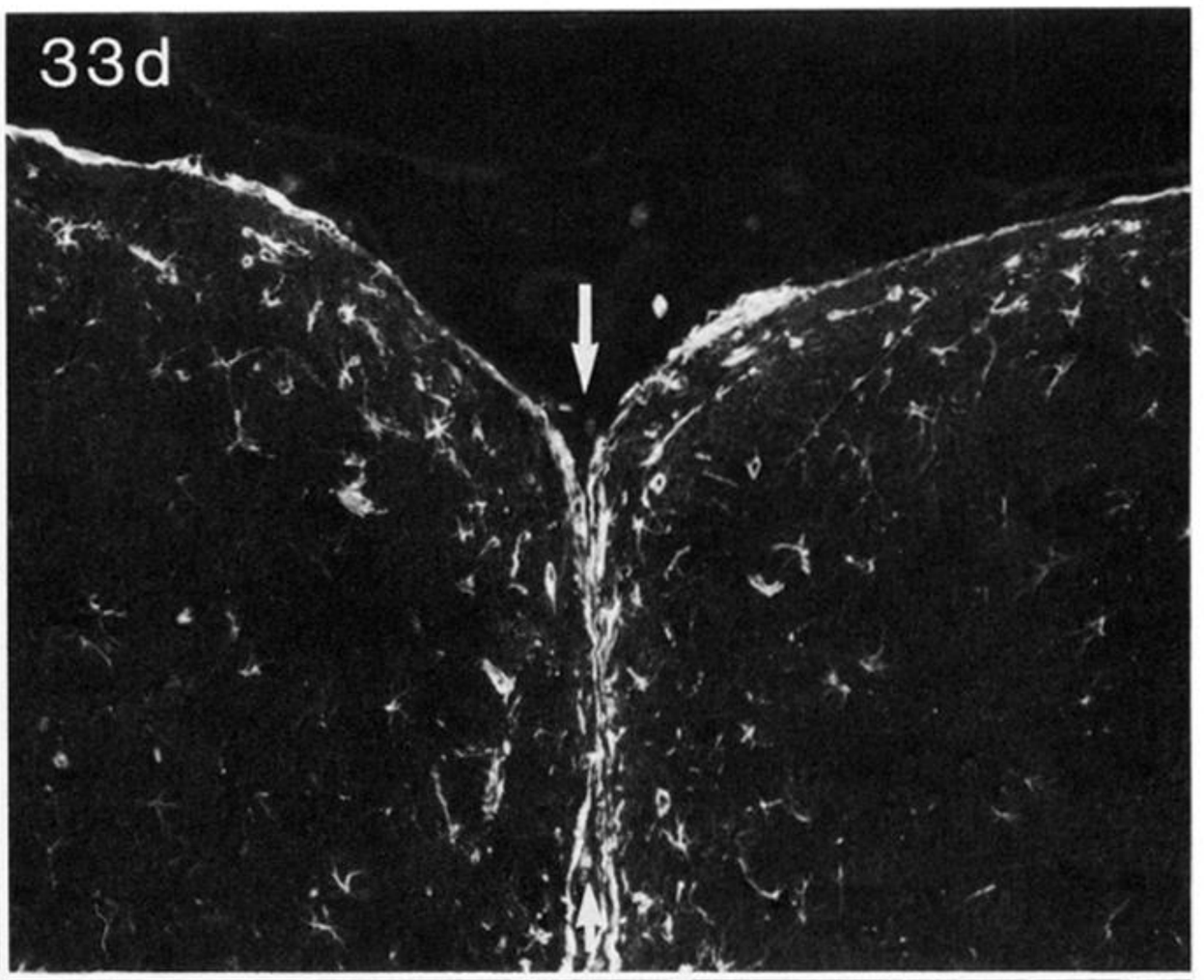

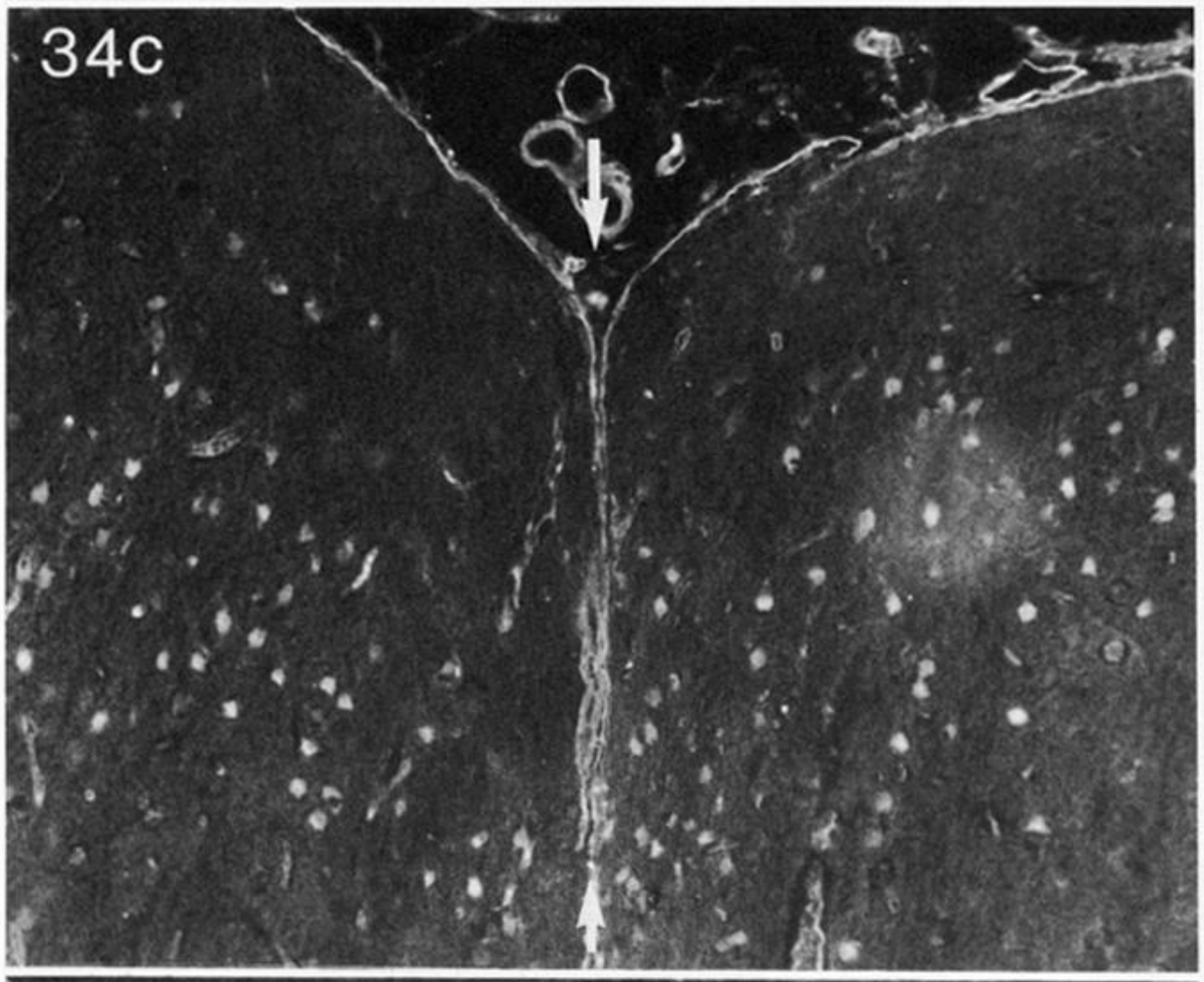

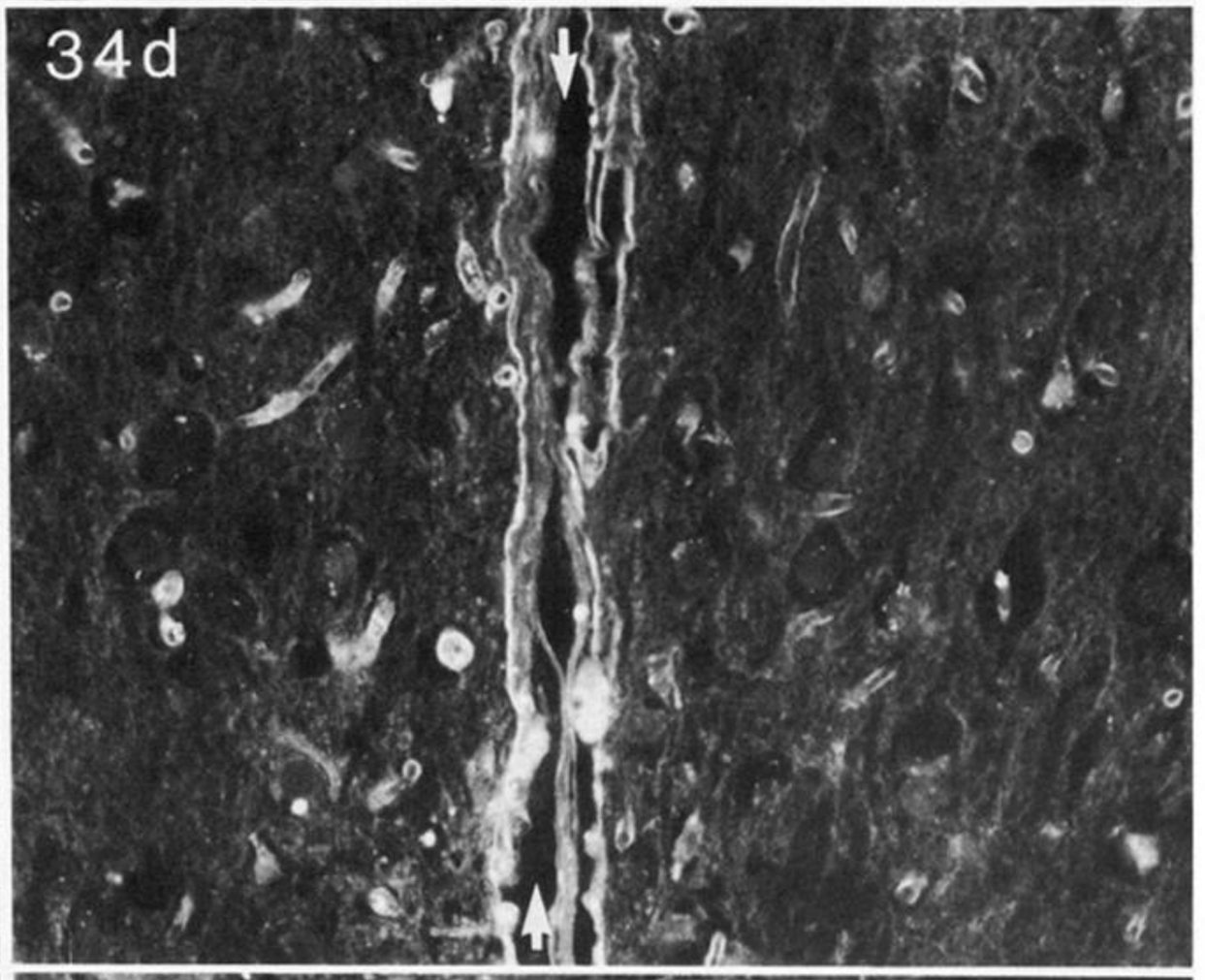

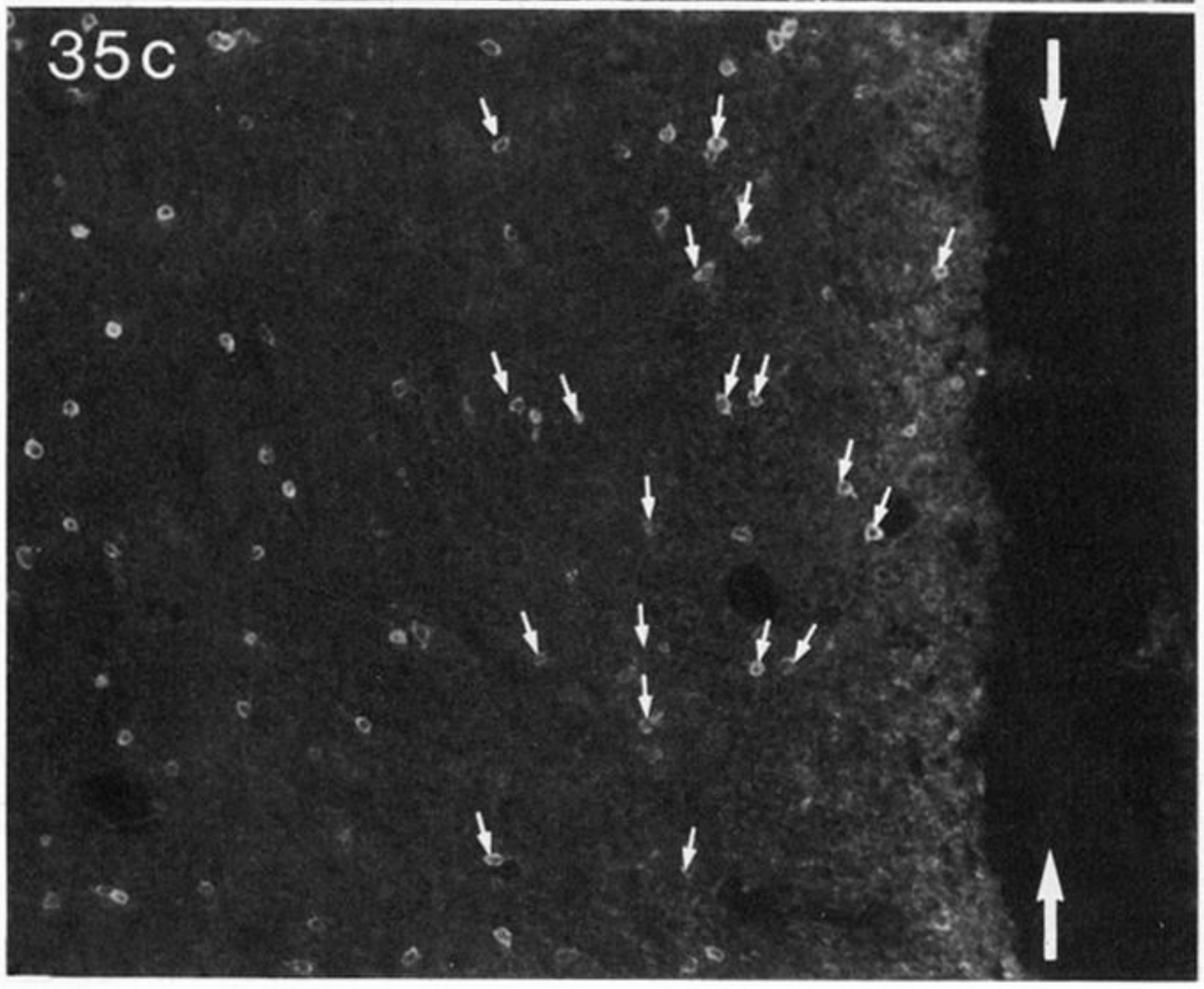

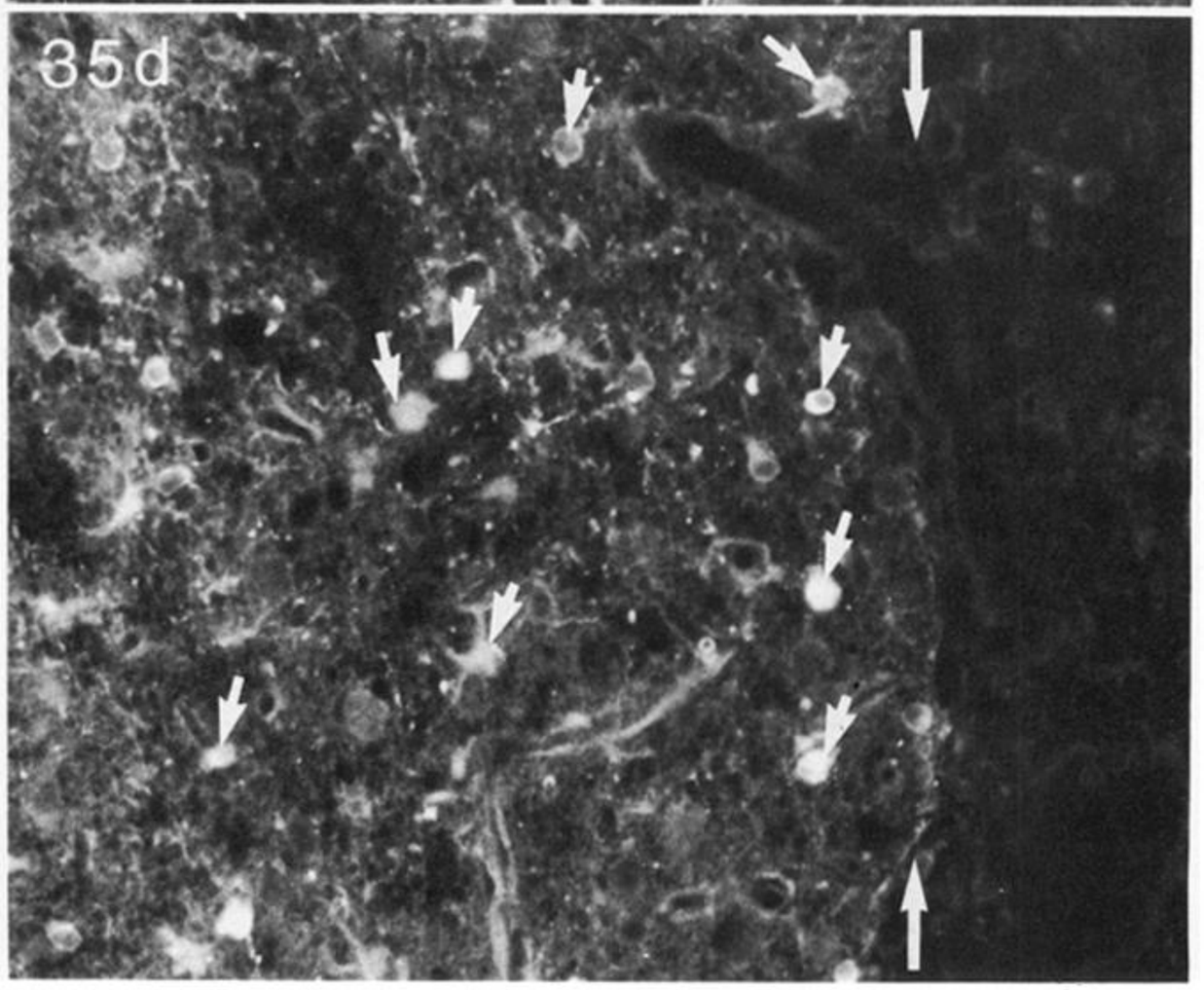

FIGURES 33*c*, *d*, 34*c*, *d* AND 35*c*, *d*. For description see p. 487.

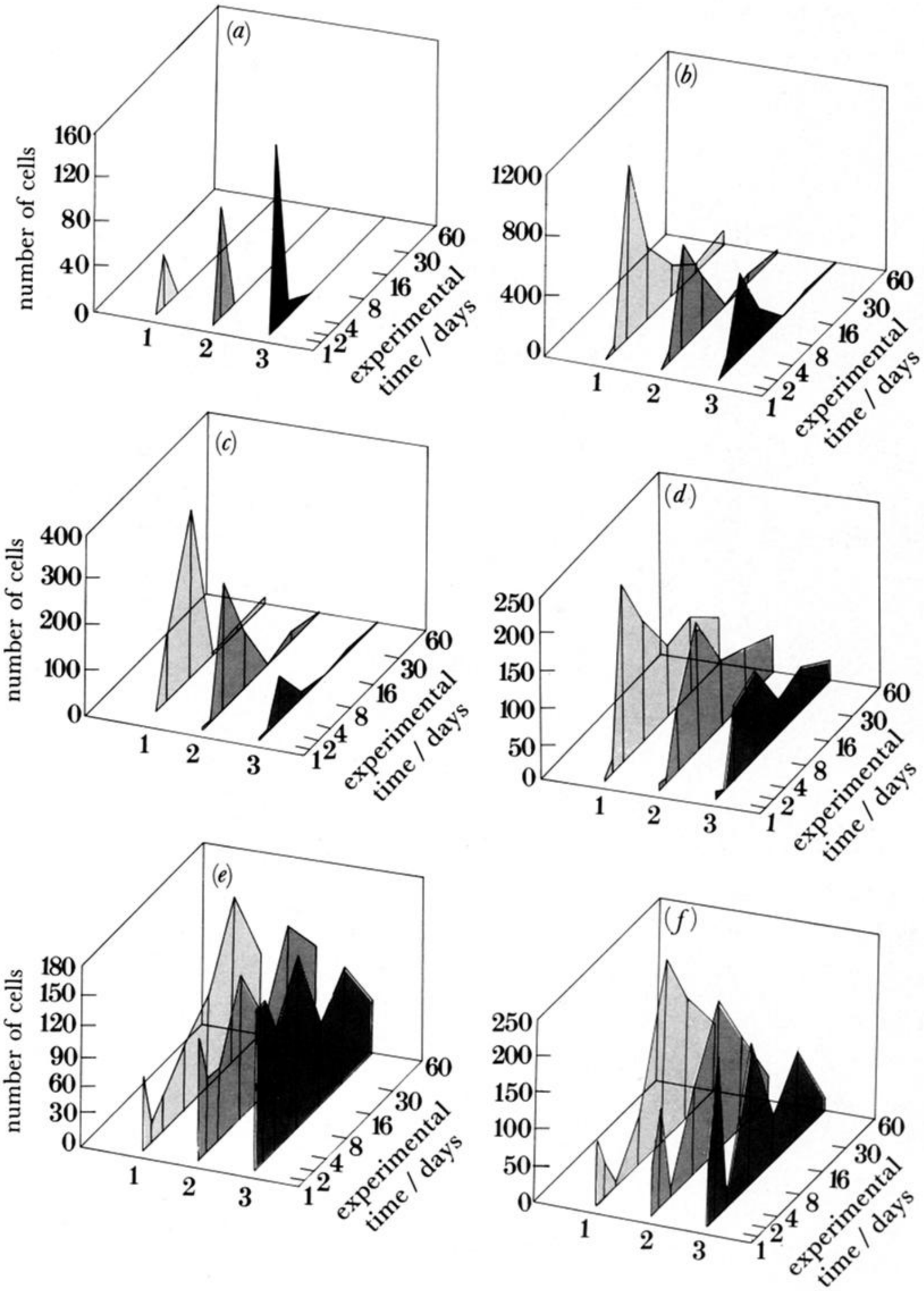

FIGURE 36. Graphs to show the numbers and distribution of the mesenchymal and glial cells associated with the lesion with increasing distance from the midline at the different experimental times. (*a*) monocytes; (*b*) macrophages; (*c*) fibroblasts; (*d*) astrocytes; (*e*) oligodendrocytes; (*f*) microglia. Key: 1, cells between midline and 100 μm on either side; 2, cells between 100 and 200 μm on either side; 3, cells between 2 and 300 μm on either side.